



Paul, Adityo (2017) *Structural and functional studies of recombinant human MsrB3A*. MSc(R) thesis.

<http://theses.gla.ac.uk/8546/>

Copyright and moral rights for this work are retained by the author

A copy can be downloaded for personal non-commercial research or study, without prior permission or charge

This work cannot be reproduced or quoted extensively from without first obtaining permission in writing from the author

The content must not be changed in any way or sold commercially in any format or medium without the formal permission of the author

When referring to this work, full bibliographic details including the author, title, awarding institution and date of the thesis must be given

Enlighten:Theses  
<http://theses.gla.ac.uk/>  
theses@gla.ac.uk

# Structural and functional studies of recombinant human MsrB3A

---



by  
Adityo Paul

Thesis submitted in fulfilment of the requirements for the degree of Master of  
Science (by research)

Institute of Molecular, Cell and Systems Biology

School of Life Sciences

University of Glasgow

August 2017

# Abstract

---

In humans, MsrB3 occur in two different isoforms, which is a distinct characteristic found in no other organism. MsrB3A is the MsrB3 isoform which is localised within the endoplasmic reticulum of the human cell, while, the MsrB3B isoform is found in the mitochondria along with MsrB2. The primary role of MsrB3A is to repair the oxidised methionine residues in nascent polypeptides and the unfolded protein chains found in the endoplasmic reticulum, which become oxidised by ROS species produced within the endoplasmic reticulum. However, the exact mode of action of MsrB3A and the stereospecificity of MsrB3A is not entirely clear.

Hence, this thesis aims - (i) to determine the structure of MsrB3A, and (ii) to find out the functionality and stereospecificity of MsrB3A protein. The mature gene sequence for MsrB3A protein lacking the sequence for the N-terminal signal peptide was successfully cloned into recombinant *E. coli* cells and subsequently over-expressed to generate the recombinant MsrB3A protein for further studies.

From a sequence alignment, it was predicted that the 126<sup>th</sup> position cysteine residue in the amino acid sequence of MsrB3A was an active site cysteine and responsible for the function of the protein, as it was a conserved residue. Based on this assumption, the 126<sup>th</sup> position cysteine was substituted with alanine residue using site directed mutagenesis to generate a mutant protein which could be further used in determination of protein activity.

With respect to determination of MsrB3A structure, we used three approaches- (i) CD Spectroscopy for determining the secondary structural elements of MsrB3A, (ii) NMR spectroscopy and (iii) protein crystallisation to determine the tertiary structure of MsrB3A protein.

The results obtained from CD spectroscopy and NMR spectroscopy proved that the recombinant MsrB3A protein had a folded structure. It was also noted that the results which were obtained by CD spectroscopy were consistent with previous studies performed by other groups with respect to MsrB proteins. Though certain crystallisation hits were obtained, good quality crystals required for determining the crystal structure by X-ray

spectroscopy were not achieved, hence, the crystal trials were not successful and requires further work.

To address the functionality of MsrB3A, two different approaches were used- (i) a gel shift assay and (ii) a HPLC assay. The gel shift assay involved the change in mobility of SurA protein in its oxidised and reduced states which formed the basis of determining the protein functionality, when analysed on SDS-PAGE gel. Hence, when SurA was oxidised by treatment with  $H_2O_2$ , the mobility of SurA decreased with respect to its native form when analysed on SDS-PAGE gel. Hence, when the oxidised form was repaired by treatment with MsrB3A protein in presence of DTT, there was a slight shift in the mobility of oxidised SurA towards its native form, but could not gain complete mobility, suggesting an incomplete repair and indicating that MsrB3A is stereo-specific, but cannot say which isoform of methionine sulfoxide it reduces. Similar results were also achieved by HPLC assay in which approximately half of the dabsylated methionine sulfoxide concentration was reduced to dabsylated methionine, which supports and suggests that MsrB3A is stereo-specific, but further experiments using individually dabsylated methionine-R-sulfoxide and methionine-S-sulfoxide is required as substrate to have accurate determination of stereo-specificity. Another significant observation which was made by the HPLC assay was the non-functionality of the C126A MsrB3A mutant protein. When the dabsylated methionine sulfoxide was treated with the C126A MsrB3A mutant no reduction was observed upon separation using the HPLC. This indicated that the cysteine residue being substituted was an active site cysteine which is responsible for the protein function.

Therefore, to conclude, we could gain a stable recombinant protein product which could be actively used for study and experimentation.

# Table of contents

---

Title	1
Abstract	2
Table of contents	4
List of figures and tables	7
Acknowledgements	10
Author's declaration	11
List of abbreviations	12
Chapter 1: Introduction	14
General introduction	14
1.1 Methionine as an antioxidant	15
1.2 Methionine sulfoxide reductases (Msrs)	17
1.3 Methionine sulfoxide reductases and diseases	18
1.4 Methionine sulfoxide reductases isoform A	20
1.5 Methionine sulfoxide reductases isoform B	22
1.6 Endoplasmic reticulum	26
1.7 Objectives of the thesis	26
1.8 Outline of the thesis	27
Chapter 2: Materials and methods	29
2.1 Expression of human MsrB3A in <i>E. coli</i> BL 21 (DE3) Star <i>pLysS</i> cells	29
2.2.1 Protein extraction and purification	29
2.2.2 Protein concentration and quantification	31
2.3.1 Spectroscopic Techniques: CD spectroscopy	31

2.3.2 Spectroscopic Techniques: NMR spectroscopy	32
2.3.3 Protein crystallisation	32
2.4.1 Site directed mutagenesis: Conversion of 126 <sup>th</sup> position cysteine to alanine	33
2.5.1 Gel shift assay	34
2.5.2 High pressure liquid chromatography (HPLC) assay	35
<b>Chapter 3: MsB3A: Protein expression, extraction and purification</b>	<b>36</b>
3.1 Introduction	36
3.2 Results	40
3.2.1 Protein expression, extraction and purification	40
3.2.2 Structural studies	54
3.2.2.1 CD spectroscopy	54
3.2.2.2 NMR spectroscopy	56
3.2.2.3 Protein crystallisation	59
3.3 Discussions	61
3.3.1 Protein expression, extraction and purification	61
3.3.2 Structural studies of recombinant MsrB3A	62
3.4 Future Work	62
<b>Chapter 4: Creation of C126A MsrB3A mutant by site directed mutagenesis</b>	<b>64</b>
4.1 Introduction	64
4.2 Results	66
4.2.1 Site directed mutagenesis	66
4.2.2 Protein expression, extraction and purification	70
4.3 Discussions	75
<b>Chapter 5: MsrB3A functional assay I - Gel shift assay</b>	<b>76</b>
5.1 Introduction	76

5.2 Results	78
5.2.1 Protein expression, extraction and purification	78
5.2.2 Gel shift assay	82
5.3 Discussions	86
5.4 Future Work	87
<b>Chapter 6: MsrB3A functional assay II - HPLC assay</b>	<b>88</b>
6.1 Introduction	88
6.2 Results	90
6.3 Discussions	95
6.4 Future Work	96
<b>Conclusions</b>	<b>97</b>
7.1 Introduction	97
7.2 Potential substrates for MsrB3A in human endoplasmic reticulum	97
7.3 Enzyme kinetics and substrate affinity of MsrB3A within the ER	98
7.4 Determination of physiological role of MsrB3A during oxidative stress	99
7.5 Other areas of research	100
<b>Appendix</b>	<b>101</b>
<b>List of references</b>	<b>103</b>

# List of figures and tables

---

**Figure 1.1:** Structure of cysteine and methionine.

**Figure 1.2:** ROS-induced oxidation of methionine residue to methionine sulfoxide and further oxidation by ROS species to methionine sulfone.

**Figure 1.3:** Oxidation of methionine to methionine sulfoxide and reduction pathway of methionine sulfoxide to methionine.

**Figure 1.4:** Schematic representation of the steps occurring at the active site of MsrA to form the sulfenic acid intermediate.

**Figure 3.1:** Multiple sequence alignment of amino acid sequences of MsrB3A from various organisms.

**Figure 3.2:** SDS-PAGE gel analysis of MsrB3A protein expression in Luria-Bertani (LB) broth media.

**Figure 3.3:** SDS-PAGE gel analysis of MsrB3A protein extraction using BugBuster™ Protein Extraction Reagent.

**Figure 3.4:** SDS-PAGE gel analysis of MsrB3A protein purification using TALON® Superflow™ Affinity Resin.

**Figure 3.5:** SDS-PAGE gel analysis of MsrB3A protein extraction using a French Press from LB media.

**Figure 3.6:** Immobilised metal affinity chromatography (IMAC) purification of His-tagged MsrB3A protein from LB media.

**Figure 3.7:** Gel filtration chromatography purification of MsrB3A protein from LB media.

**Figure 3.8:** SDS-PAGE gel analysis of MsrB3A protein expression in terrific broth (TB) media.

**Figure 3.9:** SDS-PAGE gel analysis of protein extraction of MsrB3A using a French Press.

**Figure 3.10:** Immobilised metal affinity chromatography (IMAC) purification of His-tagged MsrB3A protein from TB media.

**Figure 3.11:** Desalting of IMAC purified MsrB3A samples.

**Figure 3.12:** Ion exchange chromatography purification of MsrB3A protein.

**Figure 3.13:** Gel filtration chromatography purification of MsrB3A protein from TB media.

**Figure 3.14:** Circular Dichroism (CD) spectra of 1 mg/ml MsrB3A protein in its native state (black curve), when reduced with 1 mM TCEP (blue curve), when treated with 2 mM EDTA (red curve) respectively, in 20 mM HEPES, 150 mM NaCl, pH 7.5 buffer at 298K.

**Figure 3.15:** NMR spectra of MsrB3A protein.

**Figure 4.1:** Multiple sequence alignment of the mature wild-type MsrB3A DNA sequence with the DNA sequence of C126A MsrB3A mutant samples containing the mutation TGC→GCC to substitute cysteine with alanine.

**Figure 4.2:** Multiple sequence alignment of the wild-type MsrB3A amino acid sequence with the translated amino acid sequences of C126A MsrB3A mutant protein showing the substitution.

**Figure 4.3:** DNA profile for C126A MsrB3A mutant DNA sequence (A) 1 and (B) 9, depicting the purity of the highlighted region (GCC), which encodes for alanine residue.

**Figure 4.4:** SDS-PAGE analysis of (A) Protein expression and (B) Protein extraction of C126A MsrB3A mutant protein.

**Figure 4.5:** Immobilised metal affinity chromatography (IMAC) purification of C126A MsrB3A mutant protein.

**Figure 4.6:** Gel filtration chromatography purification of C126A MsrB3A mutant protein.

**Figure 5.1:** SDS-PAGE analysis of (A) Protein expression and (B) Protein extraction for SurA protein.

**Figure 5.2:** Immobilised metal affinity chromatography (IMAC) purification of SurA protein.

**Figure 5.3:** Gel filtration chromatography purification of SurA protein.

**Figure 5.4:** Gel shift assay (mobility of SurA).

**Figure 5.5:** Gel shift assay (functional assay of MsrB3A)-I.

**Figure 5.6:** Gel shift assay (functional assay of MsrB3A)-II.

**Figure 6.1:** HPLC assay (Reference).

**Figure 6.2:** HPLC assay (MsrB3A wild-type).

**Figure 6.3:** HPLC assay (C126A MsrB3A mutant)

**Table 1.1:** Different isoforms of MsrB in mammals.

**Table 2.1:** Nested PCR reaction mixture.

**Table 2.2:** Nested PCR reaction parameters.

**Table 3.1:** Crystallisation screening condition for MsrB3A.

**Table 3.2:** Optimisation of crystallisation screening condition for MsrB3A.

# Acknowledgements

---

It is my great privilege to present this thesis report for which I am grateful to my supervisor, Professor Neil Bulleid for his experienced guidance, valuable suggestions, time and moral support throughout the period of my research and dissertation work. I am also highly obliged to my co-supervisor, Dr. Brian Smith for helping me with my NMR experiments and providing valuable suggestions on how to study the protein structures. I would also like to express my heartiest gratitude to the following people-

- a. Dr. Zhenbo Cao and Dr. Ojore B.V. Oka for their valuable time, suggestions and help in conducting my experiments throughout my research period.
- b. Mrs. Marie Ann Pringle and Mrs. Lorna Mitchell for helping me with my PCR experiments and primer designing.
- c. Dr. Marcel van Lith and Dr. Philip Robinson for providing valuable suggestions during my research.
- d. All the present and past members of Lab 232 for their friendship.
- e. To my mother without whose moral support and financial assistance have helped me to study at the University of Glasgow.

# Author's declaration

---

I hereby declare that all the results presented in this dissertation are the result of my own work, except in places where references are made distinctly to signify the contribution of others, and that no such work has been submitted before by me for any other degree at the University of Glasgow or at any other institution.

---

(Adityo Paul)

# List of abbreviations

---

3D - Three dimensional

µm - micrometre

µg - micrograms

µl - microlitres

CD - Circular dichroism

cm - centimetre

Co<sup>2+</sup> - cobalt ion

C.V. - Column Volume

Cys - cysteine

DTT - Dithiothreitol

EDTA - Ethylene diamine tetra-acetic acid

ER - Endoplasmic reticulum

Fig. - Figure

FPLC - Fast protein liquid chromatography

GE - General electric

H-bonding - hydrogen bonding

HEPES - 4(2-hydroxyethyl)-1-piperazineethane sulfonic acid

His - Histidine

HPLC - High performance liquid chromatography or high pressure liquid chromatography

HSQC - Heteronuclear single quantum coherence spectroscopy

IMAC - Immobilised metal affinity chromatography

IPTG - Isopropyl-β,D-thiogalactopyranoside

KDa - Kilodaltons

LB - Luria-Bertani medium

M - Molar

M9 - Minimal salt medium

Met - Methionine

Met-SO - Methionine sulfoxide

MHz - Megahertz

ml - millilitre

mM- millimolar

*msr* - methionine sulfoxide reductase genes

MsrS- methionine sulfoxide reductases

MsrA - methionine reductase reductase isoform A

MsrB - methionine reductase reductase isoform B

MsrB1 - methionine reductase reductase isoform B type 1

MsrB2 - methionine reductase reductase isoform B type 2

MsrB3(A/B) - methionine reductase reductase isoform B type 3 (isoform A or B)

MsrPQ - methionine reductase reductase isoform PQ reducing system

NADP(H) - Nicotinamide adenine dinucleotide phosphate or Dihydroxy nicotinamide adenine dinucleotide phosphate

nm - nano-metre

NMR - nuclear magnetic resonance

O.D. - optical density

oxd. - oxidised

PCR - Polymerase chain reaction

PDB - Protein data bank

PEG - Polyethylene glycol

psi- pounds per square inch

ROS - reactive oxygen species

RPC - reverse phase chromatography

S-atom - sulphur atom

SDS-PAGE - Sodium dodecyl sulphate- polyacrylamide gel electrophoresis

SelR - Selenoprotein R or mammalian MsrB1

*spp.* - species

TB - terrific broth medium

TCEP - Tris(2-carboxyethyl) phosphine

UV - Ultra-violet

# Chapter 1: Introduction

## General introduction

It is well known that cysteine, homocysteine, methionine and taurine are the sulphur containing amino acids which occur in nature, but only cysteine and methionine (Fig. 1.1) are the two-sulphur containing amino acids that are naturally incorporated into proteins. From the literature, the major functions of cysteine are widely known and studied. Cysteine plays a vital role as active site residues in many enzymes like proteases, phosphatases and proteinases for enzyme catalysis, provides structural support to many proteins via disulphide linkages, or acts as antioxidants to help in redox recycling of glutathione and thioredoxin and many other such vital functions.

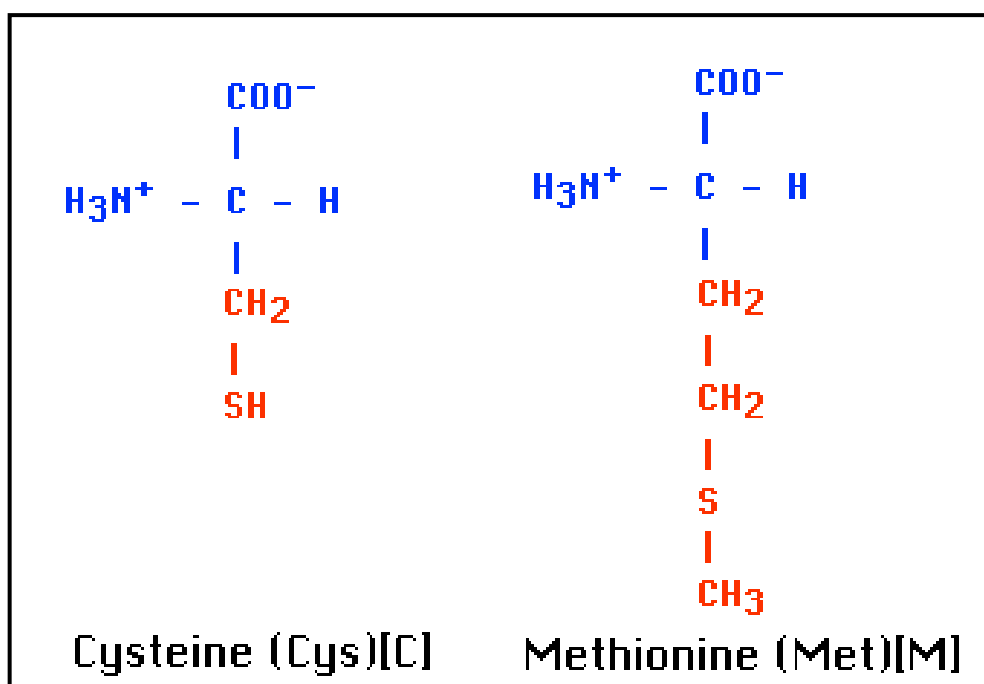


Figure 1.1: Chemical structures of cysteine and methionine residue.

The chemical structure in blue represents the basic amino acid backbone. The alkyl group which defines the amino acid is represented in red. The alkyl group of cysteine contains a sulfhydryl group (-SH), while in methionine the sulphur atom is contained within the alkyl chain.

On the other hand, the most well-known function of methionine is its vital role as initiator of protein synthesis. Yet from studies, it has been found that methionine can also act as an effective antioxidant (Levine et al., 1996) and also helps in regulation of cellular function via redox reactions in the cell (Gonias et al., 1988, Brot and Weissbach, 1991, Vogt, 1995). However, to keep up the role of antioxidant the oxidised methionine must also be recycled back to its reduced state. This is done by a specialised set of enzymes called methionine sulfoxide reductases (Msrs), which are then subsequently reduced either by thioredoxin or glutathione following NADP(H) reducing pathway. The role of methionine to regulate cellular activities are further discussed in the following sections.

## **1.1 Methionine as an antioxidant**

From previous studies, it has been determined that methionine residues present at the protein surface acts like antioxidants protecting the host protein against ROS-induced oxidative stress, thereby, helping the host proteins to retain their activity, for example, in  $\alpha$ -2-macroglobulin the surface bound methionine residues actively become oxidised by ROS-species to protect the critically important tryptophan residue present in the active site, thereby, acting as an antioxidant (Reddy et al., 1989, Reddy et al., 1994). Another good example of the antioxidant function of surface bound methionine residues in proteins are the high density lipoproteins which reduce cholesteryl ester hydroperoxides to alcohols with concomitant oxidation of two methionine residues to methionine sulfoxides (Garner et al., 1998).

However, in the case of unfolded proteins and nascent polypeptides the situation is not the same. From studies, it has been noted that the sulphur atom of methionine residues within unfolded proteins gets readily attacked by reactive oxygen species (Fig. 2), thereby, converting them to methionine sulfoxides (Levine et al., 1996, Nakao et al., 2003). This oxidation, in turn, can cause changes in hydrophobicity of proteins (Chao et al., 1997, Levine et al., 1996, Vogt, 1995) or major conformational changes in the oxidised proteins that may result in dysfunctional or non-functional protein molecules; hindering essential cellular activities (Vogt, 1995, Berlett et al., 1998, Sigalov and Stern, 1998, von Eckardstein et al., 1991). A direct result of the accumulation of dysfunctional or non-functional

proteins is the increase in ROS species, leading to increased oxidative stress. Another direct consequence of prolonged accumulation of oxidised methionine residues is the formation of free radicals, such as methionine sulfone, with greater oxidative potential (Fig. 1.2). In humans, accumulation of such free radicals, especially in the brain, leads to neurodegenerative disorders like Alzheimer's disease, which degrades the nerve cells in the brain (Butterfield and Kanski, 2002, Schoneich, 2002). It has also been predicted that excessive methionine oxidation may result in conformational switches between the  $\alpha$ -helical and  $\beta$ -sheet structures, like those occurring in neurodegenerative disorders like in Alzheimer's disease, Parkinson's disease, etc., (Dado and Gellman, 1993, Nakao et al., 2003). Similar situations have also been reported in genomic studies related to cancer. It was noted that down-regulation of methionine sulfoxide genes within human breast cancer cells, increased the proliferation rates of the cancer cells along with rapid degradation of the extracellular matrix (De Luca et al., 2010).

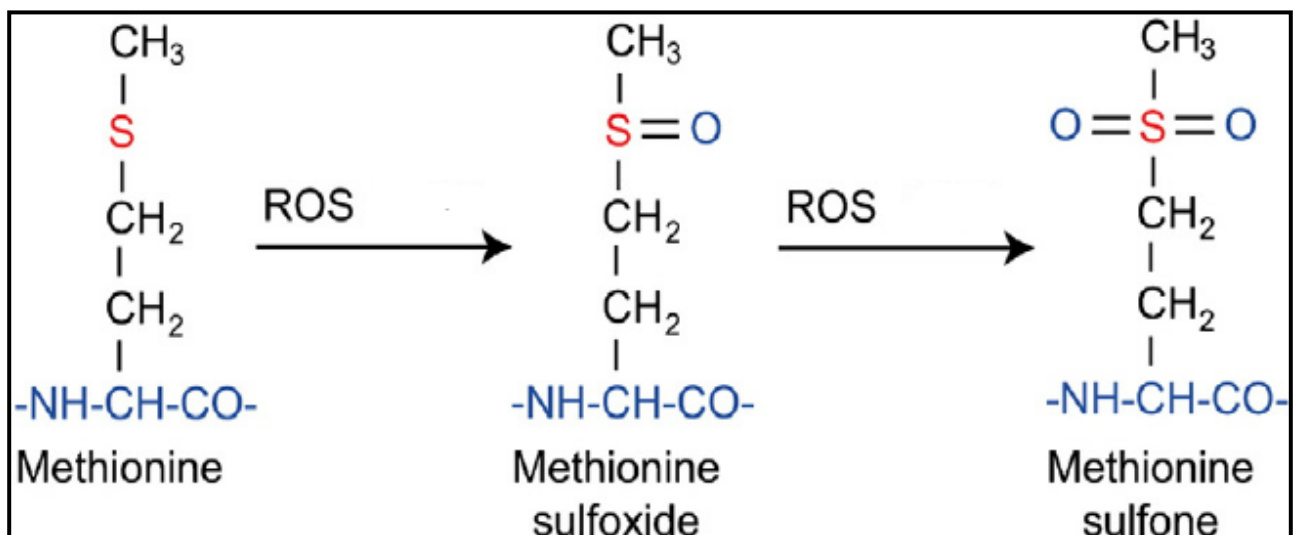


**Figure 1.2:** ROS-induced oxidation of methionine (Met) residue to methionine sulfoxide (Met-SO) and further oxidation by ROS species to methionine sulfone. (Picture is taken from Drazic, 2014)

Met residues on exposure to ROS species gets readily oxidised to Met-SO. At higher concentrations of ROS species and absence of repair mechanism, the Met-SO gets further oxidised to methionine sulfone.

Hence, to recycle the activity of surface bound methionine residues, as well as, to repair and protect the oxidised methionine residues in unfolded proteins and nascent polypeptides, an endogenous group of repair enzymes called methionine

sulfoxide reductases (Msrs) are present within the cells, which actively reduce the methionine sulfoxide to methionine. This helps to restore the antioxidant properties of surface bound methionine residues, as well as, themselves acting as antioxidants, protecting unfolded proteins and nascent polypeptides against ROS-induced oxidative stress. Methionine sulfoxide reductases are discussed further in detail in the next section.

## **1.2 Methionine sulfoxide reductases (Msrs)**

Methionine sulfoxide reductases are a group of oxidoreductase enzymes that act like antioxidants and protect the proteins against ROS induced oxidative stress. Hence, the methionine sulfoxide reductase (Msr) proteins help in regulating protein function, can be involved in signal transduction and prevent accumulation of faulty proteins lowering the chances of further oxidative stress. Any malfunction or down-regulation in the expression of the Msr enzymes results in compromised antioxidant defence, enhanced age-associated disorders such as neurodegeneration and reduced life-span (Moskovitz, 2005).

Whenever methionine residues get oxidised by reactive oxygen species, a racemic mixture of stereoisomers of methionine sulfoxide are formed- methionine-S-sulfoxide and methionine-R-sulfoxide (Schöneich et al., 1993). Due to the formation of two different stereoisomers of methionine sulfoxide, methionine sulfoxide reductases are also grouped into 2 major categories- MsrA which catalyses the reduction of methionine-S-sulfoxide and MsrB which catalyses the reduction of methionine-R-sulfoxide (Fig. 1.3) (Lowther et al., 2002, Grimaud et al., 2001, Moskovitz et al., 2000, Moskovitz et al., 2002, Singh et al., 2001, Stadtman et al., 2003). Besides the two major forms of Msrs, a third group is present in eubacteria and unicellular eukaryotes in minute quantities, which could selectively reduce free methionine-R-sulfoxides (Boschi-Muller and Branlant, 2014). Both these enzymes are vital for protecting the proteins against toxicity of reactive oxygen species by preventing excessive accumulation of oxidised proteins within the cells. Therefore, they are found in almost all living organisms, starting from bacteria to plants and mammals as discussed further in chapter 3.

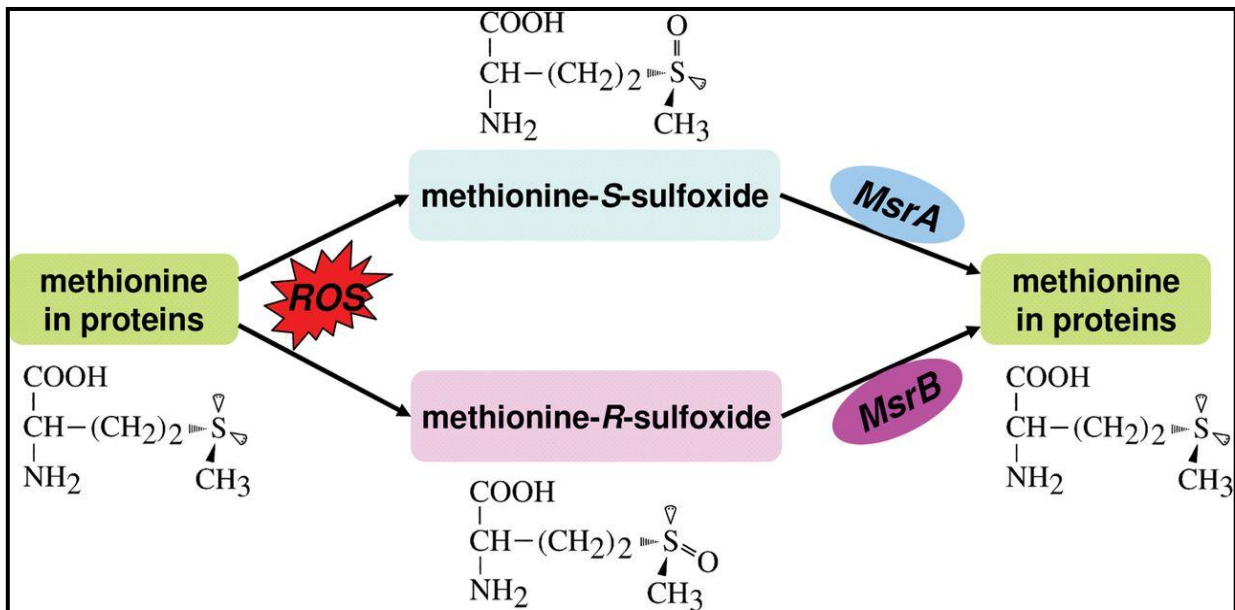


**Figure 1.3: Oxidation of methionine to methionine sulfoxide and reduction pathway of methionine sulfoxide to methionine. (Picture taken from Kim, 2007).**

Free or protein bound methionine residues present on protein surface or in nascent polypeptides are readily oxidised by ROS (shown in spiky red shape) to form mixture of diastereomers of methionine sulfoxide. Methionine-S-sulfoxides stereospecifically reduced by MsrA (shown in solid blue circle), while MsrB (shown in solid purple circle) reduces methionine-R-sulfoxides to methionine, respectively, in the presence of reducing agents like- DTT or thioredoxin reduction system.

Apart from the antioxidant function, Msrs have been shown also to regulate protein function by switching the activation and inactivation of specific methionine residues within protein molecules. For example, the potassium channels of neurons have been seen to be somehow regulated by the expression of MsrA (Ciorba et al., 1997). Similar cases have also been noted in the regulation of calmodulin activity (Sun et al., 1999). Hence, the significance of Msrs in the cells can be well established from above.

### **1.3 Methionine sulfoxide reductases and diseases**

As discussed earlier, any disruption or loss in the enzymatic activity of methionine sulfoxide reductase enzymes has negative impact on cellular functions caused by loss of antioxidant function and disruption in the regulation of activity of

various proteins. From various genomic studies conducted in different organisms, it has been observed that loss or mutation of the *msr* genes leads to increase in oxidative stress, along with reduced life span. In humans, it has been predicted to be indirectly responsible for diseases, such as, neurodegenerative disorders like Alzheimer's disease, Parkinson's disease, etc., and other diseases like cancer, age-related deafness, etc. These have been discussed further in the subsequent paragraphs.

A recent study conducted on the methionine sulfoxide reductase enzymes of important human pathogens such as *E. coli* and *Pseudomonas aeruginosa*, has shown that the novel MsrPQ system played a vital role in protecting important periplasmic proteins (Goemans et al., 2014, Silhavy et al., 2010), which help in the assembly of proteins in the periplasmic space of the bacterial cell wall (Gennaris et al., 2015), against the oxidative stress induced by reactive oxygen species (ROS). Besides identification of new and novel Msrs in bacterial cells, the structure and mode of action of bacterial Msrs have been well determined throughout literature.

But in case of higher organisms, the situation is not the same. This can be attributed to the complexity of the different cellular compartments in the eukaryotic cells owing to difference in the expression of the proteins. Although in higher organisms, not much progress has been made with respect to the structure and mode of action of the different Msrs present in different compartments of the cell, yet from expression studies conducted on yeast, plants, fruit flies (*Drosophila spp.*), and mammalian cells, it was observed that the cells in which the *msr* genes were over-expressed showed greater resistance to ROS-induced oxidative stress and had longer life-spans (Moskovitz et al., 1997, Moskovitz et al., 2002, Kryukov et al., 2002, Kumar et al., 2002, Kwak et al., 2012).

In humans, methionine oxidation can indirectly be associated with many major disorders, especially, neurodegenerative disorders like Alzheimer's disease, Parkinson's disease, Creutzfeldt-Jakob disease, etc. The association of the neurodegenerative disorders with methionine oxidation is discussed as follows.

In Alzheimer's disease, oxidation of the 35<sup>th</sup> methionine residue in the  $\beta$ -amyloid peptide in the brain leads to the process of formation of free radicals at higher rates within the brain's nervous tissue, leading to toxicity and conformational changes

(Butterfield and Kanski, 2002, Schoneich, 2002, Pogocki, 2003, Schöneich et al., 2003). In a study, it was also observed that, with increase in the free radical formation and protein modification of the  $\beta$ -amyloid peptide caused by the reduced activity of MsrA protein in the brain, re-fibrillation of the  $\beta$ -amyloid peptide in presence of metal ions occurs which could further aggravate Alzheimer's disease (Gabbita et al., 1999). In case of Parkinson's disease, methionine oxidation has a more direct effect. The oxidation of methionine residues in  $\alpha$ -synuclein protein causes the protein to lose its fibrillation (Uversky et al., 2002). However, it was also noted that on continued exposure the oxidised methionine residue might get further oxidised to form methionine sulfone (Fig. 1.2), which might lead to the oxidation of other amino acids present in the  $\alpha$ -synuclein protein in presence of metal ions. This in turn would cause re-fibrillation of the  $\alpha$ -synuclein protein, leading to progression of Parkinson's disease (Yamin et al., 2003).

Recent studies have also shown loss of MsrA antioxidant activity leads to aggressive progression of breast cancer and degradation of the extracellular matrix (De Luca et al., 2010). It has also been noted that mutation or inhibition of *msrB* gene in humans may cause deafness, which progresses with age (Ahmed et al., 2011). Hence, it can be said that methionine sulfoxide reductases are essential not only as an antioxidant but also in regulating vital cellular activities performed by the proteins.

As we discussed earlier, methionine sulfoxide reductases occur mainly in 2 broad categories- MsrA and MsrB, whose function, type, distribution and mode of action of the proteins are discussed in detail in the following sub-sections.

#### **1.4 Methionine sulfoxide reductase isoform A (MsrA)**

As stated earlier, methionine sulfoxide reductase isoform A or MsrA are a group of oxidoreductase class of enzymes which can effectively reduce methionine-S-sulfoxide to methionine. But to maintain the antioxidant functions, the Msrs need to be recycled back to their active forms. Hence, different reducing pathways are present in different organisms to recycle the activity of Msrs, such as, by help of

respiratory chain electrons, thioredoxin-thioredoxin reductase-NADPH based reduction pathway, etc. (Gennaris et al., 2015, Gonzalez Porque et al., 1970).

Throughout the literature, the functionality of MsrA, its mode of action and structure are widely known due to the widespread studies conducted on it. As we know from the previous section, Msrs or Msrs coupled with methionine residues in certain cases play important roles in providing antioxidant defence against reactive oxygen species (ROS), as well as, in some cases also help in regulation of protein function or helps in protein folding. Hence, it is quite evident that MsrA should be present throughout the cell compartments in both prokaryotic and eukaryotic cells to promote proper functioning of cellular activities.

Most organisms starting from bacteria to higher organisms like mammals, all contain the MsrA and MsrB genes within their genome. Yet thermophiles that grow in extremely hot locations, lack MsrA, MsrB or both the genes, suggesting that the proteins might be essential for organisms living at moderate temperatures (Kryukov et al., 2002). In bacterial genomes, both the MsrA and MsrB genes are clustered and linked with each other within the bacterial plasmid. Hence, they tend to occur in close association with each other (Kryukov et al., 2002, Ezraty et al., 2005). Yeast (*Saccharomyces cerevisiae*), other unicellular eukaryotes and *Drosophila* spp. Have only a single gene each for both MsrA and MsrB (Kryukov et al., 2002). But plants contain multiple sets of genes for both MsrA and MsrB proteins (Bechtold et al., 2004, Vieira Dos Santos et al., 2005, Novoselov et al., 2002). In mammals, the MsrA protein has only a single gene, but MsrA protein is transported to the cytosol, nucleus or mitochondria depending on the alternative splicing of its N-terminal signal peptide, which is responsible for directing MsrA to its target location (Kim and Gladyshev, 2005b, Black, 2003).

As mentioned earlier, MsrA is the most widely studied methionine sulfoxide reductase enzyme. Hence, its structure and series of reaction which takes place at the active site is known in detail and well understood (Boschi-Muller and Branlant, 2014). Though the mode of action for reducing methionine sulfoxide to methionine is different for different Msr isoforms, but all Msrs follow the same sulfenic acid pathway for the reduction of methionine sulfoxide to methionine, with the help of a catalytic cysteine residue present at the active site of the enzyme (Boschi-Muller et

al., 2000, Boschi-Muller et al., 2005). When the substrate binds at the active site of the enzyme a nucleophilic attack is initiated by the catalytic cysteine on the S-atom of the sulfoxide molecule. Simultaneously, protonation of the oxygen atom in the sulfoxide molecule occurs producing a sulfurane intermediate in the reduction process. This reaction step also serves as the rate-limiting step during the formation of the sulfenic acid intermediate (Fig. 4). From 3D structural analysis of MsrA in complex with substrate, it is found that the oxygen atom of sulfoxide molecule is stabilised by hydrophilic amino acid residues that comprise of a network of H-bonding interactions at the active site of the enzyme (Ranaivoson et al., 2008). This aids in the catalytic activity of active site cysteine and help produce the sulfenic acid intermediate (Boschi-Muller and Branlant, 2014).

## **1.5 Methionine sulfoxide reductase isoform B (MsrB)**

Methionine sulfoxide reductase isoform B or MsrB constitutes the second major group of Msrs which are responsible for the reduction of methionine-R-sulfoxide to methionine. Although, in most organisms, the MsrB is present mainly in a single form in close association with MsrA to reduce the entire racemic mixture of methionine sulfoxide to methionine, the MsrB differ from each other in different organisms and have different amino acid sequences. A common feature of most MsrB is the presence of a conserved resolving cysteine residue present towards the N-terminal of the amino acid sequence (Fig. 3.1). In contrast to the above, MsrB protein exists in three different forms in mammalian cells (Jung et al., 2002, Kryukov et al., 2002, Stadtman et al., 2003). Table 1.1 illustrates the differences in the different types of MsrB isoforms that occur in the mammalian cells. MsrB1 (or SelR) is the MsrB isoform in mammalian cells that is localised within the nucleus and cytoplasm, and is specialised due to the presence of a selenocysteine residue at the active site that helps in the protein function. Due to the presence of the selenocysteine residue, the protein is about 1,000 X more active than Msrs in general (Kim and Gladyshev, 2005a). MsrB2 (or CBS-1) and MsrB3 are the two other MsrB proteins found in mammals and are localised within the mitochondria and endoplasmic reticulum, respectively. However, in humans, the MsrB3 occur in two different isoforms- MsrB3A and MsrB3B- which is a unique feature that is observed in

no other organism. It is also surprising to note that MsrB3B is localised in the mitochondria and is also a unique feature, in which two different MsrB isoforms are present to regulate cell function and antioxidant defence. On the other hand, MsrB3A is localised within the endoplasmic reticulum and is responsible in protecting the nascent and unfolded polypeptides against ROS induced oxidative stress within the endoplasmic reticulum. Hence, the significance of MsrB proteins would be further discussed in detail in chapter 3.

**Table 1.1: Different isoforms of MsrB in mammals.**

<u>MsrB1</u>	<u>MsrB2</u>	<u>MsrB3</u>
Localised in the nucleus and cytoplasm.	Present in the mitochondria.	Localised within the endoplasmic reticulum.
Contains modified amino acid- selenocysteine at the active site and helps in protein function.	Has normal cysteine residue at its active site to help in its function.	Also has cysteine residue at its active site to help in its function.
It is 1000 times more active than other MsrB isoforms, due to the presence of selenocysteine.	Inhibited by substrate concentrations above 1 mM.	Active for substrate concentrations above 1 mM.
Has well defined crystal structure and mode of function has been well established.	Has no definite crystal structure yet, though an NMR ensemble has been determined for mouse MsrB2.	No structural data available till now.
Exists as a single isoform.	Exists as a single isoform.	Exists as a single isoform in most mammals. In humans, it again has two forms- MsrB3A (localised in the ER) and MsrB3B (found in the mitochondria) because of alternative splicing.

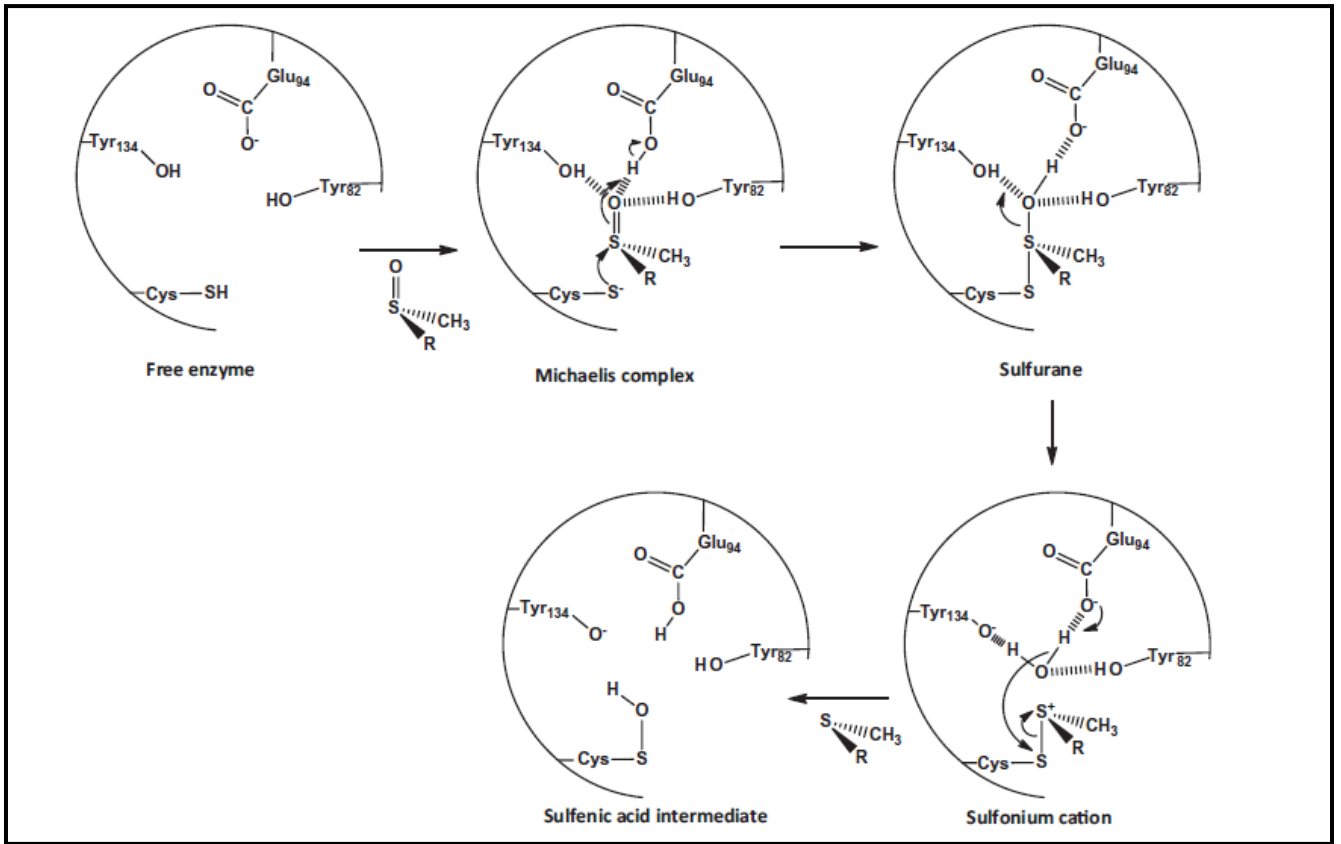


Figure 1.4: Schematic representation of the steps occurring at the active site of MsrA to form the sulfenic acid intermediate. (Picture taken from Boschi-Muller, 2014)

## **1.6 Endoplasmic reticulum (ER)**

The endoplasmic reticulum (ER) is the major site of protein synthesis and protein-folding. It comprises of molecular chaperones which help the proteins to fold, as well as, a well distinguished set of sensory proteins that helps to detect misfolded or unfolded proteins. Due to the presence of high concentrations of unfolded proteins and nascent polypeptides in the ER matrix, it is also a major site for the reactive oxygen species to target such unfolded and nascent polypeptides.

The accumulation of unfolded or misfolded proteins within the ER lumen leads to greater aggregation of intracellular ROS, thereby, enhancing the magnitude of the ER oxidative stress. Consecutively, different repair mechanisms are present within the ER which help to prevent protein misfolding due to ROS induced oxidative stress (Liu and Kaufman, 2003, Zhang and Kaufman, 2008, Malhotra and Kaufman, 2007). Since, the MsrB3A is localised within the ER of the cells in humans, therefore, this thesis aims to study the structure and function of MsrB3A as the primary subject. Another interesting feature which was found in the ER was the absence of MsrA protein or its isoform, suggesting that either MsrB3A is somehow able to reduce both the diastereomers of methionine sulfoxide or an epimerase enzyme is present within the ER which helps in switching of the stereoisomer forms from S- to R-form, thereby, helping to reduce the methionine sulfoxide to methionine.

## **1.7 Objectives of the thesis**

The first objective of the thesis was to clone the mature MsrB3A gene in to recombinant *Escherichia coli* cells and successfully over-express the recombinant MsrB3A protein to gain sufficient quantity of protein for structural and functional studies.

As discussed earlier in Table 1.1, there is no available structure for MsrB3A. Hence, on one hand, this thesis made an attempt to determine the structure of MsrB3A protein. The knowledge gained from the structural experiments might then be used for elucidating the events occurring at the active site of the protein, as well as, to find potential substrates within the immortalised human cell lines which

would provide more detailed outlook into human disorders like Alzheimer's disease and Parkinson's disease.

Consecutively, the another aim of this thesis was to establish whether the 126<sup>th</sup> position cysteine in the MsrB3A protein sequence is an active site cysteine responsible for the protein function. This was based on the hypothesis that the 126<sup>th</sup> position cysteine present in the MsrB3A protein sequence is a resolving cysteine residue involved in the protein function as it coincided with the conserved region containing selenocysteine of the MsrB1 (or SelR) obtained in the multiple sequence alignment (Fig. 3.1) towards the N-terminal of the protein chain. From the literature, it is known that selenocysteine is present at the active site and is responsible for the protein function. Hence, it could be assumed that the 126<sup>th</sup> position cysteine residue in the MsrB3A protein sequence might be a resolving cysteine residue responsible for the protein function. Therefore, using site directed mutagenesis the 126<sup>th</sup> position cysteine residue was substituted for alanine to create a non-functional mutant MsrB3A protein and protein function was determined using gel shift assay and a HPLC assay, respectively, to test the hypothesis.

## **1.8 Outline of the thesis**

The above objectives were addressed in the results chapters which are being divided between chapters 3 to 6 in an orderly manner. Chapter 2 mainly deals with the various techniques that was used in the experiments to determine the results and meet the objectives.

In the first half of chapter 3, we aim for the successful expression, extraction and purification of the recombinant MsrB3A protein in sufficient quantity to be used for structural and functional studies. In the next part of chapter 3, results related with the determination of structure of MsrB3A protein were discussed in detail.

Chapter 4 was based on the creation of 126<sup>th</sup> position cysteine mutant protein (C126A MsrB3A mutant), using site directed mutagenesis. While chapters 5 and 6 deal with the functional assay for MsrB3A protein using a gel shift assay and a HPLC assay, respectively.

The results chapters (chapter 3 to 6) are followed by an conclusions chapter which mainly summarises the entire thesis and also highlights the potential areas of further research which is required to gain more detailed knowledge about MsrB3A

protein, as well as, their role in maintenance of antioxidant defence and regulation of protein function within the endoplasmic reticulum.

# Chapter 2: Materials and methods

---

## **2.1 Expression of human MsrB3A in *E. coli* BL21 (DE 3) Star *pLysS* cells**

The human MsrB3A gene linked with N-terminus 6X His-tag was cloned into a pET21a (+) plasmid. The construct was transformed in *E. coli* BL21 (DE 3) Star *pLysS* cells for expressing the recombinant MsrB3A protein. The transformed *E. coli* cells were then grown in selective Luria Broth (LB) media (Appendix) containing 0.1 mg/ml ampicillin, until the O.D.<sub>600</sub> reached 0.5. The expression of the recombinant MsrB3A protein was then induced by 0.5 mM IPTG, supplemented with 0.5 mM ZnCl<sub>2</sub>. The induction was done for 3 hours at 37°C. The expression was analysed on 15% SDS-PAGE gel. Later, the expression was further increased by growing the transformed *E. coli* cells in selective terrific broth (TB) media containing 0.1 mg/ml ampicillin and then induced for protein expression using 0.25 mM IPTG, supplemented with 0.5 mM ZnCl<sub>2</sub> at 18°C.

After protein expression, the cell culture was centrifuged at 3,836xg for 15 minutes using Beckman JA 14 Fixed Angle Rotor and Beckman Coulter J2-HS centrifuge. The supernatant was disposed aseptically and the cell pellet was re-suspended in 20 ml of 50 mM HEPES 150 mM NaCl and 5 mM Imidazole, pH 7.5 buffer.

### **2.2.1 Protein extraction and purification**

To check for expression on a bench scale, the cell culture after induction of protein expression was treated with 1X BugBuster™ Protein Extraction Reagent from Novagen, as per the procedure provided within the kit, to lyse the recombinant cells to release the intracellular proteins. The cell suspension was then centrifuged at 16,162Xg in a micro-centrifuge and the samples were analysed on 15% SDS-PAGE gel.

The clarified solution (supernatant) was subsequently applied to TALON® SuperFlow™ Affinity Resin from GE Healthcare Life Sciences for the purification of the 6X His-tagged MsrB3A proteins which binds with the Co<sup>2+</sup> ions present in the resin. The purified samples were then collected and analysed on 15% SDS-PAGE gel to check for purity.

The resuspended cells from scaled-up cell cultures were lysed using a French Press at 950 psi pressure. After cell lysis, the cell suspension was centrifuged at 11,424xg for 20 minutes using Beckman JA 17 Fixed Angle Rotor and Beckman Coulter J2-HS centrifuge, following which the supernatant was collected. The supernatant was then filtered using a 0.45 µm Minisart® High Flow syringe filter from Sartorius before being applied to Fast protein liquid chromatography (FPLC).

The following purification steps were involved using the FPLC -

- a. Immobilised metal affinity chromatography (IMAC): - The filtered supernatant was applied to a 5 ml HisTrap™ HP column (from GE Healthcare) that was pre-equilibrated with 50 mM HEPES 150 mM NaCl and 5 mM Imidazole, pH 7.5 buffer (binding buffer). The column was then washed with 50 ml (10 column volumes or 10 C.V.) of the binding buffer to enable binding of the His-tagged proteins while the non-binding contaminants flow out of the column. Elution for His-tagged protein was carried out with increase in gradient of elution buffer (50 mM HEPES 150 mM NaCl and 500 mM Imidazole, pH 7.5) from 0 to 100%, over 50 ml (10 C.V.). The elution buffer was further applied for 15 ml (3 C.V.) at 100% concentration to completely elute out the proteins. The elution samples were then collected in accordance to their absorption peaks at 280 nm and analysed by SDS-PAGE gel electrophoresis.
- b. Desalting: - The IMAC purified samples was then applied to HiPrep™ 26/10 Desalting column to filter out the salt and imidazole present in the samples with a buffer containing 50mM HEPES, pH 8.0 buffer.
- c. Ion exchange chromatography: - The desalted samples were applied to 2X 5 ml Hi-Trap™ Q HP columns which were pre-equilibrated with 50 mM HEPES, pH 8.0 (binding buffer) to purify the protein based on their charge difference. The samples in the column were then washed with 20 ml (2 C.V. each) of binding buffer (50 mM HEPES, pH 8.0) for the proteins to bind. The proteins were eluted out of the column by applying a 50 ml (5 C.V. each) linear concentration gradient for elution buffer (50 mM HEPES and 500 mM NaCl, pH 8.0) by varying the concentration of elution buffer from 0 to 100%. The 100% concentration of elution buffer was maintained for further 10 ml (1 C.V. each) to completely elute out any remaining protein. The elution

samples were then collected in accordance to their absorption peaks at 280 nm and analysed by SDS-PAGE gel electrophoresis.

- d. Gel filtration chromatography: - In this step, the ion exchange purified samples were first collected and concentrated to 1ml as described below in section 2.2.2. After concentration, the samples were purified based on their molecular size using Superdex 200 10/300 GL gel filtration chromatography column. The concentrated sample was applied to the column and subsequently eluted out using 1 C.V. of 20 mM HEPES and 150 mM NaCl, pH 7.5 buffer (elution buffer). The purified samples in which the peaks were observed at 280 nm UV absorbance were analysed by SDS-PAGE gel electrophoresis.

### **2.2.2 Protein concentration and quantification**

The purified protein was concentrated using a Sartorius VivaSpin Turbo 15 Concentrator (MWCO= 10,000 Da), at 3,000xg until the desired volume. After concentration, the protein solution was collected in an Eppendorf tube.

Absorbance of the concentrated protein solution was measured at 280 nm with the help of L-Vis plate and the SpectroStar Nano UV Spectrometer. The protein concentration was quantified using the Beer- Lambert's law.

The extinction coefficient ( $\epsilon$ ) for MsrB3A and SurA protein was calculated using the ProtParam bioinformatic tool by providing the amino acid sequence for the respective proteins as input.

$$\begin{aligned}\epsilon \rightarrow \text{Extinction coefficient at 280 nm (M}^{-1}\text{cm}^{-1}) &= 13,325 \text{ M}^{-1}\text{cm}^{-1} \text{ (for MsrB3A)} \\ &= 29,450 \text{ M}^{-1}\text{cm}^{-1} \text{ (for SurA)}\end{aligned}$$

After protein quantification, the solution was aliquoted and flash frozen using liquid nitrogen.

### **2.3.1 Spectroscopic techniques: CD spectroscopy**

The concentrated MsrB3A protein aliquots were diluted to a concentration of 1 mg/ml using 20 mM HEPES 150mM NaCl, pH 7.5 buffer. The samples were then examined at near and far UV ranges to determine the secondary structure and

folding under different conditions (native, in the presence of 1 mM TCEP for reducing conditions and 1 mM EDTA to strip off any metal ions linked to the MsrB3A protein).

### **2.3.2 Spectroscopic techniques: NMR spectroscopy**

$^{15}\text{N}$  labelled MsrB3A was expressed by growing the recombinant *E. coli* cells in M9 liquid medium (Appendix) containing  $^{15}\text{NH}_4\text{Cl}$  salt. The recombinant MsrB3A protein was extracted, purified and concentrated as per the methods described in section 2.2.1 and 2.2.2.

NMR spectra was acquired from 600  $\mu\text{l}$  sample of 0.372 mM MsrB3A protein in 50 mM sodium phosphate and 100 mM NaCl buffer at pH 6.5, containing 10%  $\text{D}_2\text{O}$ . The sample was added to a clean NMR tube (*Wilmad 535-pp7*) using an NMR pipette for measuring the NMR spectra. The NMR spectra was measured at 298 K using 600 MHz *Bruker Avance III* HD NMR spectrometer equipped with TCI cryo-probe. The  $^{15}\text{N}/^1\text{H}$  HSQC sequence spectra was obtained using the Fast HSQC (FHSQC) pulse program (Mori et al., 1995). The  $^{15}\text{N}/^1\text{H}$  HSQC spectra data was collected for 5 minutes.

### **2.3.3 Protein crystallisation**

Purified protein samples at 40 mg/ml and 20 mg/ml were added to four 96 well crystallisation screening plates- *Morpheus*<sup>®</sup> HT-96, Structure Screen 1 & 2 HT-96, *JCSG-plus*<sup>TM</sup> HT-96, and *PACT premier*<sup>TM</sup> designed by Molecular Dynamics in sitting drop configuration using the robotic arm (Cartesian Robot). The plates were then sealed using clean transparent plastic and were incubated at 16 °C for 3 months. The plates were observed every week under a microscope to check for any crystal growth in the 3 months of incubation period.

Optimisation of crystallisation conditions was made by varying the salt concentration in the crystallisation buffer over different pH range in a 24 well crystallisation condition screening plate. Again, the crystallisation plates were sealed using clean transparent plastic and incubated at 16 °C for 3 months.

### 2.4.1 Site directed mutagenesis: conversion of 126<sup>th</sup> position cysteine to alanine

Synthetic DNA primers- Forward Primer (5'-GACCGTAAACGCTACGCCATCAATAGCGCGGCC-3') and Reverse Primer (5'-GGCCGCGCTATTGATGGCGTAGCGTTTACCGGTC-3') incorporating the mutation of cysteine to alanine (TGC→GCC) in the 126<sup>th</sup> position of the amino acid sequence of MsrB3A were designed and ordered from Agilent Technologies. The primers were then amplified using pET21a (+) plasmid containing the mature gene sequence of the MsrB3A wild-type DNA as the parental DNA strand, ACCUZYME™ DNA polymerase from Bioline Reagents Ltd. and nested-PCR for 25 cycles. The PCR mixture and nested PCR cycle parameters used are represented by Table 2.1 and 2.2, respectively.

**Table 2.1: Nested PCR reaction mixture.**

<u>Constituents</u>	<u>Control (µl)</u>	<u>Sample (µl)</u>
10X AccuBuffer	5	5
ACCUZYME™ DNA polymerase (2.5 U/µl)	1	1
25 mM MgCl <sub>2</sub>	2	2
Primers (conc.= 25 ng/µl)	0	5
<i>Forward primer</i>		
<i>Reverse primer</i>		
10 mM dNTP mix (dATP, dGTP, dCTP, and dTTP)	1	1
DMSO	1	1
dsDNA template (conc.= 50 ng/µl)	1	1
ddH <sub>2</sub> O	39	34
<b>Total reaction volume (µl)</b>	<b>50</b>	

**(Note-** The DNA polymerase enzyme is added at the end just before starting the PCR reaction.)

**Table 2.1: Nested PCR reaction parameters.**

<u>Step</u>	<u>Temperature (°C)</u>	<u>Time (mins.)</u>	<u>Cycles</u>
Melting	95	5	1
Melting	95	0.5	30
Annealing	60	0.5	
Elongation	72	1	
Elongation	72	10	1

The resulting amplified PCR product was then treated with *Dpn I* restriction endonuclease to digest the methylated parental DNA strand. The *Dpn I* digested product was then transformed into *E. coli* XL1 Blue super-competent cells. The transformed cells were then grown in selective LB Agar media containing 0.1 mg/ml ampicillin for 24 hours at 37 °C.

Colonies were selected from the culture plate and marked. The selected colonies were then grown over-night in selective LB broth containing 0.1 mg/ml ampicillin at 37 °C. The plasmid DNA was then isolated from the over-night cultures using alkaline lysis method for DNA purification. The DNA purity and concentration was measured using L-Vis plate, the SpectroStar Nano UV Spectrometer and MARS Data Analysis software. Cysteine to alanine (TGC→GCC) mutation was verified by DNA sequencing services provided by GATC Biotech.

### **2.5.1 Gel shift assay**

The transformed *E. coli* BL 21 (DE3) cells harbouring the pKD 11 plasmid containing the SurA gene linked with 6X-His-tag at the C-terminus (obtained by request from Prof. J.F. Collet) was first grown in selective terrific broth media containing 0.1 mg/ml kanamycin up to an O.D.<sub>600</sub> of 0.5. Protein over-expression was induced using 0.5 mM IPTG and was carried out for 16 hours at 20°C. The SurA protein was then purified and concentrated similarly to the steps involved in MsrB3A purification as described in section 2.2.1 and 2.2.2.

An aliquot of the purified and concentrated SurA was first diluted to 200  $\mu\text{M}$  and was then oxidised *in-vitro* by incubating the protein with 100 mM  $\text{H}_2\text{O}_2$  at 30°C for 3 hours (Gennaris et al., 2015) in 20 mM HEPES and 150 mM NaCl, pH 7.5 buffer. The  $\text{H}_2\text{O}_2$  was then removed from the solution by gel filtration chromatography using a pre-equilibrated 5 ml HiTrap™ Desalting column and AKTAPurifier FPLC system. Equilibration of the column was done using 20 mM HEPES and 150 mM NaCl, pH 7.5 buffer. The purified samples were pooled together, concentrated and quantified as described in section 2.2.2

*In-vitro* repair of oxidised SurA was done by incubating 20  $\mu\text{M}$  SurA with different concentrations of MsrB3A at 37°C for one hour, in the presence and absence of 10 mM DTT. Following the treatment with MsrB3A the samples were analysed on 10% SDS-PAGE gels to check the mobility of SurA.

### **2.5.2 High pressure liquid chromatography (HPLC) assay**

The HPLC assay was done according to the procedure described by (Kumar et al., 2002). 0.2 mg/ml MsrB3A (wild-type) or C126A MsrB3A mutant protein was mixed with 0.5 mM dabsylated methionine sulfoxide and added to 50 mM NaCl, 20 mM DTT and 20 mM Tris, pH 7.0 buffer in a total sample volume of 0.2 ml. The reaction mix was incubated at 30°C for 5, 10, 20 and 30 minutes and then quenched using 0.5% SDS.

The reaction products were then separated based on their hydrophobicity using reverse phase chromatography (RPC) column (Sephasil peptide C18 5 $\mu\text{m}$  ST 4.6/250 column) and ÄKTAmicro™ Chromatography system. The reaction mix was then applied to the column which was pre-equilibrated with 5 C.V. of 100 mM sodium acetate and 30% acetonitrile, pH 6.0 buffer (binding buffer) and subsequently washed with 1 C.V. of binding buffer to enable binding of reaction products. The reaction products were separated from each other by the help of a concentration gradient over 2 C.V. of 100 mM sodium acetate and 70% acetonitrile, pH 6.0 buffer (elution buffer) from 0 to 100% of the elution buffer. The 100% concentration of elution buffer was maintained for further 1 C.V. to completely elute out any remaining products. Sample mix containing only dabsylated methionine and dabsylated methionine sulfoxide respectively, were used as reference to determine the retention time.

# Chapter 3: MsrB3A: Protein expression, purification and structural studies.

---

## 3.1 Introduction

Methionine sulfoxide reductases occur in two major forms- MsrA and MsrB, which catalyses the reduction of methionine sulfoxide to methionine, thereby, acting as antioxidants within the cell in response to oxidative stress. MsrA catalyses reduction of methionine-S-sulfoxide while MsrB catalyses the reduction of methionine-R-sulfoxide.

The structure and function of MsrA is widely known and well-characterised due to the studies performed on it (Brot et al., 1981, Tête-Favier et al., 2000, Vouquier et al., 2003, Hansel et al., 2002, Antoine et al., 2003, Yermolaieva et al., 2004). Although MsrB proteins have been identified quite recently, not much is known about them. However, MsrB has been reported to occur in various organisms from bacteria to mammals in different forms localised to specific organelles (Grimaud et al., 2001, Jung et al., 2002, Kryukov et al., 2002, Kumar et al., 2002, Olry et al., 2002, Etienne et al., 2003, Spector et al., 2003).

In mammals, only a single gene encoding for the MsrA protein is present in mitochondria, cytosol and nucleus (Kim and Gladyshev, 2005b, Kim et al., 2010, Vouquier et al., 2003). In contrast to MsrA, MsrB is encoded by three different genes (B1-B3) and targeted to different cellular compartments (Kim and Gladyshev, 2004b). MsrB1 is present in the nucleus and cytosol, while MsrB2 is targeted to the mitochondria. MsrB3 is found within the endoplasmic reticulum of most mammals. But in humans, an isoform of MsrB3 is also targeted to the mitochondria which is a unique feature that has not been observed in any other mammal.

As stated in the previous paragraph, MsrB3 occurs in two different isoforms in humans, namely, MsrB3A and MsrB3B. This is due to the alternative splicing of the first exon, which results in contrasting N-terminal signal peptides. Although recent studies conducted on mice have found that the mouse MsrB3 contains consecutive ER and mitochondrial targeting signals in the N-terminus, the MsrB3 protein is only localised within the ER (Kim and Gladyshev, 2004a). Another reason for the presence

of two isoforms of MsrB in the mitochondria in humans could be due to the inhibition of MsrB2 at high substrate concentrations, while MsrB3B can then help reduce methionine-R-sulfoxide at concentrations higher than 1 mM (Kim and Gladyshev, 2004b).

Although, both MsrA and MsrB perform the same function of methionine sulfoxide reduction to methionine, they both differ from each other with respect to their mode of action and arrangement of the amino acids at the active site of the protein. Previous studies conducted on MsrA has helped to understand and establish the mode of action of MsrA to reduce methionine-S-sulfoxide to methionine (Dokainish and Gauld, 2013). But the same cannot be said for MsrB. Although the mode of function for MsrB has been found for some human pathogens such as *Neisseria gonorrhoeae* (Robinet et al., 2011), by sequence analysis (Fig. 3.1) it has been observed that the MsrB sequences in various organisms differ from each other, hence differing in their mode of action, arrangement of amino acids at their active site, substrate binding capacity and localisation to specific regions of the cell. For example, MsrB1 in eukaryotic cells possess a seleno-cysteine (represented by codon 'U', in the amino acid sequence) in its active site that helps in the reduction of methionine-R-sulfoxide (Kim and Gladyshev, 2004b, Kim and Gladyshev, 2007). But MsrB2 and MsrB3 do not contain any specialised amino acid but only cysteine residue at the active site to reduce methionine-R-sulfoxide (Kim and Gladyshev, 2005a), as observed in the sequence alignment. It is also noted that all MsrB have  $Zn^{2+}$  as co-factors which are strongly bound. From sequence analysis it is observed that all MsrB has two  $Zn^{2+}$  binding sites in the form of -CXXC- motifs (Kumar et al., 2002), as a characteristic feature.

As stated earlier, the structure and function of MsrA have been well defined throughout literature for most organisms, owing to the widespread study in the past two decades. But the same cannot be said for MsrB. Although, MsrB structures have been found for some micro-organisms, particularly human pathogens like *N. gonorrhoeae*, *N. meningitides* (Ranaivoson et al., 2009, Lowther et al., 2002) etc., they lack homology to the mammalian enzymes. In case of mammals, only the structure for mouse MsrB1 has been determined (Aachmann et al., 2010). Though, recently the crystal structure of human MsrB1 (PDB id- 3MAO) and structure of mouse MsrB2 (NMR Ensemble; PDB id- 2L1U (*unpublished data by Aachmann et al.*),

2010)) has been determined. The structure of MsrB3 protein remains unknown. Hence, we shall also try to focus on finding the structure for human MsrB3A. Since MsrB3A has been recently identified, its mode of action and structure are still unknown. Hence, our primary aim is to express the MsrB3A gene within recombinant *E. coli* to generate optimal quantities of MsrB3A protein, which can then be utilised to study the structure and mode of action. Secondly, we shall conduct structural experiments using circular dichroism (CD) spectroscopy, nuclear magnetic resonance (NMR) spectroscopy and X-ray crystallography to determine the structure of MsrB3A.

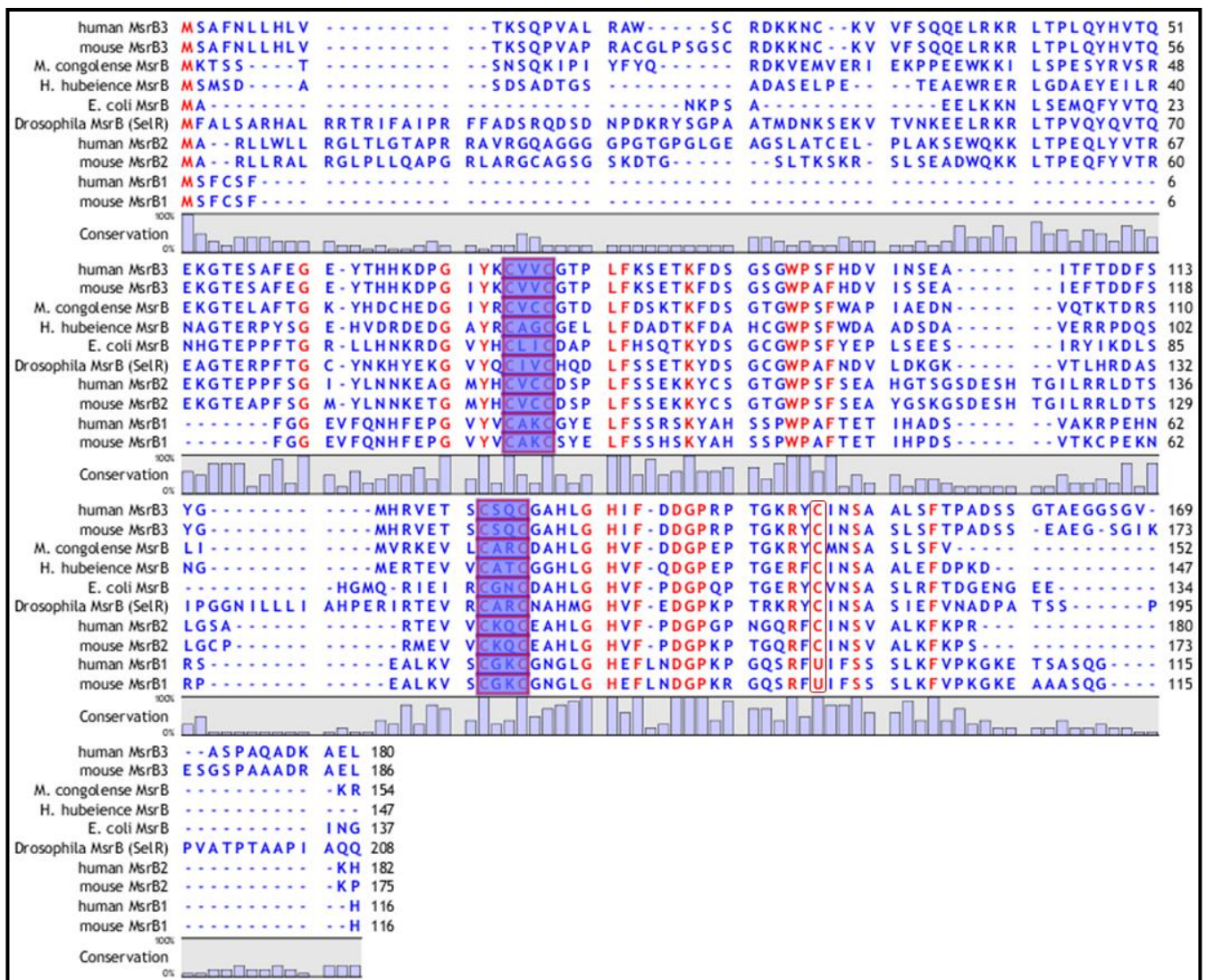


**Figure 3.1: Multiple sequence alignment of amino acid sequences of different MsrB variants from various organisms.**

Alignment of full length sequences of MsrB proteins from humans {GenBank Accession Number- EAW97151.1 (MsrB3), AAH18030.1 (MsrB2), NP\_057416.1 (MsrB1)}; mouse {GenBank Accession Number- EDL24407.1 (MsrB3), EDL08114.1 (MsrB2), NP\_001333597.1 (MsrB1)}; *Drosophila melanogaster* MsrB (GenBank Accession Number- Q8INK9.3); *Escherichia coli* MsrB (GenBank Accession Number- EMZ45312.1); *Methanobacterium congolense* MsrB (GenBank Accession Number- SCG84896.1); *Halobacterium hubeiense* MsrB (GenBank Accession Number- CQH58376.1). The amino acid residues coloured in blue have the least conserved residue domains, while the amino acid residues coloured in red are the most conserved residue regions. The highlighted region represents the Zn<sup>2+</sup> binding motif region -CXXC- which remains conserved throughout the different sequences shown. The conserved cysteine region marked by the red rounded edged rectangle represents the functional cysteine as described by Kumar, 2002. (Note- Both MsrB3A and MsrB3B have identical protein sequences, except that MsrB3B has an extension at its N-terminal generated by alternative splicing.)

## **3.2 Results**

### **3.2.1 Protein expression, extraction and purification**

To study human MsrB3A in detail, the human MsrB3A gene lacking the N-terminal signal peptide for the endoplasmic reticulum was replaced by 6X His-tag sequence and cloned into pET 21a (+) plasmid. The construct was used for transformation in *E. coli* BL 21 (DE 3) Star *pLysS* cells to express the recombinant MsrB3A protein, as stated in section 2.1. The first step was to check whether the protein could be expressed on a bench scale using the recombinant bacteria. The transformed *E. coli* cells were grown in selective LB broth media and protein expression was induced using IPTG. Protein expression was then visualised on 15% SDS-PAGE gel (Fig. 3.2). Lanes 1 and 2 represent the cell samples before and after protein induction by IPTG. As we can observe from lane 1 that the recombinant *E. coli* cells have a band in between the 17 and 22 KDa region. This could be due to “leaky expression” of the recombinant MsrB3A protein as recombinant *E. coli* BL 21 (DE 3) Star cells are known to have some basal level expression of the gene of interest as stated by the vendor. Another factor contributing to the leaky expression of recombinant MsrB3A protein is the absence of chloramphenicol in the culture media which was essential for the activation of pLysS plasmid to produce the T7 lysozyme which then reduces the basal level or leaky expression of the gene of interest in uninduced cells. Hence, from lane 2 we observe a slightly thicker band indicating there is a small increase in the quantity of protein expressed after the induction of protein expression by IPTG, which might be due to the expression of MsrB3A. Another evidence of the leaky expression would be the expression of the C126A MsrB3A mutant protein which is discussed in detail in Chapter 4. Upon comparison of the elution curves of gel filtration chromatography in Fig. 3.7, 3.13 and 4.6, it can be clearly observed that the peak always lie in the same region.

Following protein expression, the cell culture was treated with BugBuster™ 10X Protein Extraction reagent from Novagen to extract the recombinant MsrB3A protein. The extraction sample, pellet and supernatant (clarified solution) were then analysed on 15% SDS-PAGE gel (Fig. 3.3). Lane E represents the extraction cell

culture sample after treatment with BugBuster™ 10X Protein Extraction reagent. Lanes P and Sn represents the pellet and supernatant respectively. Lane P has a faint band, while lane Sn has a thick band when compared with lane E. This suggests that the expressed recombinant MsrB3A protein is soluble.

Subsequently, the clarified solution (supernatant) obtained from the protein extraction was applied to TALON® Superflow™ Affinity Resin which contains  $\text{Co}^{2+}$  ions conjugated to the beads, for purification of the recombinant MsrB3A protein. The 6X His-tag present in the protein construct binds strongly with the metal ion present in the bead, hence, separating the recombinant protein from the unwanted proteins. Following purification, the purified samples obtained were analysed on 15% SDS-PAGE gel as shown in Fig. 3.4. Lane Sn represents the clarified solution (supernatant), lanes FT and W represents the 1<sup>st</sup> and 2<sup>nd</sup> washes respectively. Lane El represents the elution.

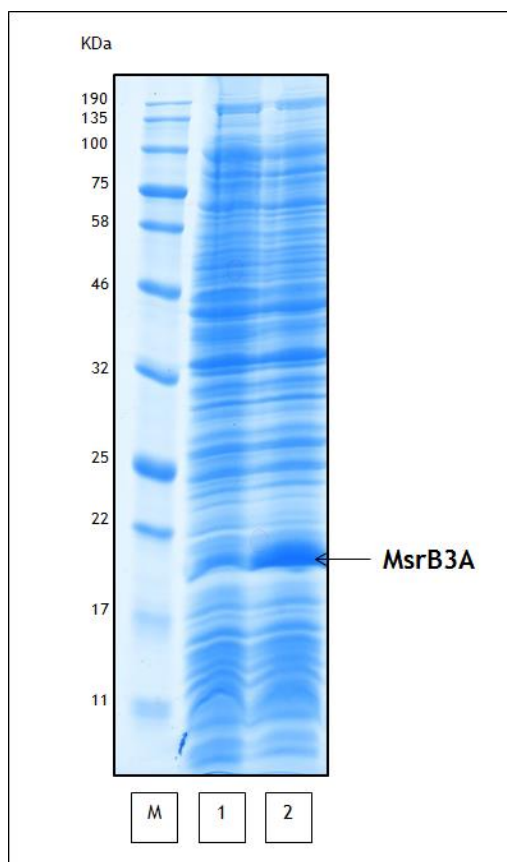


**Figure 3.2: SDS-PAGE gel analysis of MsrB3A protein expression in Luria-Bertani (LB) broth media.**

Lane M represents the Blue pre-stained Protein Standard as reference of protein size. Lane 1 represents the sample from cell culture just before induction of protein expression using IPTG, while lane 2 represents the sample from cell culture after 3 hours of induction of protein expression using IPTG.

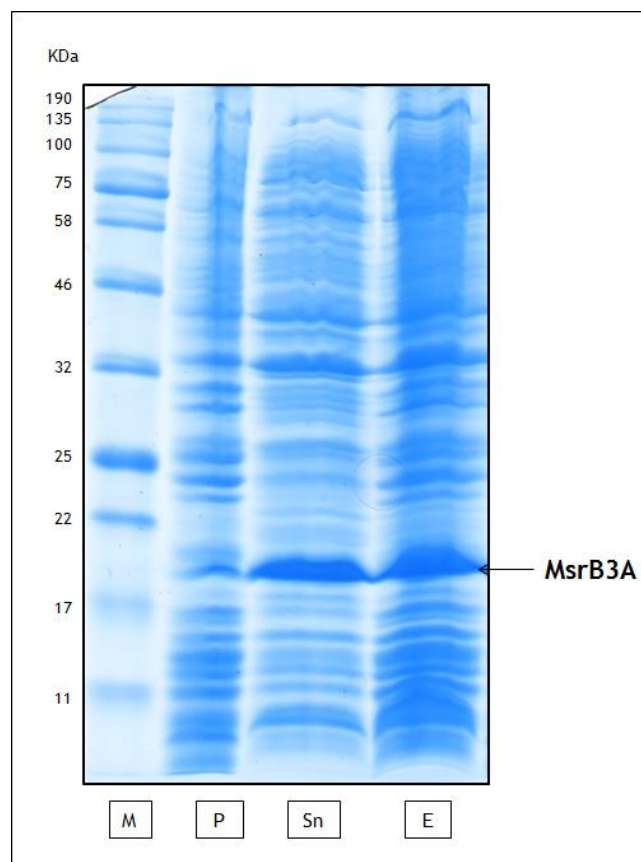


**Figure 3.3: SDS-PAGE gel analysis of MsrB3A protein extraction using BugBuster™ Protein Extraction Reagent.**

Lane M represents the Blue pre-stained Protein Standard as reference of protein size. Lanes P and Sn represent the pellet and supernatant samples obtained after the cell extract was centrifuged at 16,162xg in a micro-centrifuge, respectively. Lane E represents extraction sample after cell culture was treated with 1X BugBuster™ Protein Extraction Reagent.

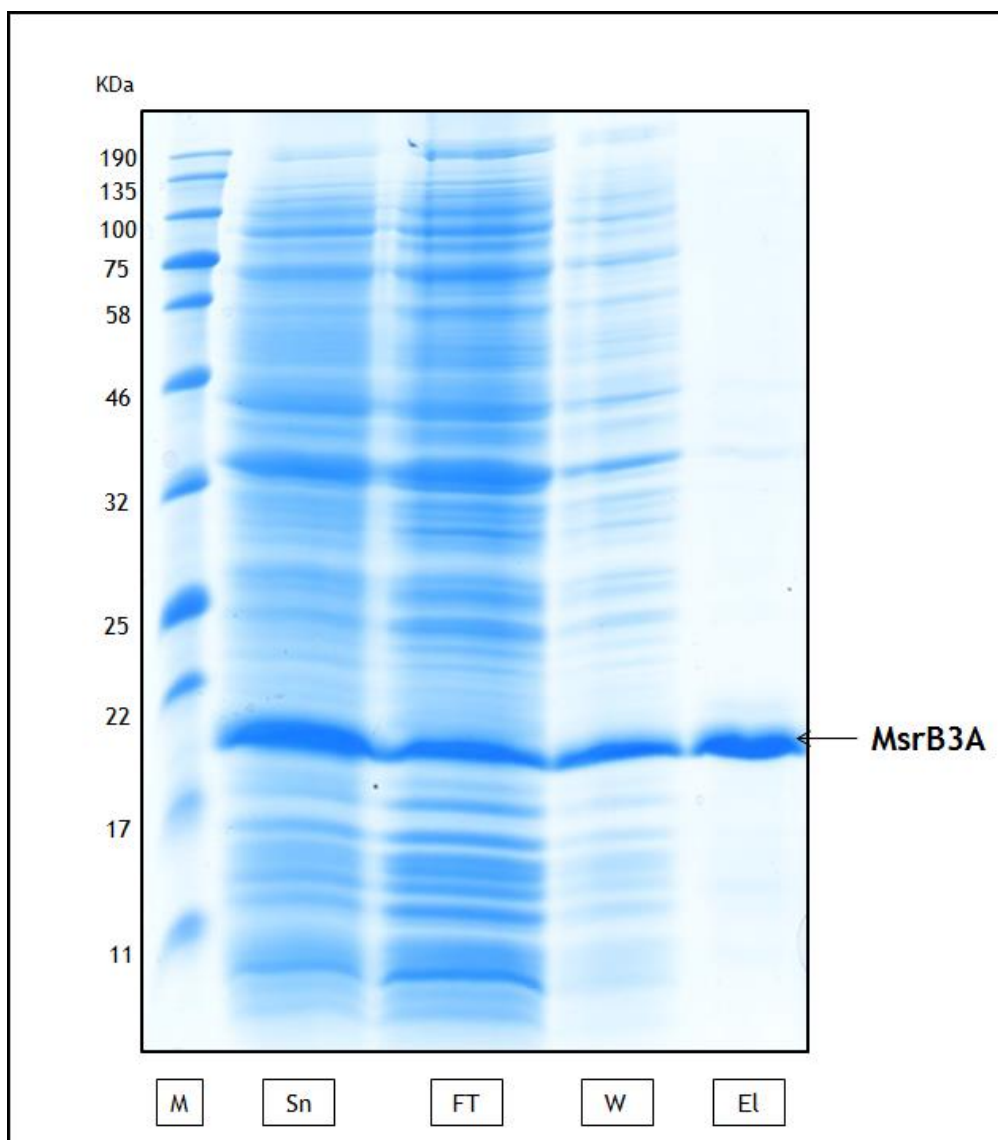


**Figure 3.4: SDS-PAGE gel analysis of MsrB3A protein purification using Talon® Superflow™ Affinity Resin.**

Lane M represents the Blue pre-stained Protein Standard as reference of protein size. Lane Sn represents the non-purified supernatant (clarified solution) sample which is applied to the Talon® Superflow™ Affinity Resin. Lane FT and W represent the sample from the flow-through or 1<sup>st</sup> wash and 2<sup>nd</sup> wash of the resin using 50 mM HEPES 150mM NaCl, pH 7.5 (wash) buffer. Lane EL represents the purified MsrB3A protein eluted out when 50 mM HEPES 150 mM NaCl 500 mM imidazole, pH 7.5 (elution) buffer was applied to the resin.

A clear, single and distinct band was obtained in the elution. This meant that the protein could be purified easily using immobilised metal affinity chromatography (IMAC). We can also notice in figure 8 that MsrB3A is also present in lanes FT and W. This could be due to the saturation of the beads which can bind with the protein suggesting that the concentration of protein was far greater than the quantity of binding sites available.

Hence, after successfully establishing that the recombinant MsrB3A can be expressed on bench scale, the protein expression was scaled up by growing the recombinant *E. coli* in 2 l of selective LB broth media and then inducing protein expression using IPTG. Cell lysis was carried out using a French Press, as discussed in section 2.1. The cell lysate was then analysed using 15% SDS-PAGE gel (Fig. 3.5). As we can observe in lane P, there is still some amount of MsrB3A present in the pellet, indicating that the procedure was not efficient and a fraction of the cells was not lysed. However, the supernatant obtained after centrifugation of the cell lysate was first filtered as discussed in Section 2.2.1, before applying to 5 ml HisTrap™ HP column for IMAC chromatography using the AKTA FPLC system for purification. After purification using IMAC chromatography, the eluted proteins were analysed on a 15% SDS-PAGE gel (Fig. 3.6). As we can observe, the samples in lane 5 to 7 contains considerable amount of the recombinant MsrB3A. Yet small quantities of contaminant proteins were still present in the samples. Hence, to get a better purification the samples were pooled together and concentrated as discussed in section 2.2.2. Following concentration, the sample was applied to Superdex 200 10/300 GL gel filtration chromatography column for further purification based on molecular size difference (Fig. 3.7). The eluted samples obtained after purification, were analysed on a 15% SDS-PAGE gel to check for purity. Typical concentrations achieved after protein expression in LB broth media and purification ranged between 0.5 to 0.6 mg/l of culture. Although, we could successfully isolate the recombinant MsrB3A, the quantity of protein required was not sufficient to perform structural studies and analysis of protein functions. Hence, purifying the recombinant protein on multiple occasions might result in unwanted variations in the results obtained on analysis. It is better to get a standard result from a single purified sample.

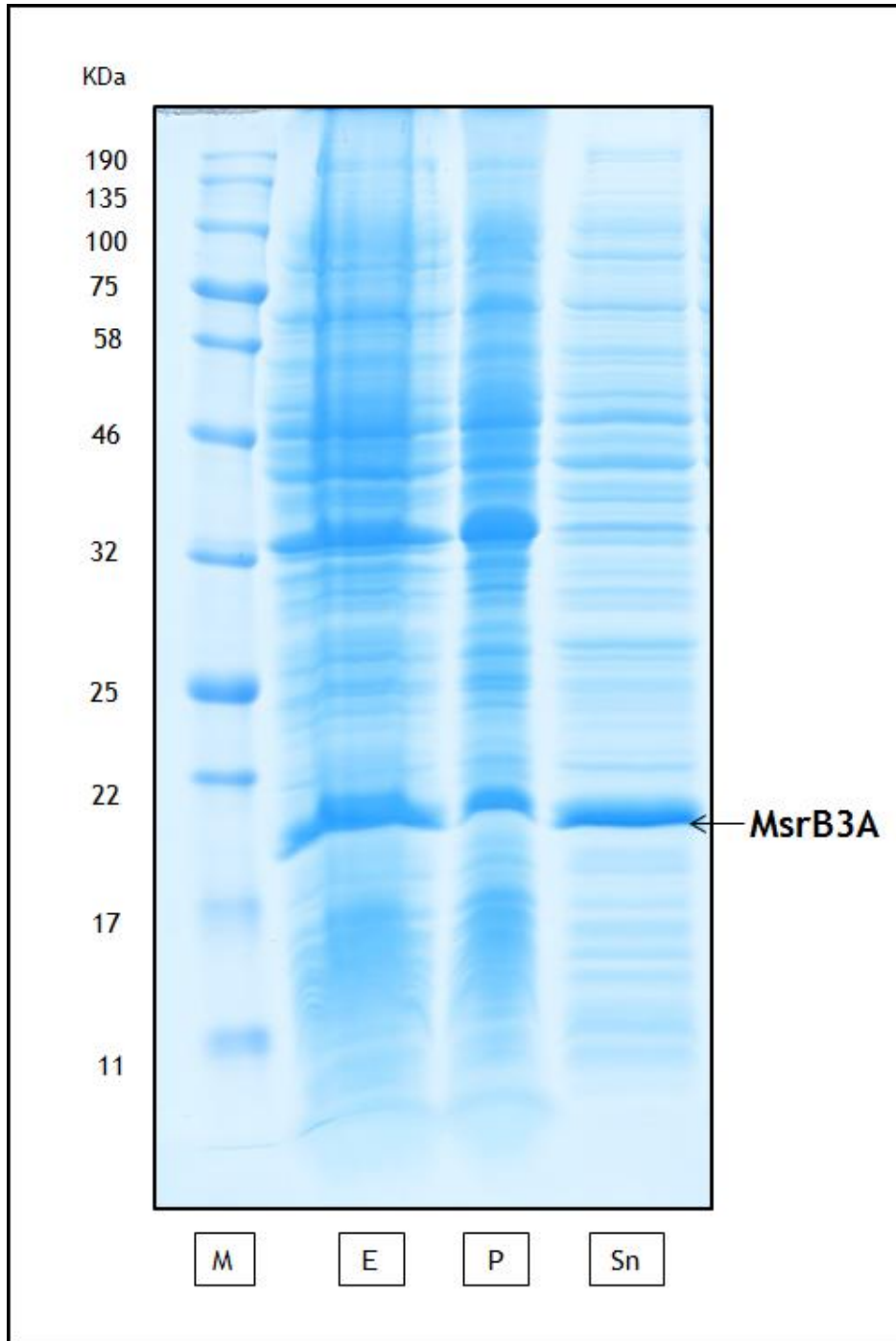


**Figure 3.5: SDS-PAGE gel analysis of MsrB3A protein extraction using French Press.**

Lane M represents the Blue pre-stained Protein Standard as reference of protein size. Lane E represents extraction sample after cell lysis using the French Press. Lanes P and Sn represents the pellet and supernatant samples obtained after the cell extract was centrifuged at 3,836Xg for 15 minutes using Beckman JA 14 Fixed Angle rotor and Beckman-Coulter J2-HS cold centrifuge, respectively.

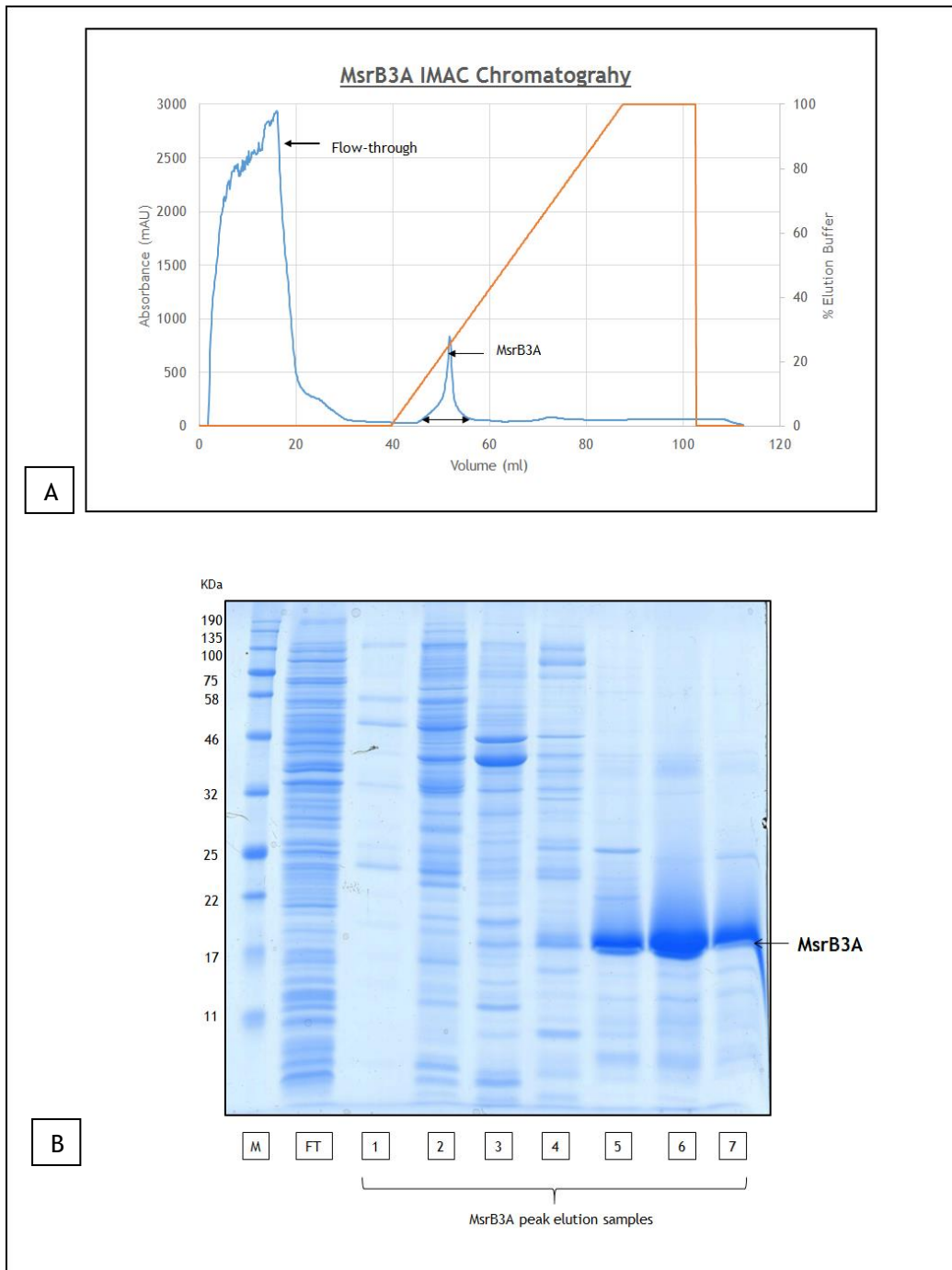


**Figure 3.6: Immobilised metal affinity chromatography (IMAC) purification of His-tagged MsrB3A protein.**

- A.** The graph represents a typical FPLC Chromatogram obtained using a 5 ml HisTrap™ HP affinity column for purifying the 6X His-tagged MsrB3A protein. The bound protein was eluted by using a 500 mM Imidazole concentration gradient represented by the orange curve.
- B.** SDS-PAGE gel analysis of the samples of the purified fractions collected from the peaks obtained as shown in A. Lane M represents the Blue Protein Standard used as reference. Lane FT represents the sample from the flow through elution peak, while lanes 1 to 7 represent the fractions collected from the MsrB3A elution peak in successive order and is represented in the graph by an arrow.

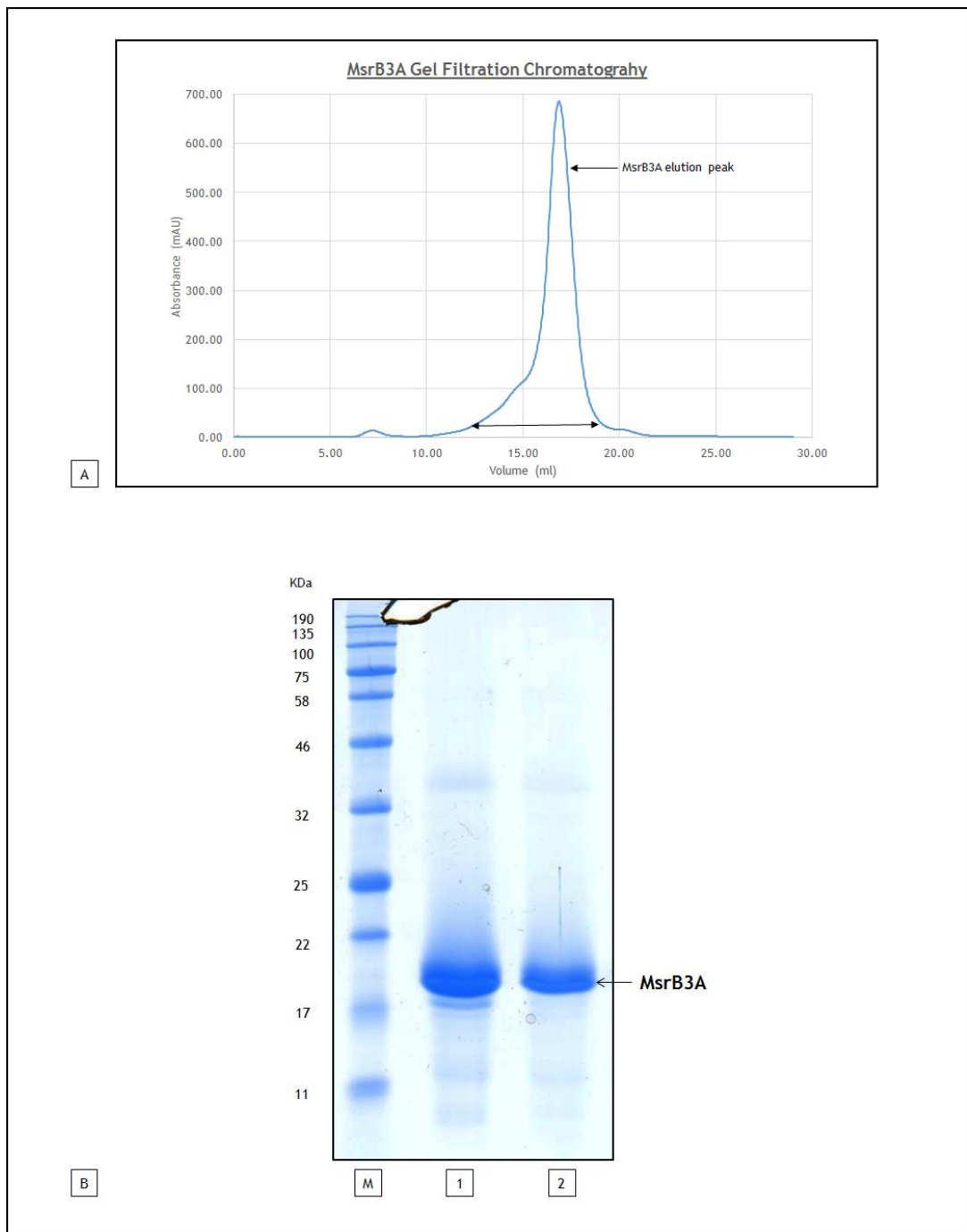


**Figure 3.7: Gel filtration chromatography purification of MsrB3A protein.**

- A. The graph represents a typical FPLC Chromatogram obtained using a Superdex 200 10/300 GL gel filtration chromatography column for purifying the MsrB3A protein based on the principle of molecular size exclusion.
- B. SDS-PAGE gel analysis of the samples of the purified fractions collected from the peaks obtained as shown in the graph. Lane M represents the Blue Protein Standard used as reference. Lanes 1 and 2 represent the samples from the fractions collected from the MsrB3A elution peak in successive order and is represented in graph by an arrow.

To generate sufficient quantity of recombinant MsrB3A protein for further experiment, the recombinant *E. coli* cells were grown in selective terrific broth (TB) media, as described in section 2.1. Although, the recombinant *E. coli* cells were first grown at 37°C like in LB media, once the OD<sub>600</sub> of 0.5 was reached, the protein induction was carried out at 18°C using IPTG. The primary reason for this was to have a slower growth rate while keeping the cells in their logarithmic phase of growth. Protein expression was checked by analysing the samples on a 15% SDS-PAGE gel (Fig. 3.8). As we can observe from the thick band in lane 2, the quantity of recombinant protein increased after induction of protein expression using IPTG with respect to lane 1 (before protein induction). The cells were then lysed using French Press for protein extraction and the cell lysates were analysed using 15% SDS-PAGE gel (Fig.3.9).

In the same way as the earlier purification, the clarified solution (filtered supernatant) was applied to the 5 ml HisTrap™ HP column for IMAC chromatography using the AKTA FPLC system. As we can observe from the elution profile in Fig. 3.10, the quantity of recombinant protein purified was almost three times more than the amount produced when LB media was used. The only drawback of the increase in concentration of recombinant protein was the increase in concentration of contaminant proteins. Hence, we removed the unwanted proteins based on surface charge difference using ion exchange chromatography (Fig. 3.12). As the elution buffer for IMAC chromatography consisted of 150mM NaCl and imidazole, we first removed the salt from the samples, using the HiPrep™ 26/10 Desalting column and 50 mM HEPES pH 8.0 buffer, as discussed in section 2.2.1. This was done to avoid interference from the salt molecules with the resin of the ion exchange column. Fig. 3.11 illustrates the elution profile of desalting step. The desalted samples were then applied to the 5 ml Hi-Trap™ Q HP columns to purify the recombinant MsrB3A protein from the contaminants based on the surface charge difference (Fig. 3.12). The fractions collected after ion exchange chromatography were then concentrated up to 1 ml as described in section 2.2.2. The concentrated sample was then applied to the Superdex 200 10/300 GL gel filtration chromatography column to obtain recombinant MsrB3A protein with high degree of purity (Fig. 3.13, panel B). As we can also observe in panel A, there are two elution peaks which occur adjacent with each other. This could be due to formation of dimers which may result in the formation of a separate peak.

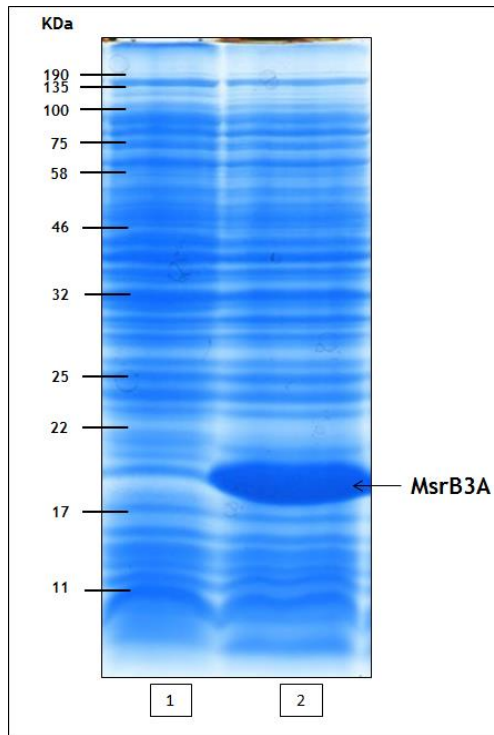


**Figure 3.8: SDS-PAGE gel analysis of MsrB3A protein expression in terrific broth (TB) media.**

Lanes 1 and 2 represent the samples from cell culture just before and after over-night induction of protein expression using IPTG.

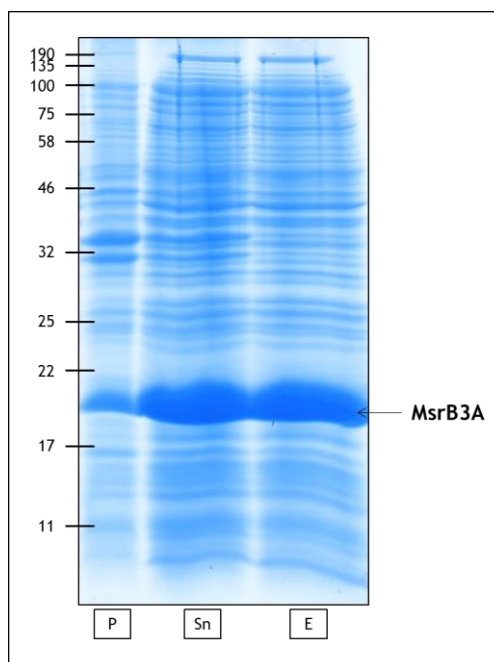


**Figure 3.9: Protein extraction of MsrB3A using French Press.**

Lane E represents extraction sample after cell lysis using French Press. Lanes P and Sn represent the pellet and supernatant samples obtained after the cell extract was centrifuged at 3,836xg for 15 minutes using Beckman JA 14 Fixed Angle rotor and Beckman Coulter J2-HS cold centrifuge, respectively.

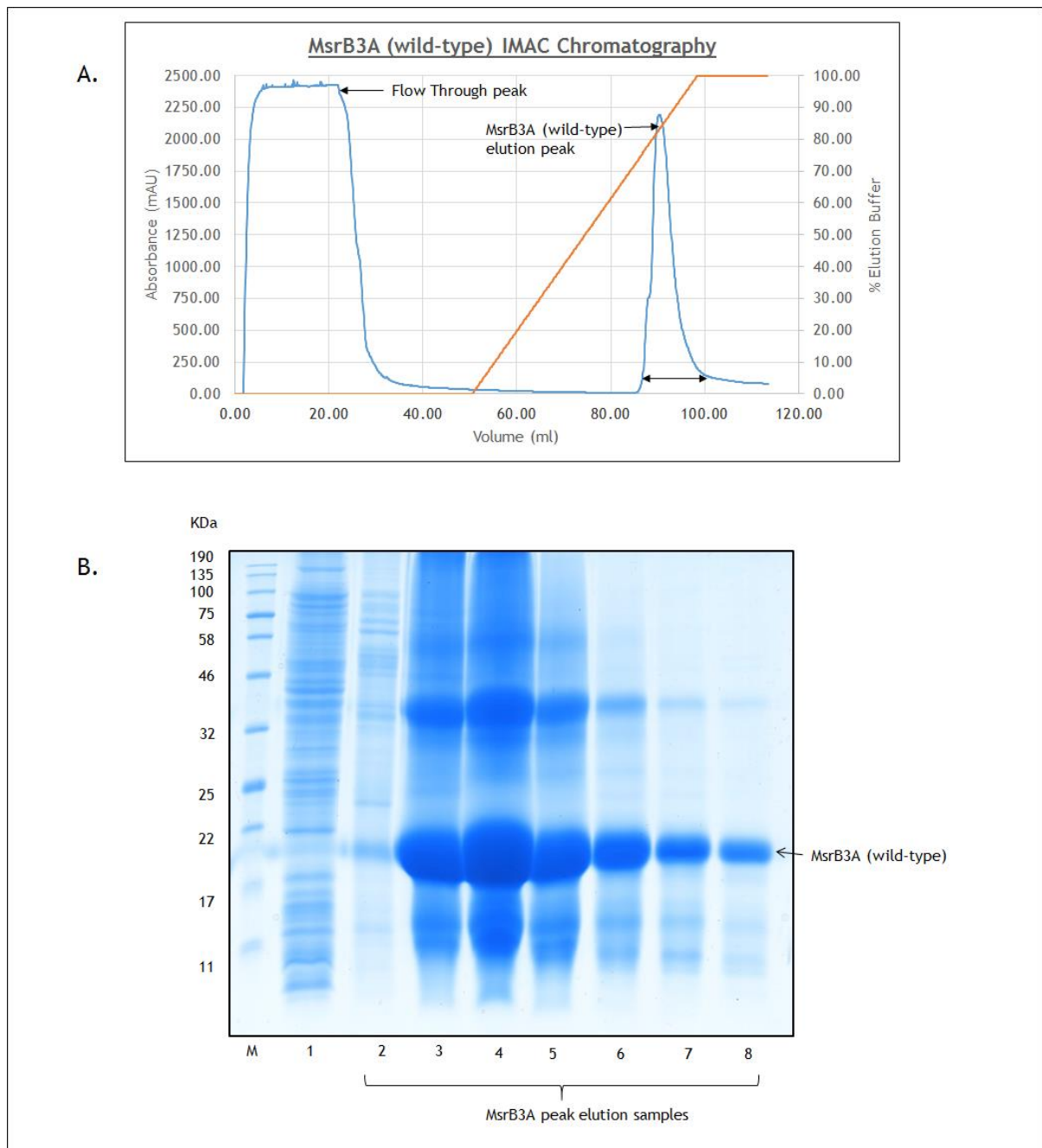


**Figure 3.10: Immobilised metal affinity chromatography (IMAC) purification of 6XHis-tagged MsrB3A protein.**

- A.** Typical FPLC chromatogram obtained by using a 5 ml HisTrap™ HP affinity column. The bound protein was eluted using a 500 mM Imidazole concentration gradient represented by the orange curve.
- B.** SDS-PAGE gel analysis of the samples of the purified fractions collected from the peaks obtained as shown in A. Lane 1 represents the sample from the flow through elution peak, while lanes 2 to 8 represent the samples from the fractions collected from the MsrB3A elution peak in successive order.

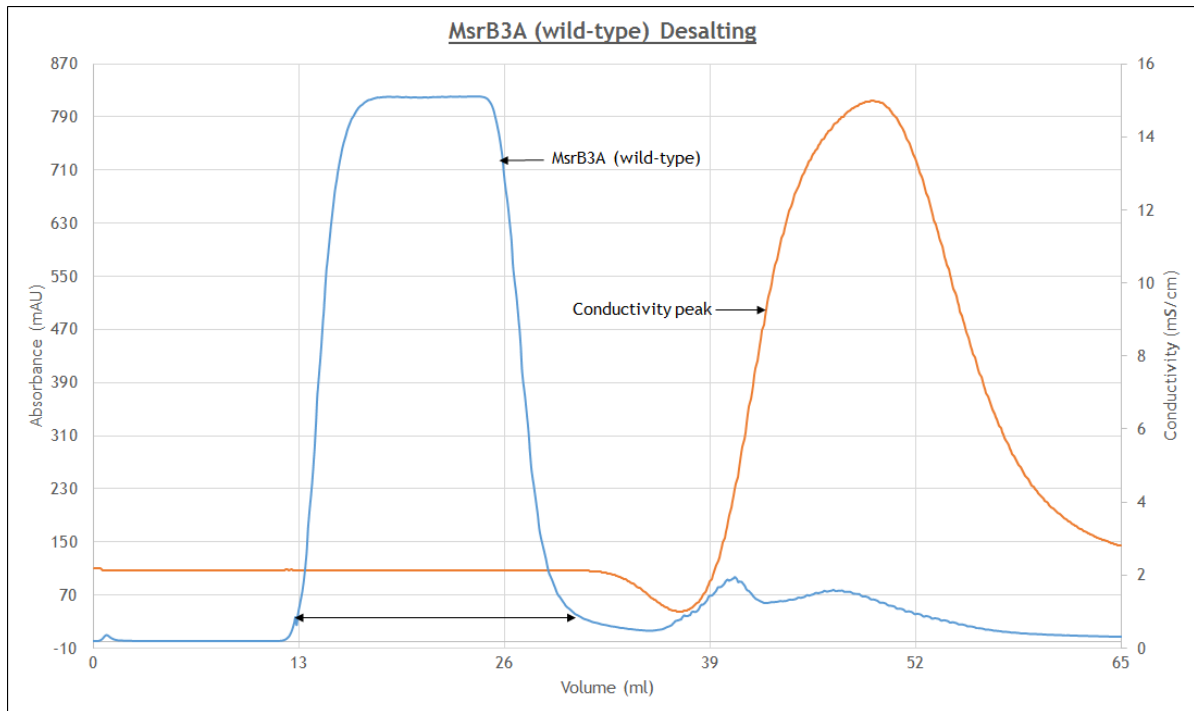


**Figure 3.11: Desalting of IMAC purified MsrB3A samples.**

The graph represents a typical FPLC Chromatogram obtained using HiPrep 26/10 Desalting column. As shown in the graph, the blue curve represents the absorbance of the protein sample at 280 nm and the salt represented by the conductivity curve in orange separated from the protein.

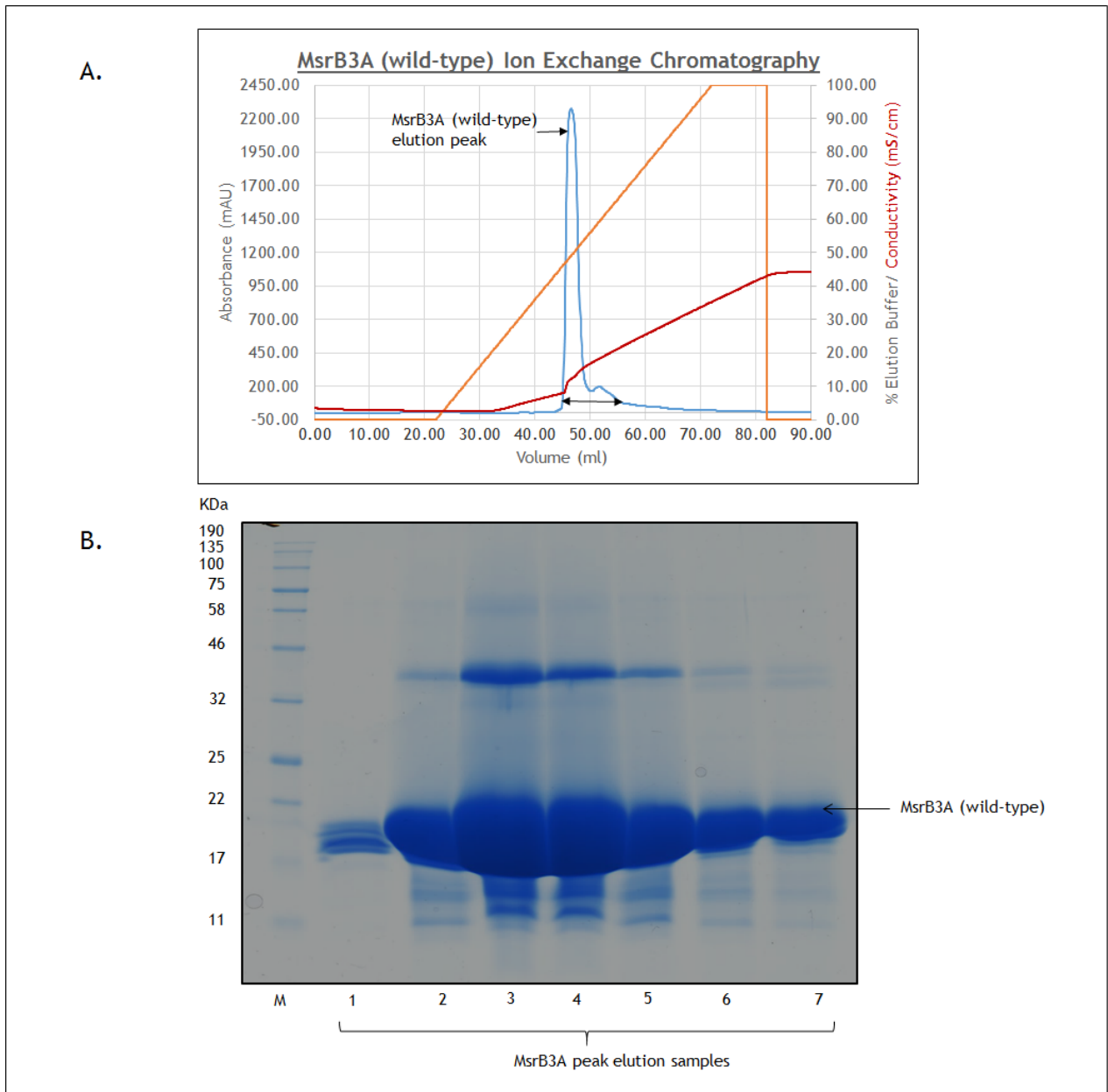


**Figure 3.12: Ion exchange chromatography purification of MsrB3A protein.**

- A.** Typical FPLC chromatogram obtained using two 5 ml Hi-Trap™ Q HP columns for purifying the MsrB3A protein based on the surface charge difference. The bound protein was eluted by using a 500 mM NaCl concentration gradient represented by the orange curve and increase of salt concentration is shown by the conductivity curve in red.
- B.** SDS-PAGE gel analysis of the samples of the purified fractions collected from the peaks obtained as shown in graph. Lanes 1 to 7 represent the samples from the fractions collected from the MsrB3A elution peak in successive order and is represented in the graph by a double headed arrow.

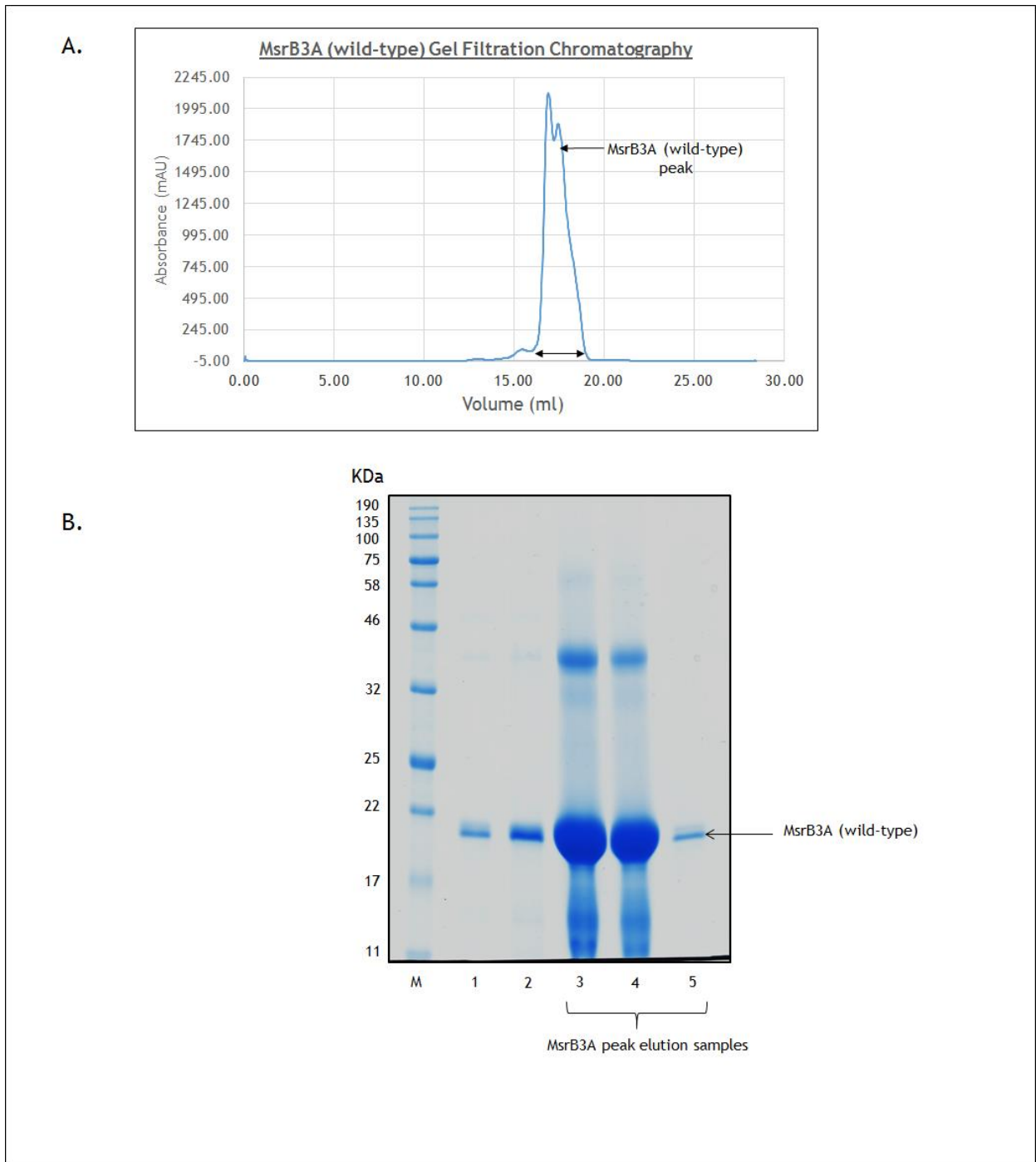


**Figure 3.13: Gel filtration chromatography purification of MsrB3A protein.**

- A.** Typical FPLC chromatogram obtained using a Superdex 200 10/300 GL gel filtration chromatography column for purifying the MsrB3A protein based on the principle of molecular size exclusion.
- B.** SDS-PAGE gel analysis of the samples of the purified fractions collected from the peaks obtained as shown in the graph. Lanes 3 to 5 represent the samples from the fractions collected from the MsrB3A elution peak in successive order and is represented in graph by an arrow.

A noticeable feature in all the purification steps is the presence of a distinct band between the 32 and 46 kDa marker bands, suggesting the formation of dimers by the recombinant MsrB3A protein. The net quantity of recombinant MsrB3A protein achieved after purification and concentration ranged between 4.5 to 6.0 mg/l of culture.

### 3.2.2 Structural studies of recombinant MsrB3A

We approached determining the overall secondary structure of purified MsrB3A using circular dichroism (CD) spectroscopy, followed by an evaluation of the tertiary structure using NMR (nuclear magnetic resonance) spectroscopy and protein crystallography (X-ray crystallography) experiments as described below.

#### 3.2.2.1 CD spectroscopy

Fig. 3.14 represents the CD spectral graphs of MsrB3A protein taken under different conditions, obtained at far UV (panel A) and near UV (panel B) respectively. As we can clearly observe from the figure that the recombinant MsrB3A protein has a folded structure owing to the strong CD signals giving rise to the curves obtained in the figure at both far and near UV range respectively.

In both panels A and B, the native state of the MsrB3A protein is represented by the black curve. The blue curve represents MsrB3A protein after reduction using 1mM TCEP, as TCEP is a better reagent for sample analysis in CD spectroscopy (Getz et al., 1999). The red curve represents the MsrB3A protein after treatment with 1mM EDTA. We use EDTA as a chelating agent to extract the  $Zn^{2+}$  ions present in MsrB3A protein, to study the effect of change in its secondary structure.

Secondary structure estimation of MsrB3A protein was done for the native MsrB3A protein (black curve) using CONTIN/LL CD data analysis software (Sreerama and Woody, 2000, Provencher and Glöckner, 1981).

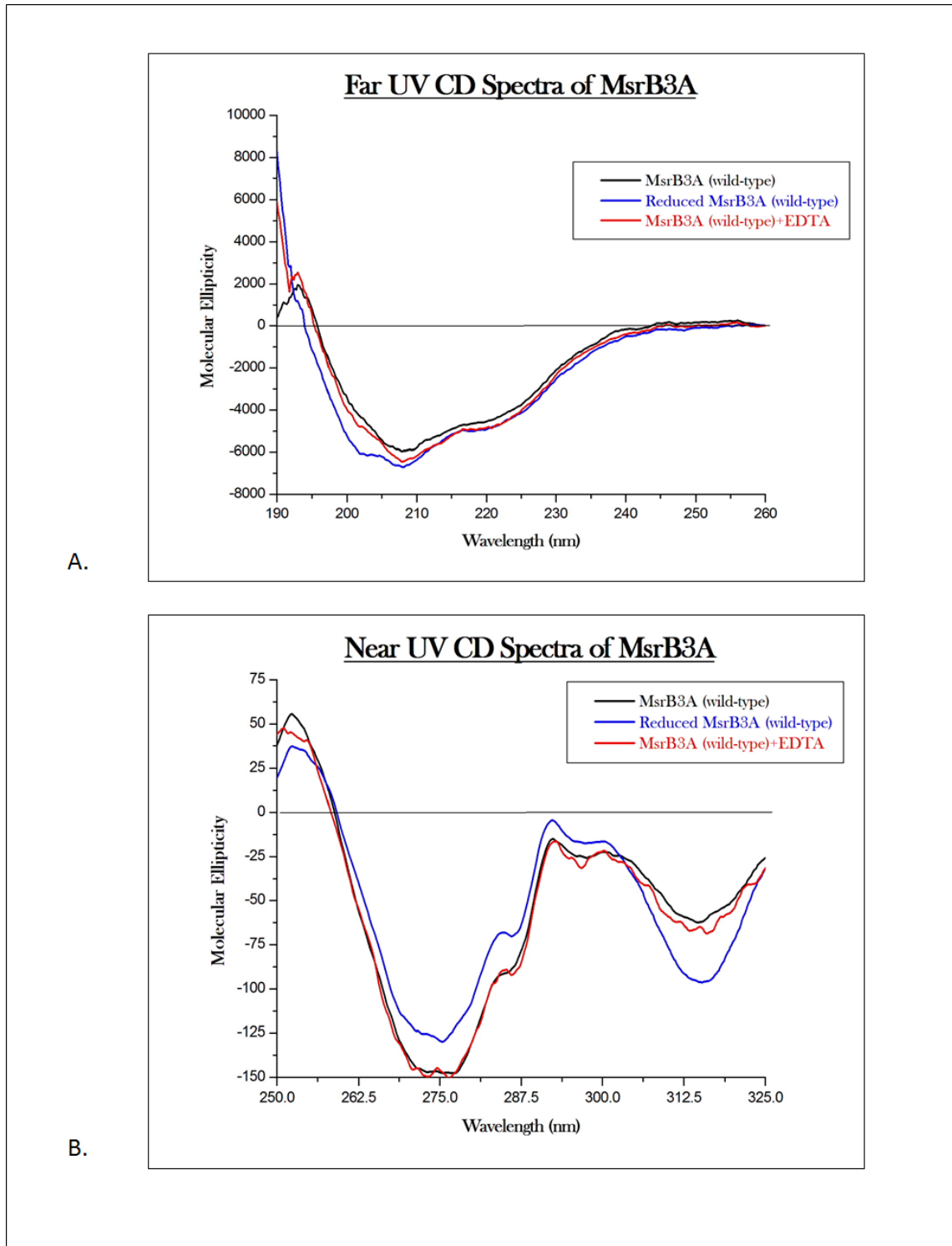


**Figure 3.14: CD Spectra of 1 mg/ml MsrB3A protein in its native state (black curve), when reduced with 1 mM TCEP (blue curve) and when treated with 2 mM EDTA (red curve) respectively, in 20 mM HEPES 150 mM NaCl, pH 7.5 buffer at 298 K.**

- A. Panel showing the far UV CD spectra of MsrB3A protein.
- B. Panel showing the near UV CD spectra of MsrB3A protein.

Accordingly, it was predicted to have 35%  $\beta$ -sheeted structure, 11%  $\alpha$ -helix, 21% turns and 33% random secondary structures. This result is also in accordance with the structural composition predicted (Kryukov et al., 2002) for most MsrB proteins.

In panel A, we observe that the reduced MsrB3A protein (blue curve) has a slightly broader and deeper peak between the 195 to 215 nm region in comparison to its native state for the far UV CD spectra, indicating partial unfolding of the protein structure.

The same is also depicted in panel B for near UV spectra. We observe decrease in the positive peak between 250 to 260 nm and negative peak between 260 to 300 nm range, followed by the increase in the negative peak in the 300 to 325 nm region of the near UV region in comparison to the native MsrB3A protein (black curve). It can be said that EDTA treatment had no effect on the secondary structure of MsrB3A, as the red curve (EDTA treated MsrB3A protein) for the near UV region superimposed with the black curve. The slight discrepancies observed in the red curve could be the interference caused by EDTA.

### 3.2.2.2 NMR spectroscopy

Fig. 3.15 represents the two dimensional [ $^1\text{H}$ ,  $^{15}\text{N}$ ]-HSQC spectra obtained for MsrB3A using 600 MHz *Bruker Avance III* HD NMR spectrometer at 298 K. As we can observe in panel A, the contours are spread over a wide region, indicating that the MsrB3A protein has a folded structure. Each series of contour in the spectra represents a peak for the backbone H-N pair in each amino acid residue.

Panel B represents the 2D [ $^1\text{H}$ ,  $^{15}\text{N}$ ]-HSQC spectra obtained when MsrB3A was reduced (represented by blue contour) using 1 mM TCEP. The NMR spectra for the reduced MsrB3A was then compared with the native MsrB3A by super-imposing the 2D [ $^1\text{H}$ ,  $^{15}\text{N}$ ]-HSQC spectra of native MsrB3A (represented by the red colour) over the NMR spectra of the reduced MsrB3A. Chemical shifts could be clearly observed, across various lengths, along with emergence

of new contour regions. This suggests a change in conformation possibly due to unfolding in the reduced MsrB3A protein. This support the results obtained by CD spectroscopy.

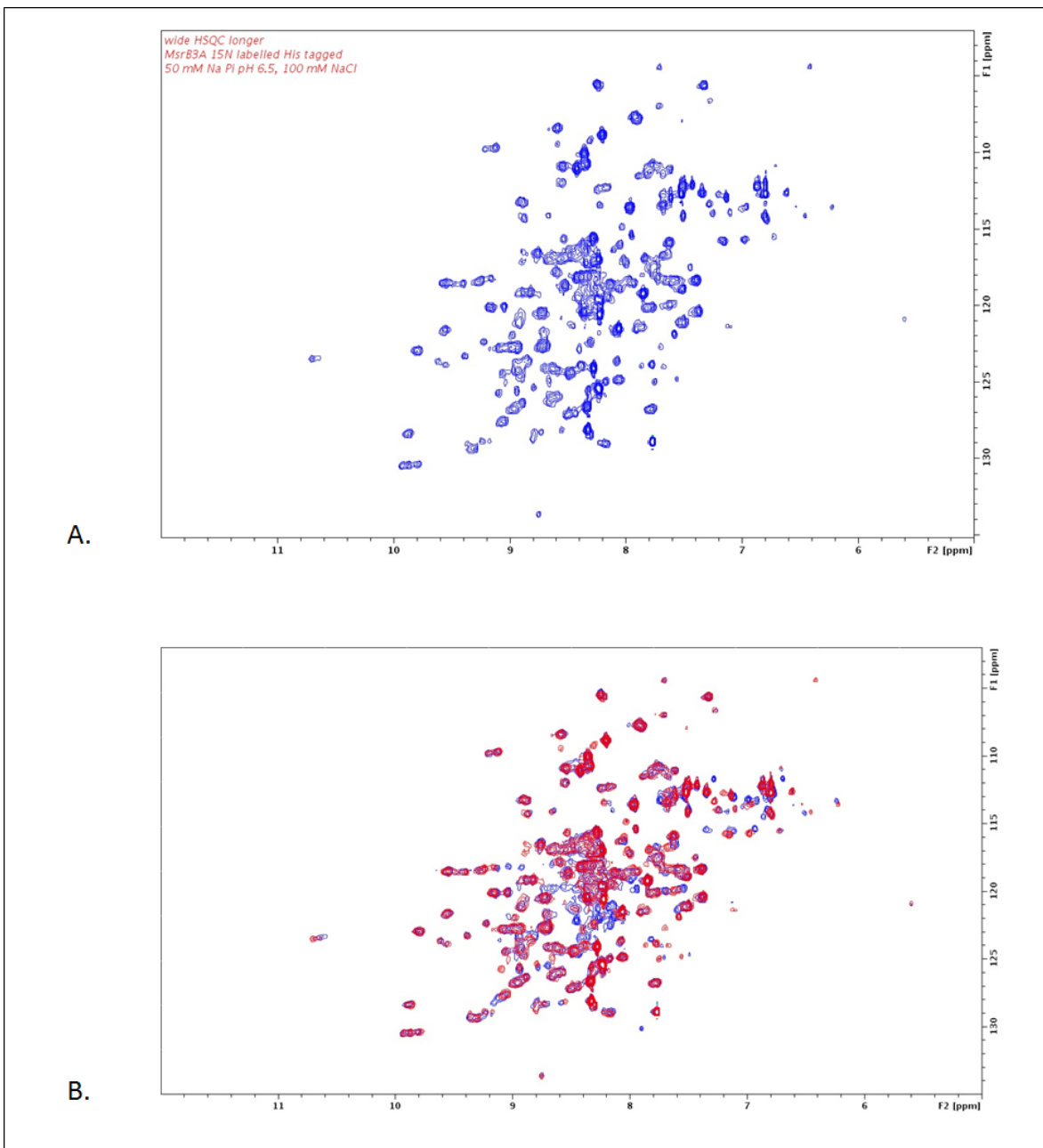


**Figure 3.15: NMR spectra of MsrB3A.**

Panel A represents the 600 MHz [ $^1\text{H}$ ,  $^{15}\text{N}$ ]-HSQC spectra of 372  $\mu\text{M}$  MsrB3A protein in 50 mM  $\text{NaPO}_4$  100 mM NaCl pH 6.5 buffer containing 10%  $\text{D}_2\text{O}$  at 298 K, in its native state (represented as the blue contours).

Panel B represents the 600 MHz [ $^1\text{H}$ ,  $^{15}\text{N}$ ]-HSQC spectra of 372  $\mu\text{M}$  MsrB3A protein after it was reduced by 1 mM TCEP in 50 mM  $\text{NaPO}_4$  100 mM NaCl pH 6.5 buffer containing 10%  $\text{D}_2\text{O}$  at 298 K (represented as the blue contours), superimposed by the 600 MHz [ $^1\text{H}$ ,  $^{15}\text{N}$ ]-HSQC spectra of the native state of MsrB3A obtained earlier in panel A (represented by the red contours).

### 3.2.2.3 Protein crystallisation

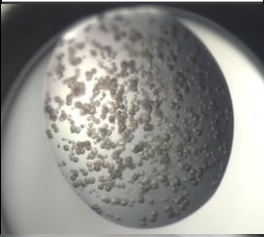
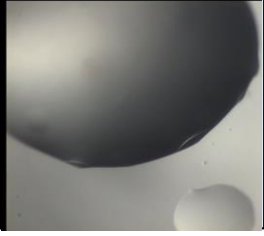
X-ray crystallography is another technique used for determining protein structure. Although it is the best technique to determine protein structure in atomic scale resolution, it is not always successful. The primary reason is the availability of protein crystals which are a must for the technique. Protein crystal formation is highly elusive on its own and requires a lot of trial and errors with different crystallisation conditions, thereby, making it a tedious and time-consuming process, when compared to NMR spectroscopy.

With the aim of obtaining MsrB3A protein crystals, we set up 4X 96 well crystallisation screening plates made by Molecular Dynamics, as discussed earlier in section 2.3.3. In certain crystallisation screening plates hits were obtained for crystallisation conditions (Table 3.1). As observed, the crystallisation conditions of well E2 of screening plate JCSG-*plus*<sup>™</sup> HT-96 had come up to the phase separation stage and the bubbles of the phase separation seemed to come together for crystal formation. But further incubation did not give any result. As for the well D1 of screening plate Morpheus<sup>®</sup> HT-96, tiny bulges occurring at regular intervals were observed, but up on being taken for analysis, they broke away, thereby, leading to failure of crystal structure determination.

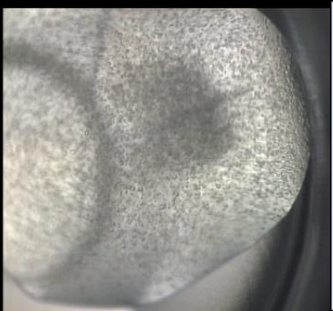
Since, phase separation was achieved in well E2 (Table 3.1), the crystallisation conditions were then optimised further to get crystals (Table 3.2). As we can observe, the phase separation was too fast. Hence, crystals could not be formed and would result in formation of asymmetric amorphous solids.

Therefore, to conclude the crystal trials did not yield protein crystals suitable for structural analysis.

**Table 3.1: Crystallisation screening conditions for MsrB3A.**

<u>Molecular Dynamics Plate Reference</u>	<u>Well</u>	<u>Crystallisation conditions</u>	<u>Figure</u>	<u>Observation</u>
JCSG-plus™ HT-96	E2	Salts- 2.0 M (NH <sub>4</sub> ) <sub>2</sub> SO <sub>4</sub> , 0.2 M NaCl ; Buffer- 0.1 M sodium cacodylate, pH 6.5		Phase Separation is observed. Tiny bubbles are tending to come closer to form crystals. No crystal formation occurs.
Morpheus® HT-96	H10	Precipitants- 10% (w/v) PEG 8000, 20% (v/v) ethylene glycol; Additives- 0.02 M amino acid mix; Buffer- 0.1 M Bis-Tris propane, pH 8.5		Crystal formation was observed. Upon analysis under X-ray generator, crystals were salt crystals.
Morpheus® HT-96	D1	Precipitants- 10% (w/v) PEG 20000, 20% (v/v) PEG 550MME; Additives- 0.02 M alcohol mix; Buffer- 0.1 M MES/Imidazole, pH 6.5		Regular structure pattern was observed. Upon sampling, the crystals were too brittle and broke away.

**Table 3.2: Optimisation of crystallisation condition for MsrB3A.**

<u>Well</u>	<u>Crystallisation conditions</u>	<u>Figure</u>	<u>Observation</u>
A1	Salts- 1.8 M (NH <sub>4</sub> ) <sub>2</sub> SO <sub>4</sub> , 0.2 M NaCl ; Buffer- 0.1 M sodium cacodylate, pH 6.3		Phase separation was achieved, but was too fast for crystal formation
C1	Salts- 1.8 M (NH <sub>4</sub> ) <sub>2</sub> SO <sub>4</sub> , 0.2 M NaCl ; Buffer- 0.1 M sodium cacodylate, pH 6.7		Phase separation was achieved, but was too fast for crystal formation

## Discussions

### 3.3.1 Protein expression, extraction and purification

The *MsrB3A* gene was successfully cloned into the pET21a (+) plasmid and expressed in *E. coli* BL 21 (DE 3) Star *pLysS* cells to express the recombinant protein product. From all the extraction and purification processes that were observed for recombinant *MsrB3A*, it could be predicted that predominantly intact proteins were obtained, as only single peaks were detected in the elution curve in all the chromatographic steps. Although, slight shoulder was also present along with the single peaks, it would be amounted to formation of dimers that were seen in all the SDS-PAGE gels of the protein extraction and purification steps. This suggests that the stable recombinant protein product was obtained up on over-expression.

As we can notice in the protein extraction in Fig. 3.3, minute amount of *MsrB3A* protein is still present in the pellet, even though a chemical process of extraction was used. A reason for this could be an improper mixing step with the chemical components of the BugBuster™ protein extraction, for which the step was not efficient. Another possible explanation could be the presence of minute amount of supernatant with the pellet, which could have resulted in the false positive result. As for the protein extraction using French Press (Fig. 3.5 and 3.9), similar condition is observed. A viable explanation for this inefficiency is the inadequate number of cell lysis cycles and use of lower driving pressure for which enough shear force could not be generated for completely lysing all the cells. Hence, the non-lysed cells might be responsible for giving the false-positive result. A good way to lower the false positive result is to increase the number of lysis cycles to 6 to be more efficient.

Since the recombinant *MsrB3A* protein was cloned with a 6X his-tag at its N-terminal, IMAC chromatography was used effectively as the primary purification stage of the protein. As we can observe in Fig. 3.4, 3.6 and 3.10, we could purify the recombinant *MsrB3A* with high degree of purity on bench scale, while, the use of His-Trap™ column did not give such results and required further purification steps. A possible reason for this is the use of the metal ion in the binding resin. The TALON® Superflow™ Affinity Resin used  $\text{Co}^{2+}$  ions which can bind with more specificity and

strength to the 6X His-tag than the Ni<sup>2+</sup> ion present in the resin of the His-Trap™ column. Another possible reason attributed to the difference in the purification process was the volume of the sample being purified. Although, we obtained recombinant MsrB3A protein with high degree of purity on bench scale, the amount purified protein was not sufficient for structural studies and functional assays. Hence, increasing the sample volume also increases the concentration of other unwanted histidine containing proteins which were the contaminants and were subsequently removed by further chromatographic purification processes.

### **3.3.2 Structural studies of recombinant MsrB3A**

The CD spectroscopic and NMR spectroscopic structural studies conducted on recombinant MsrB3A protein did confirm that the protein was folded, but whether it was correctly folded to be functional was not known. The functional studies made, as discussed in the chapter 4 and 5 proved that our recombinant protein was functional, hence, establishing that the recombinant MsrB3A was folded in its correct conformation. Though CD spectroscopy and NMR spectroscopy could shed some light on the structure of MsrB3A and change in the conformation when MsrB3A was reduced by TCEP, further experiments must be made to understand and solve the structure of MsrB3A protein.

Though some hits were achieved for screening of crystallisation conditions, but on analysis they either turned to be salt crystals or ceased at the phase separation stage. Therefore, the crystal trials were not successful. Further experiments using new crystallisation parameters must be made to obtain better crystals.

## **3.4 Future work**

From the results obtained in this chapter, much work requires to be done to determine the structure of MsrB3A protein. For example, for CD and NMR spectroscopy, further experiments involving thermal stability of MsrB3A protein, analysis of structural conformations of MsrB3A mutant proteins and their subsequent

comparison with the results obtained for the wild-type MsrB3A protein are some of the experiments which could be made.

From the results obtained in the subsequent chapters about the functionality of MsrB3A protein demonstrates that the MsrB3A protein is functional, thereby, proving that the conformation achieved for the recombinant MsrB3A protein is correct. Hence, we could then design an experiment to study the changes in the conformation of MsrB3A when it reduces the methionine sulfoxide to methionine in presence of a reducing environment using cryo-NMR spectroscopy. This experiment would also provide us an actual glimpse into the mode of function of MsrB3A protein.

Though the NMR spectroscopy could provide us with valuable insight into the structure of MsrB3A protein and helps us to collect information from different types of experiments easily, the resolving power of NMR spectroscopy is lower than x-ray crystallography as the information obtained is highly complex and requires more sophisticated equipment to handle the data-sets obtained. On the other hand, we can obtain the entire 3D structure at atomic scale by systematic analysis of data obtained by x-ray crystallography. As we know from our results obtained earlier in this chapter, we were not successful in obtaining protein crystals that are suitable for X-ray crystallographic studies. A possible reason for this could be the interference caused by the presence of the 6X His-tag. Hence, to remove the His-tag from the recombinant MsrB3A protein we need to treat the recombinant MsrB3A with TEV protease in presence of a suitable cleavage buffer which would cleave the His-tag from the recombinant protein allowing it to be separated easily by HPLC, while the His-tag remains attached to the column resin. The His-tag could then be washed using the suitable elution buffer. This way we might be able to get the tag free MsrB3A protein which we could analyse for its structure and function, as well as, it could be helpful to get protein crystals that might be suitable for structural studies.

# Chapter 4: Creation of C126A MsrB3A mutant by site-directed Mutagenesis.

---

## 4.1 Introduction

In the previous chapter, we discussed the need to study MsrB3A protein, how it was cloned, expressed and purified from recombinant *E. coli* cells, followed by structural studies using CD spectroscopy, NMR spectroscopy and protein crystal trials. From the experiments conducted by CD spectroscopy and NMR spectroscopy, it is observed that the MsrB3A protein has a folded structure, but whether it is in its correct conformation, can only be proved if the protein is functional. As discussed in the later chapters, MsrB3A is a functional protein signifying that the structural conformations obtained by CD and NMR spectroscopy are correct. But to validate and understand about the arrangement of amino acids involved in the functioning of the protein, mutant proteins having altered sequences by substitution, insertion or deletion of amino acid residues based on conserved regions obtained by sequence alignment (Fig. 3.1), are created to study the effects of mutation and understand their role in the proper functioning of the protein. Alteration of the amino acid sequences can be brought about by the help of site directed mutagenesis in the respective gene sequence encoding for the mature protein.

From literature, it is known that, mammalian MsrB (SelR) consists of a seleno-cysteine residue towards the C-terminal of the protein chain, which is said to be responsible for the catalytic activity of the protein. Hence, it can be used as a good indicator of a catalytic residue which is vital for the redox reactions when compared for finding the catalytic residue in various MsrB sequences (Stadtman, 1996, Hatfield and Gladyshev, 2002). From multiple sequence alignment (Fig. 3.1), we observe that a single cysteine residue near the C-terminal is conserved in the various MsrB sequence and shows conservation with the seleno-cysteine residue of the human and mouse MsrB1 (SelR) sequences. In case of the MsrB3A sequence, the 126<sup>th</sup> position cysteine corresponds as the conserved cysteine residue, which is also in alignment with the seleno-cysteine residue.

Based on the multiple sequence alignment and literature stated in the last paragraph, we hypothesise that the 126<sup>th</sup> position cysteine is the catalytic residue

which is responsible for the redox process in MsrB3A protein and is present in the active site of MsrB3A protein. Hence, we mutated the MsrB3A protein by substituting the 126<sup>th</sup> position cysteine for alanine to produce a non-functional protein using site-directed mutagenesis.

## 4.2 Results

### 4.2.1 Site directed mutagenesis

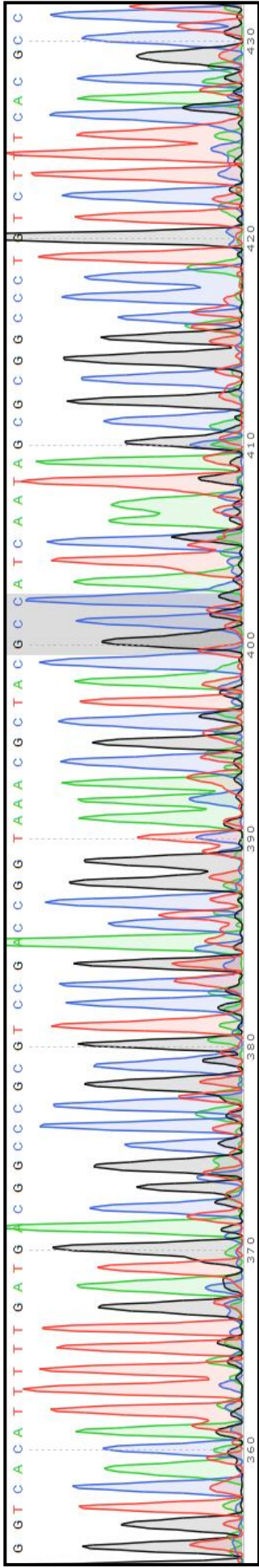
As discussed earlier in section 2.4.1, synthetic DNA primers incorporating the cysteine to alanine mutation (TGC→GCC) at the 126<sup>th</sup> position of the amino acid sequence of MsrB3A, were amplified using nested PCR on the parental DNA strand (mature DNA sequence for the recombinant MsrB3A protein) and subsequently transformed into recombinant *E. coli* XL1 Blue super-competent cells. The transformed cells were then grown over-night in selective LB agar media containing 0.1 mg/ml ampicillin at 37°C, following which the plasmid DNA was isolated using alkaline lysis method. The resulting plasmid DNA was sequenced by GATC Biotech.

Potential DNA sequences predicted to contain the mutation were aligned together with the mature DNA sequence of the recombinant MsrB3A gene lacking the signal peptide (Fig. 4.1). As we can clearly observe from the multiple sequence alignment (Fig. 4.1), the C126A MsrB3A mutant DNA sequences 1, 2, 3, 7 and 9 had the mutation, i.e., TGC→GCC, which could encode alanine in place of cysteine at the 126<sup>th</sup> position of the amino acid sequence during translation (Fig. 4.2). But only the DNA sequence of the mutated gene sequence 9, could encode the entire gene sequence of the MsrB3A protein, as seen in Fig. 4.2. Although, the mutated gene sequence for the C126A MsrB3A mutant sequence 1 had a better DNA purity profile (Fig. 4.3) than the DNA sequence of C126A MsrB3A mutant sequence 9, since, it just lacked the DNA sequence to encode the last six amino acids at the C-terminal (as seen in Fig. 4.2), it could not be used further to produce the mutant C126A MsrB3A protein.

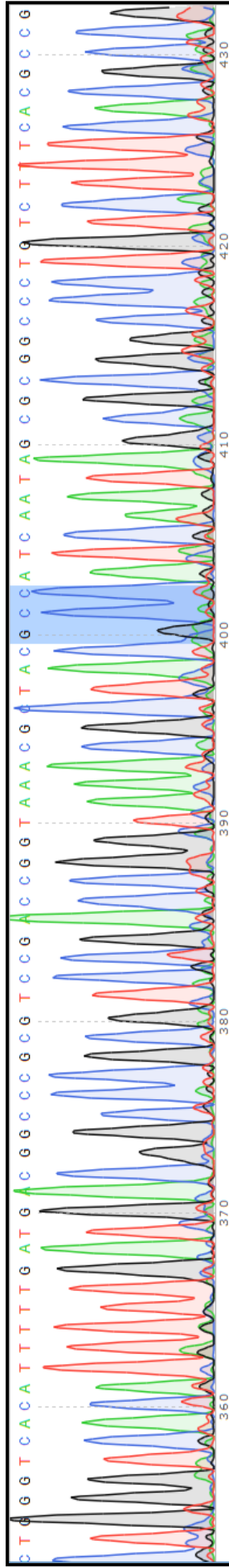
Thus, the plasmid DNA containing the C126A MsrB3A mutant DNA sequence 9 was used to transform the recombinant *E. coli* BL21 (DE3) Star *pLysS* cells to express the recombinant C126A MsrB3A mutant protein. The expression of the mutant protein, extraction and purification are discussed in detail in the next section.







A.



B.

Figure 4.3: DNA profile for C126A MsrB3A mutant DNA sequence (A) 1 and (B) 9 depicting the purity of the highlighted mutation region (GCC), which encodes for Ala residue instead of Cys.

#### **4.2.2 Protein expression, extraction and purification**

To express the recombinant C126A MsrB3A mutant protein, the transformed *E. coli* cells were first grown in selective LB broth media and then induced for protein expression using IPTG. The expression was then analysed on 15% SDS-PAGE gel (result not shown). No expression was observed in LB broth media. Similar results were also obtained when the recombinant *E. coli* cells containing the C126A MsrB3A mutant gene was expressed in TB media (Fig. 4.4 Panel A). There was no increase in the protein expression when induced by IPTG. Although, a leaky expression for the C126A mutant protein was observed in TB broth media. Hence, depending on the leaky expression obtained for the C126A MsrB3A protein we proceeded to extract the recombinant protein using French Press. Fig. 4.4 Panel B demonstrates the extraction samples when analysed on SDS-PAGE gel. As we can clearly observe, only a small quantity of the C126A MsrB3A mutant protein is obtained in the supernatant (Sn) or clarified solution. The clarified solution was then filtered as discussed in section 2.2.1, before being purified by IMAC chromatography using the AKTA FPLC system.

Fig. 4.5 represents the purification of the C126A MsrB3A mutant protein by IMAC chromatography. As we can clearly observe in lanes 3 to 13 of panel B, there are still some higher molecular weight contaminants present after IMAC chromatography purification. In panel A, we observe that two different peaks are present which may denote the presence of different forms of the mutant C126A MsrB3A protein, which gets eluted at different time interval. The IMAC purified samples are further purified by gel filtration chromatography (Fig. 4.6). In panel A we notice the presence of multiple peaks, which might suggest that the purified C126A MsrB3A mutant protein has multiple structural forms in which it gets eluted or the protein might be cleaved by the *E. coli* proteases resulting in multiple peptides. However, we only use the samples from the lanes 8 to 9 for further study, as the other samples contain a lot of contaminant proteins and less quantity of our target mutant protein. The gel filtration chromatography eluted C126A MsrB3A mutant protein samples were then collected, concentrated and quantified according to the procedure stated in section 2.2.2. Though, the quantity of C126A MsrB3A mutant

protein obtained was small but was sufficient to perform functional studies related to MsrB3A protein. Another noticeable feature in the extraction and purification steps of C126A MsrB3A mutant protein was the absence of the bands between the 32 to 46 KDa marker in the selected purified samples of gel filtration chromatography, unlike the observations made in the extraction and purification steps of wild-type MsrB3A protein.

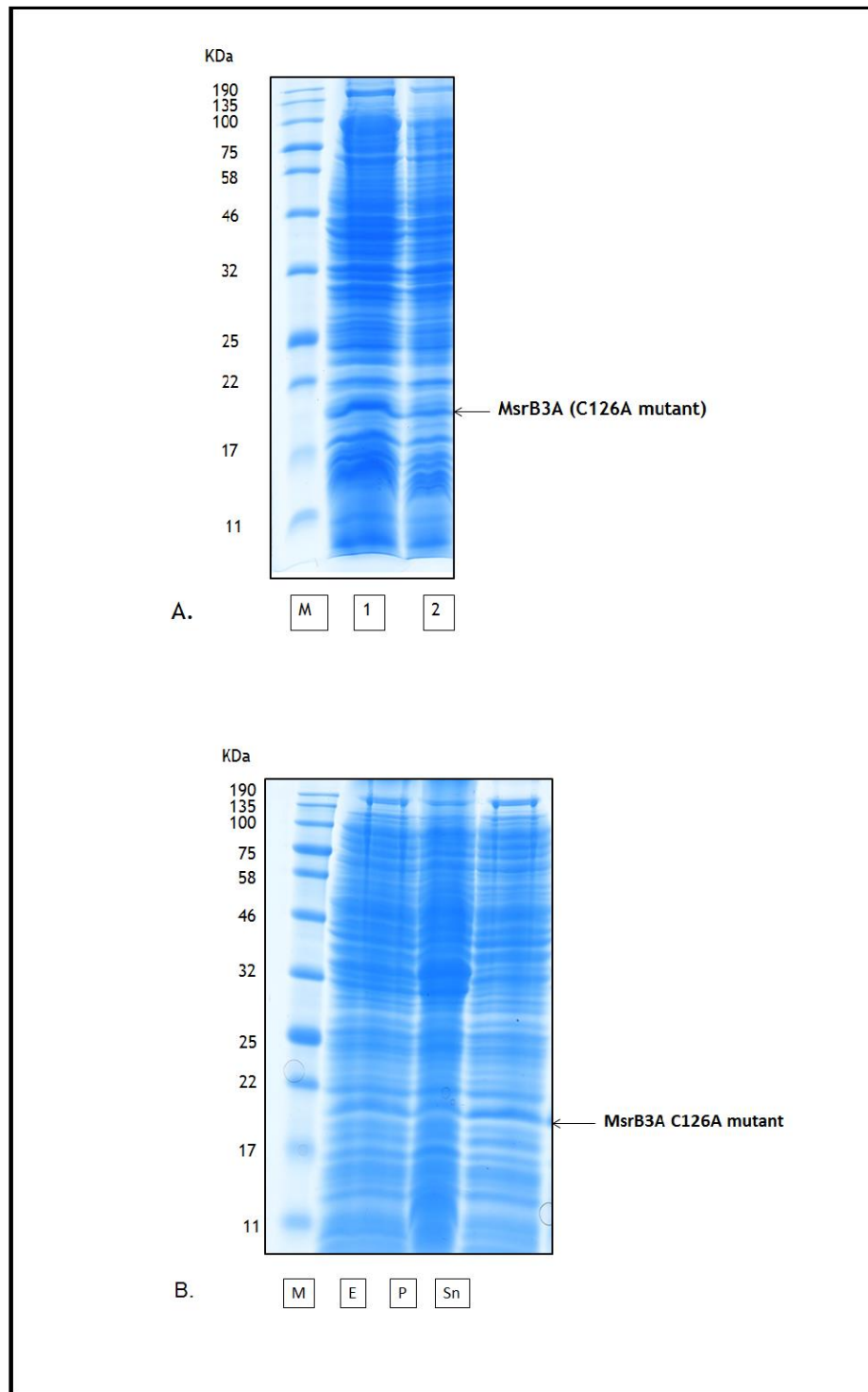


**Figure 4.4: Protein expression and extraction of C126A MsrB3A mutant.**

Lane M represents the Blue Pre-Stained Protein Standard in both panels.

Panel A represents the SDS-PAGE gel analysis for protein expression of C126A MsrB3A mutant in TB broth media. Lane 1 contains the sample from cell culture before IPTG induction, while lane 2 represents the sample from cell culture after IPTG induction.

Panel B represents the SDS-PAGE gel analysis for protein extraction of C126A MsrB3A mutant using French Press. Lane E represents extraction sample after cell lysis using French Press. Lanes P and Sn represent the pellet and supernatant respectively.

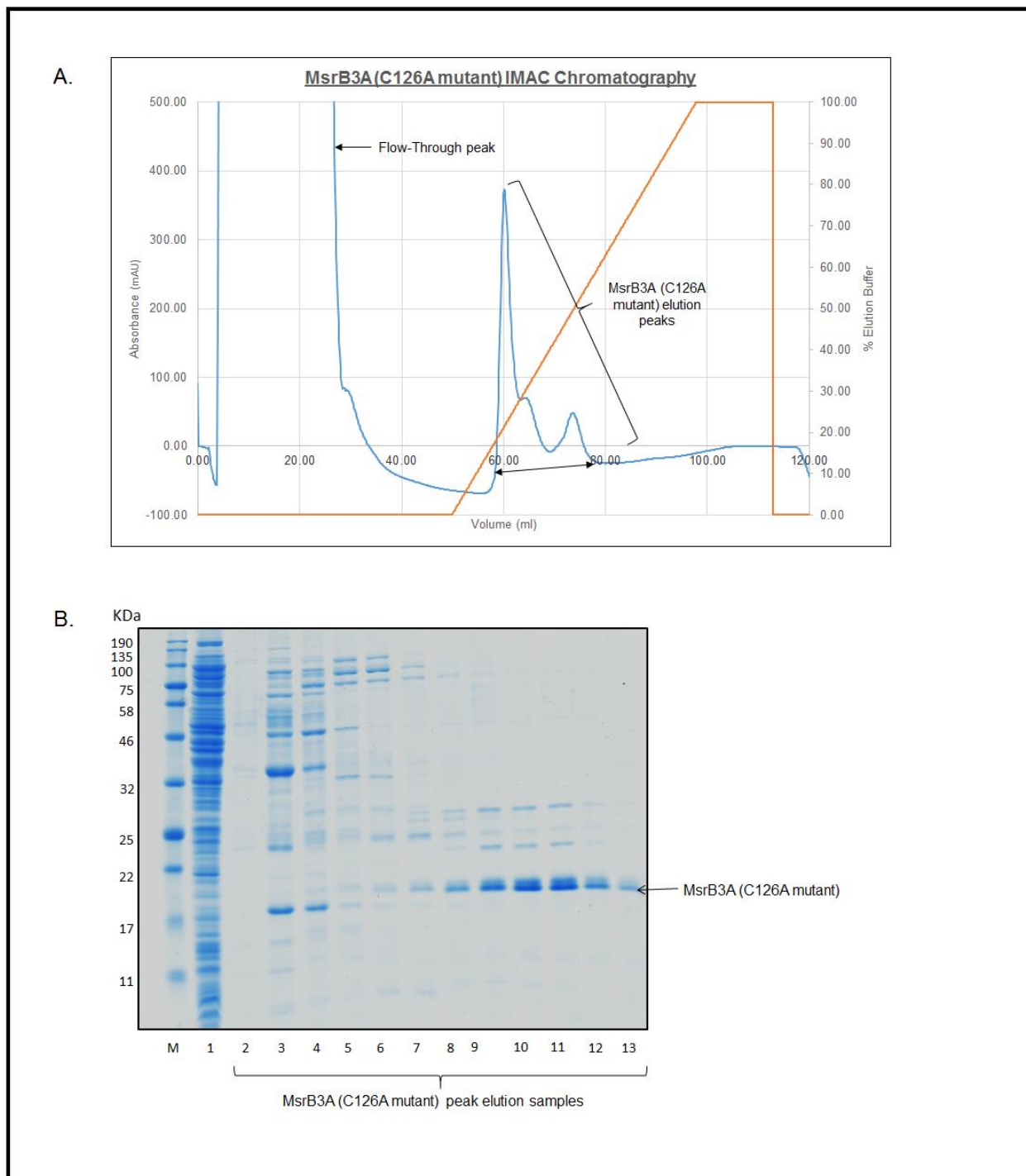


**Figure 4.5: Immobilised metal affinity chromatography (IMAC) purification of C126A MsrB3A mutant protein.**

- A.** Graph representing a typical FPLC chromatogram obtained using a 5 ml HisTrap™ HP affinity column for purifying the 6X His-tagged C126A MsrB3A mutant protein. The bound protein was eluted by using a 500 mM Imidazole concentration gradient represented by the orange curve.
- B.** SDS-PAGE gel analysis of the samples of the purified fractions collected from the peaks obtained as shown in graph. Lane 1 in illustration B represents the sample from the flow through elution peak, while lanes 3 to 13 represent the samples from the fractions collected from the MsrB3A elution peak in successive order and is represented in graph A by the double headed arrow.

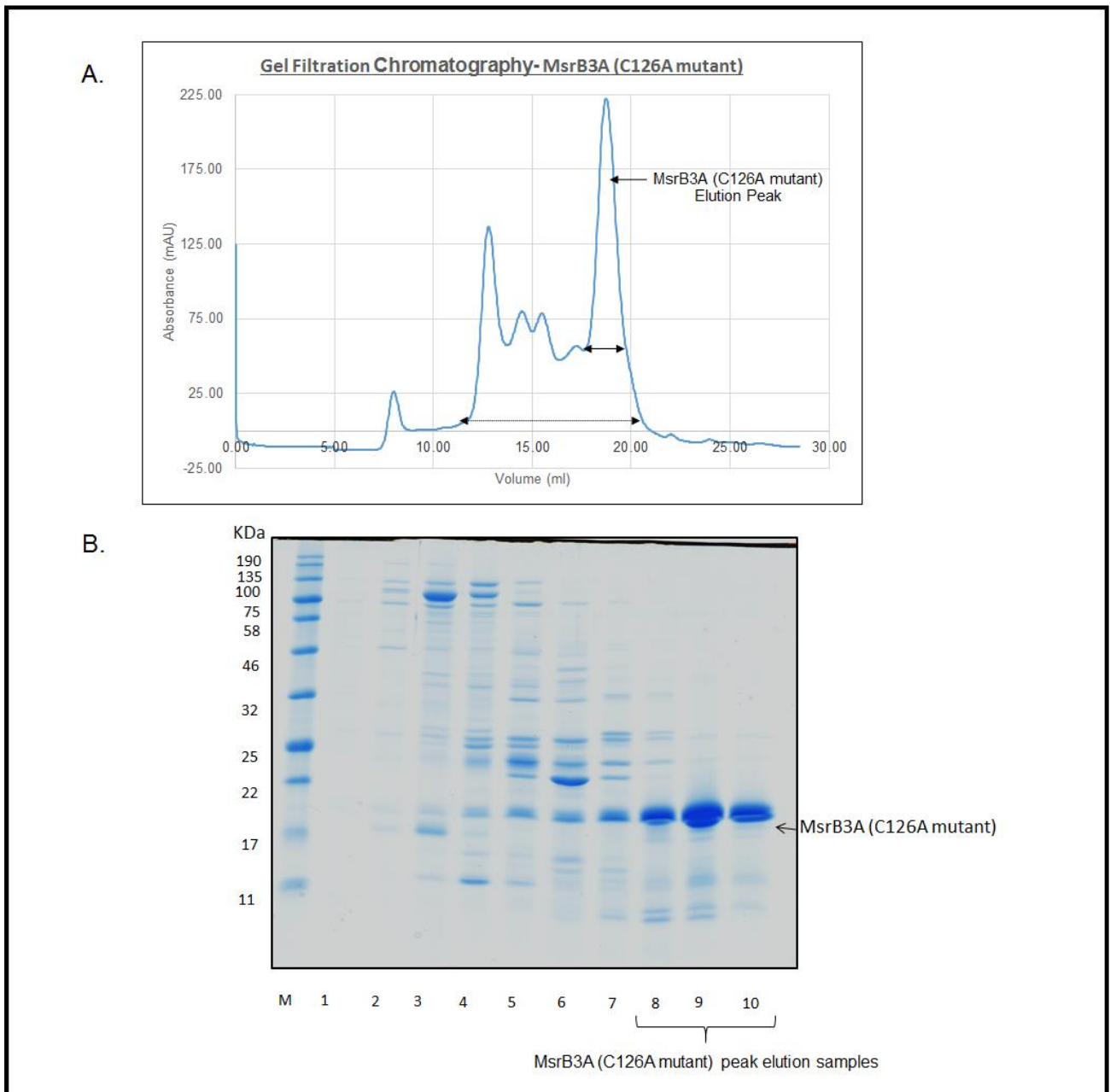


**Figure 4.6: Gel filtration chromatography purification of C126A MsrB3A mutant protein.**

- A.** Graph representing a typical FPLC chromatogram obtained using a Superdex 200 10/300 GL gel filtration chromatography column for purifying the C126A MsrB3A mutant protein based on the principle of molecular size exclusion.
- B.** SDS-PAGE gel analysis of the samples of the purified fractions collected from the peaks obtained as shown in graph. Lane M represents the Blue Protein Standard used as reference. Lanes 8 to 10 represent the samples from the fractions collected from the elution peak in successive order and is represented in graph A by the double headed arrow.

### **4.2.3 Discussions**

From the results obtained above, we could mutate the mature MsrB3A DNA sequence to encode for alanine residue in place of conserved cysteine residue at the 126<sup>th</sup> position of the MsrB3A protein sequence, as seen in Fig.5, using site directed mutagenesis. The C126A MsrB3A mutant protein was further used to verify the function of MsrB3A protein as discussed in the next two chapters.

A striking feature which we notice from Fig. 25 is the presence of multiple elution peaks in panel A. In panel B, the elution samples from these peaks show the presence of the mutant MsrB3A protein but in mixture with other contaminant proteins. This suggests that the C126A MsrB3A protein is not only unstable, but it may also signify that the cysteine residue which was substituted might also be responsible for maintaining the structural conformation of the protein. Although, we could get some insight about the structural integrity of MsrB3A, more mutagenesis studies are required to have a better understanding. Besides the creation of more MsrB3A mutants, the use of different MsrB3A mutants for structural studies is another field which could provide more detailed insight about the structural conformation and integrity of MsrB3A.

# Chapter 5: MsrB3A functional assay I - Gel shift assay

## 5.1 Introduction

In the previous chapters, we discussed the expression of human MsrB3A protein in recombinant *E. coli* cells, followed by its extraction, purification and structural studies. We also created the C126A mutant MsrB3A (substituting alanine in place of cysteine at 126<sup>th</sup> position of the amino acid chain) for functional analysis of MsrB3A.

From the literature, we know that different assays have been developed over time to study the functions of methionine sulfoxide reductases. The first such functional assay for methionine sulfoxide reduction was developed by (Brot et al., 1982). The method utilised [<sup>3</sup>H]-labelled N-acetyl methionine sulfoxide as the substrate and used ethyl acetate extraction to assay the radioactive N-acetyl methionine obtained after reduction by methionine sulfoxide reductases. Some major drawbacks of this technique included the use of radioactive isotopes, incomplete extraction of the reaction product and contamination of the substrate. Another method commonly utilised for determination of Msr function is an enzyme-coupled method that depends on the change in absorption of light by NADPH at 340 nm as described by (Moskovitz et al., 1996). In the method, the Msrs are reduced by thioredoxin which in turn is reduced by the NADPH-dependent thioredoxin reductase, thereby, utilising the change in the absorption of light by NADPH at 340 nm for determining Msr function. Although, the detection by this method is slightly less than the HPLC assay which utilises dabsylated methionine sulfoxide as substrate for Msrs, it allows to experiment with different substrates.

The HPLC assay is another method which is commonly utilised for determination of Msrs functions. As stated earlier it uses the reduction of dabsylated methionine sulfoxide to dabsylated methionine by Msrs, and is highly accurate and sensitive. We shall be discussing this technique further in chapter 6. The only drawback of the technique is that it utilises a HPLC system for separating the dabsylated methionine sulfoxide from dabsylated methionine, hence, requiring the

use of skilled labour for operating the system, as well as, for preparation of the substrate. Yet with recent developments in the HPLC systems it is becoming much easier to use this method to assay methionine sulfoxide reductases.

Recently, a more simple, easy and cost-effective method has been developed by (Le et al., 2008), which utilises the mobility shift of methionine-rich proteins between their oxidised and reduced states when analysed on SDS-PAGE gels for determining the function of different methionine sulfoxide reductases. In this method, it was noted that the oxidised forms of the methionine-rich proteins exhibited decreased mobility than their reduced forms. An improved version of the method was devised by (Gennaris et al., 2015), in which methionine-rich proteins such as, SurA, Pal, calmodulin etc., found in the bacterial cell envelope of important human pathogens, was utilised widely to determine the function of the novel MsrPQ reduction enzymes. Hence, we used SurA as our model substrate using this technique to determine the function of MsrB3A as discussed later in the chapter.

SurA is a chaperone protein that occurs mostly in the periplasm of gram negative bacteria. It aids in the folding and transport of outer membrane proteins in the periplasmic space of the bacteria (Vertommen et al., 2009). SurA has 14 methionine residues present in it, which makes it highly susceptible to attack by reactive oxygen species (ROS) (Gennaris et al., 2015, Riley et al., 2006). Since, SurA serves as one of the vital proteins responsible for biogenesis of the cell membrane in gram negative bacteria (Volokhina et al., 2011), hence, it can be used as an excellent biological substrate to determine the functionality of human MsrB3A.

Hence, SurA was over-expressed as described in section 2.5.1. It was then extracted and purified using the same methods described in section 2.2.1, except the desalting and ion exchange chromatography steps which were not required in this case.

## **5.2 Results**

### **5.2.1 Protein expression, extraction and purification-**

Fig. 5.1 represents the SDS-PAGE gels for the SurA protein expression (panel A) and extraction (panel B) respectively. Panel A represents the expression of SurA before (lane 1) and after (lane 2) being induced by IPTG respectively. As we observe in panel A, over-expression of SurA occurs when induced by IPTG, resulting in high quantities of the protein as shown by the thick band in lane 2. This also suggests that the product obtained is also stable and does not degrade rapidly.

In Panel B (Fig. 5.1), the SDS-PAGE gel represents the extraction of SurA using a French Press. Presence of a thick and distinct band in lane Sn suggests that the protein is soluble and is present in the supernatant, but presence of a distinct band in lane P tells us that a small fraction is still present in the pellet. This could be due to the inefficiency of the cell lysis step caused by low pressure applied by the piston leading to generation of lower shear stress and insufficient cycles in the French Press, for which a fraction of cells remained intact.

Fig. 5.2 represents the purification of SurA by immobilised metal affinity (IMAC) chromatography. As we can observe in lanes 2-4 of panel B, there are a few higher molecular weight contaminants still present after purification by IMAC chromatography. Hence, the IMAC purified samples were further purified by gel filtration chromatography as shown by Fig. 5.2. After purification, the samples collected were concentrated down, quantified and aliquoted as described in section 2.2.2.

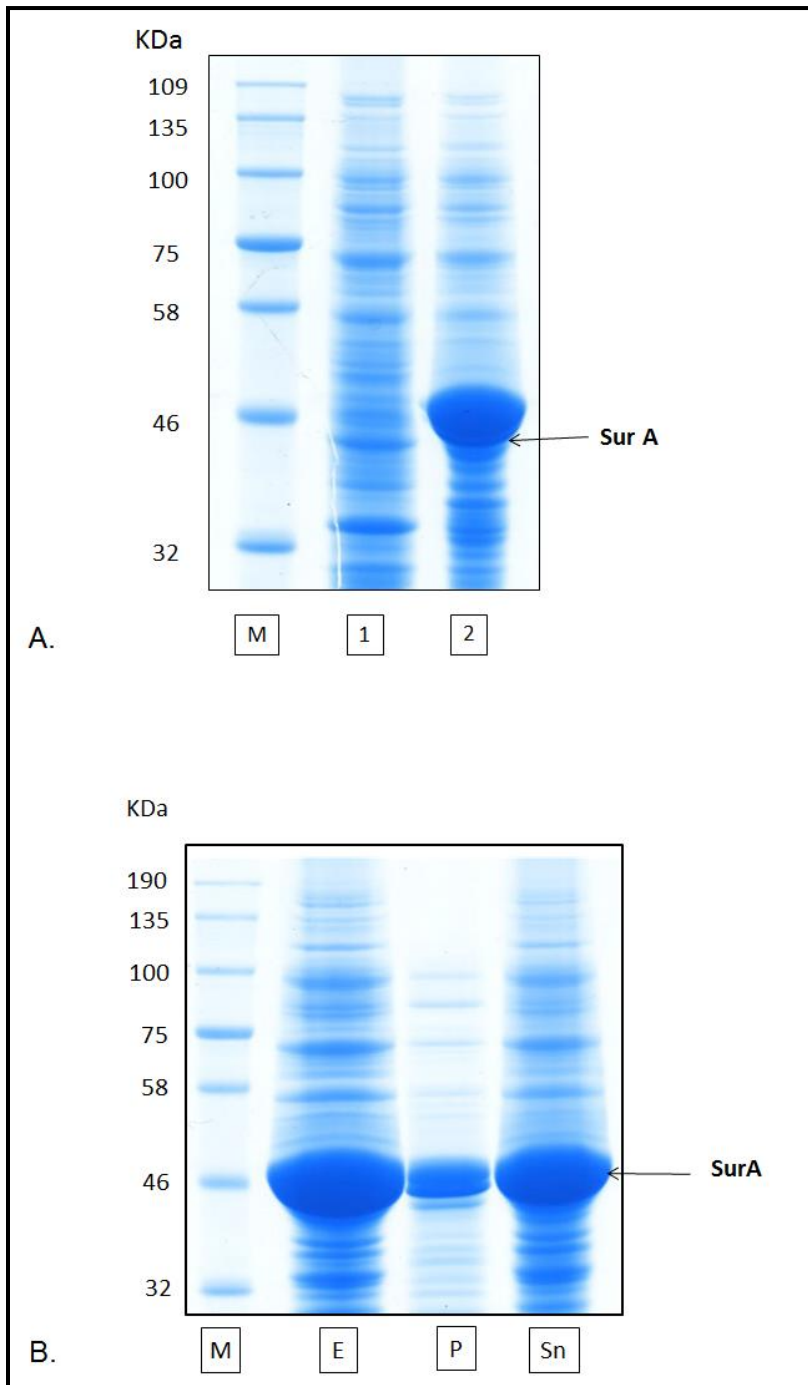


**Figure 5.1: Protein expression and extraction.**

Lane M represents the Blue Pre-Stained Protein Standard in both panels.

Panel A represents the SDS-PAGE gel analysis for protein expression of SurA. Lane 1 contains the sample from cell culture before IPTG induction, while lane 2 represents the sample from cell culture after IPTG induction.

Panel B represents the SDS-PAGE gel analysis for protein extraction of SurA. Lane E represents extraction after cell lysis using French Press. Lanes P and Sn represents the pellet and supernatant respectively.

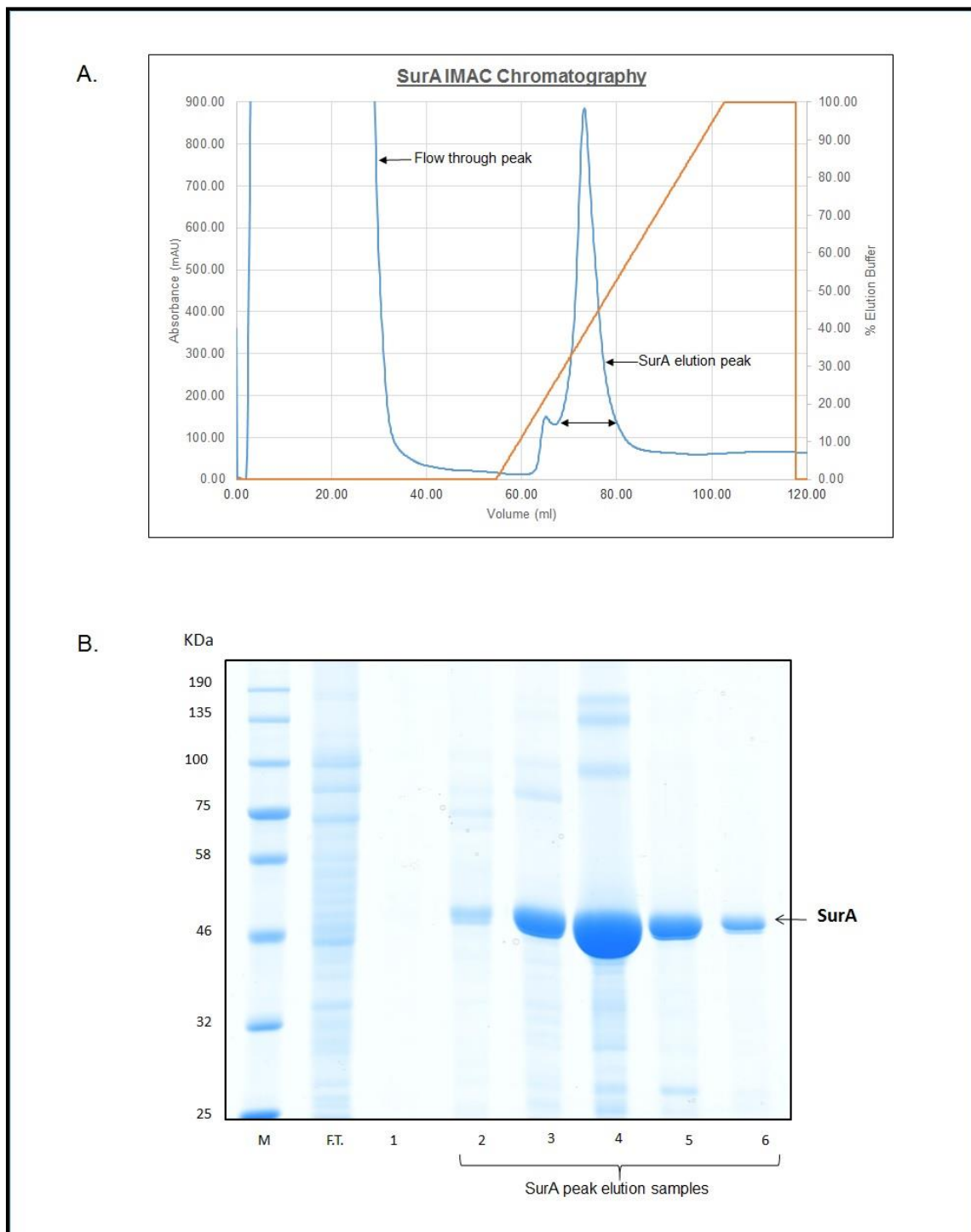


**Figure 5.2: Immobilised metal affinity chromatography (IMAC) purification of SurA protein.**

- A.** Graph representing a typical FPLC chromatogram obtained using a 5 ml HisTrap™ HP affinity column for purifying the 6X His-tagged SurA protein. The bound protein was eluted by using a 500 mM Imidazole concentration gradient represented by the orange curve.
- B.** SDS-PAGE gel analysis of the samples of the purified fractions collected from the peaks obtained as shown in graph. Lane F.T. in illustration B represents the sample from the flow through elution peak, while lanes 2 to 6 represent the samples from the fractions collected from the MsrB3A elution peak in successive order and is represented in graph A by the double headed arrow.

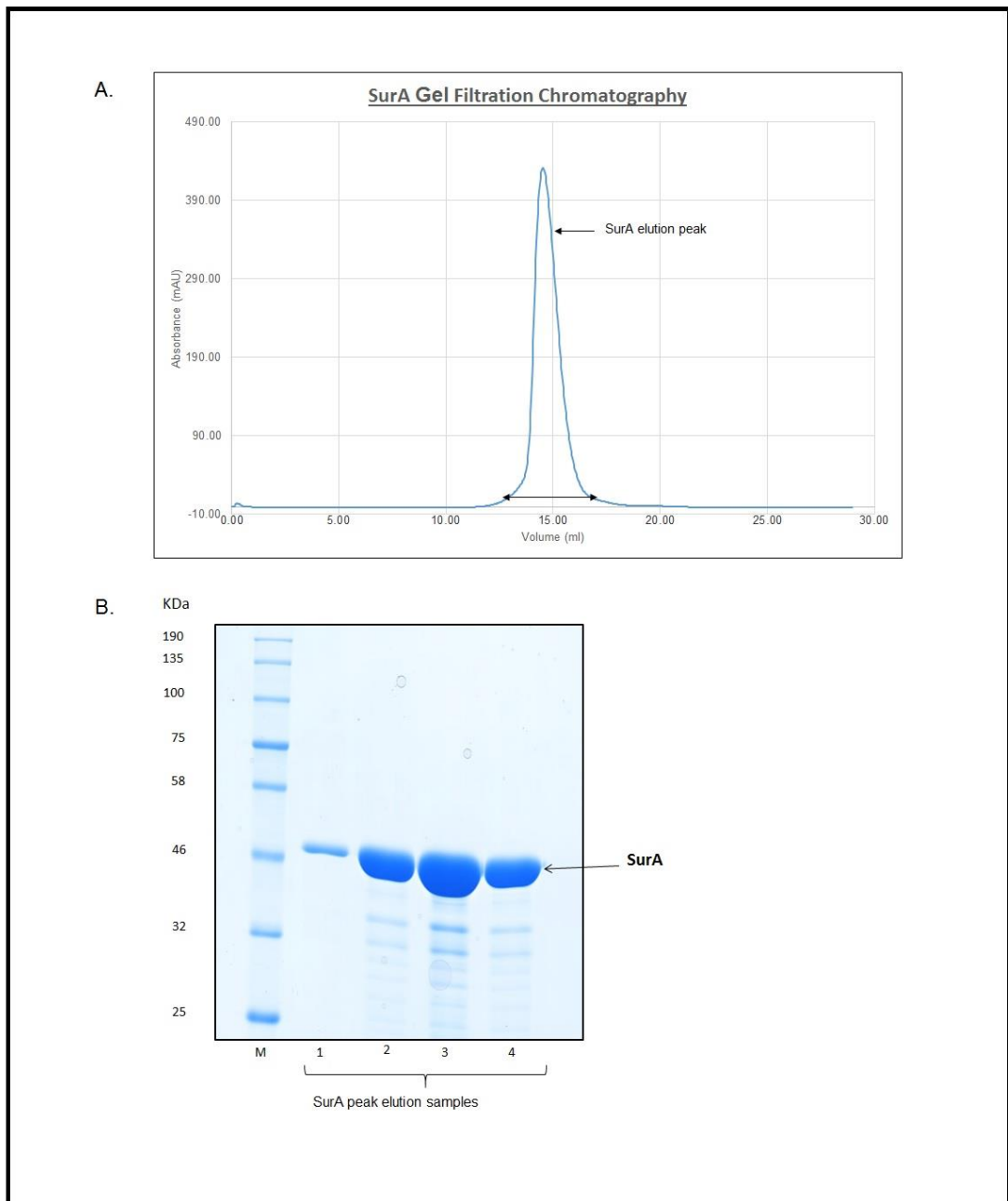


**Figure 5.3: Gel filtration chromatography purification of SurA protein.**

- A.** Graph representing a typical FPLC chromatogram obtained using a Superdex 200 10/300 GL gel filtration chromatography column for purifying the SurA protein based on the principle of molecular size exclusion.
- B.** SDS-PAGE gel analysis of the samples of the purified fractions collected from the peaks obtained as shown in graph. Lane M represents the Blue Protein Standard used as reference. Lanes 1 to 4 represents the samples from the fractions collected from the SurA elution peak in successive order and is represented in graph A by the double headed arrow.

### 5.2.2 Gel shift assay

As discussed earlier in the chapter 5 introduction, the gel shift assay is employed to observe the change in the mobility of methionine-rich proteins between their oxidised and reduced states when analysed on SDS-PAGE gel to determine the function of Msrs (Le et al., 2008). Since, SurA contains 14 methionine residues on its surface, hence, it can get rapidly oxidised by oxidising agents (in this case by incubating SurA with 100 mM H<sub>2</sub>O<sub>2</sub> at 30 °C for 3 hours in 20 mM HEPES and 150 mM NaCl, pH 7.5 buffer) to form methionine sulfoxide which in turn increases the molecular mass of the protein. Therefore, when analysed on SDS-PAGE gel the oxidised SurA moves slower than its reduced or untreated state, resulting in a mobility shift as illustrated by Fig. 5.4 panel A. The band of the oxidised SurA (lane 2) is higher than the band of the untreated or reduced SurA sample indicating that oxidised SurA travels slower than the untreated or reduced sample. Similar results were also found by (Gennaris et al., 2015), when SurA was oxidised using H<sub>2</sub>O<sub>2</sub>. Another notable feature was that when the SurA samples were treated with DTT, but there was no effect on the mobility, indicating that DTT has no effect on the mobility of SurA. Similar situations were also observed by (Le et al., 2008), when other methionine rich proteins were oxidised and treated with DTT, thereby, indicating that DTT cannot reduce methionine sulfoxide on its own and requires a reagent with higher reducing power. Hence, based on the principle of mobility shift of the methionine-rich proteins, different experiments were devised varying in parameters in which the oxidised SurA was treated with MsrB3A to reduce it in the presence and absence of DTT, as shown in Fig. 5.5.

In Fig. 5.5, we can observe a small shift in the mobility of oxidised SurA towards the mobility of its reduced state, but not entirely when it is treated with MsrB3A in presence of DTT (lane 4), suggests that MsrB3A in presence of DTT alone cannot return SurA back to its original mobility. This might indicate that MsrB3A is stereo-specific to some extent. A slight shift is also observed in lane 5 when oxidised SurA is treated with MsrB3A in the absence of DTT, but is less evident in contrast to the mobility of the oxidised SurA when treated with MsrB3A in the presence of DTT. Although, there are slight shifts in the mobility of SurA when treated by MsrB3A in

presence (lane 4) and absence (lane 5) of DTT, but are not as significant as the Sur A mobility shift assays obtained by (Gennaris et al., 2015).

In Fig. 5.6, panels A and B represent the gel shift assay when oxidised SurA is treated with MsrB3A at different concentration ratio (MsrB3A: SurA) of 1:1, 1:2, 1:5, 1:10, 1:100 and 1:1000, in the presence and in the absence of DTT respectively (lanes 3-8). Although slight shifts are detected, they are not too clear to draw definite conclusions. Panel C represents the gel shift assay in which oxidised SurA is treated with equal quantity of MsrB3A in presence and absence of DTT (lanes 3 and 4 respectively), as well as, when it was treated with equal amount of MsrB3A C126A mutant again in presence and absence of DTT (lanes 5 and 6 respectively). Similarly, to panels A and B, slight shifts can be seen but are very hard to distinguish and draw clear conclusions. It should also be noted that the shifts observed in lanes 3 to 6 are similar.

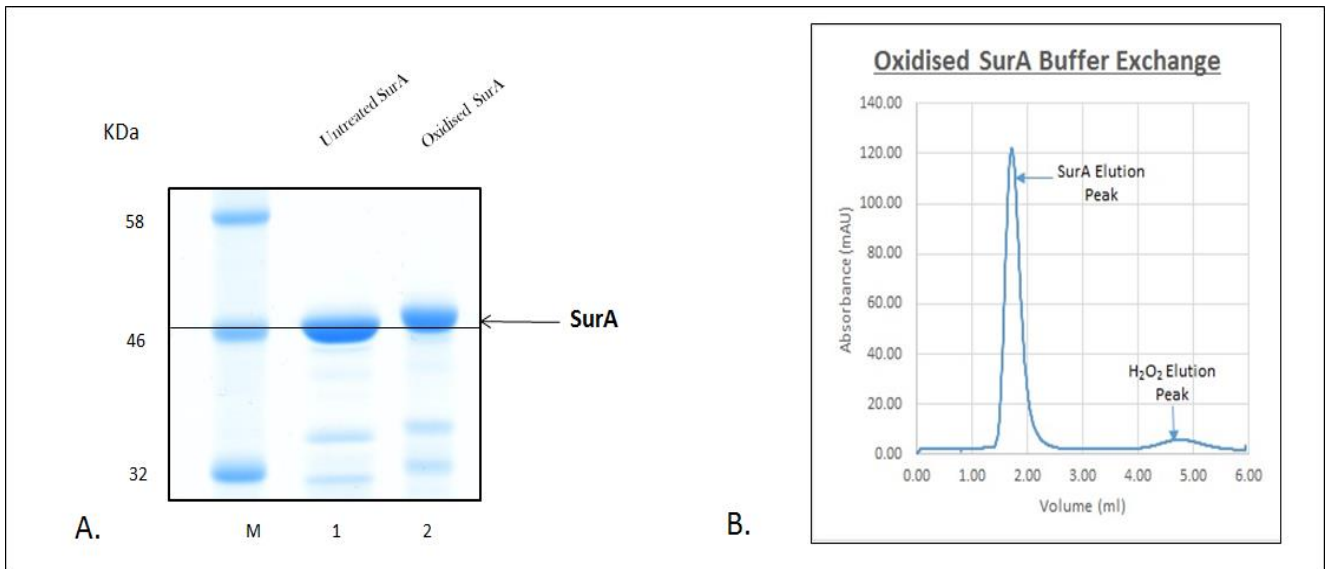


**Figure 5.4: Gel shift assay (mobility of SurA)**

Panel A represents the SDS PAGE gel showing change in the mobility of SurA when it is oxidised. Lane 1 represents the untreated SurA and lane 2 represents oxidised SurA. Lane 2 is higher than lane 1 indicating shift in mobility of the protein.

Panel B depicts the typical chromatogram of separating the oxidised SurA after treatment with H<sub>2</sub>O<sub>2</sub>.

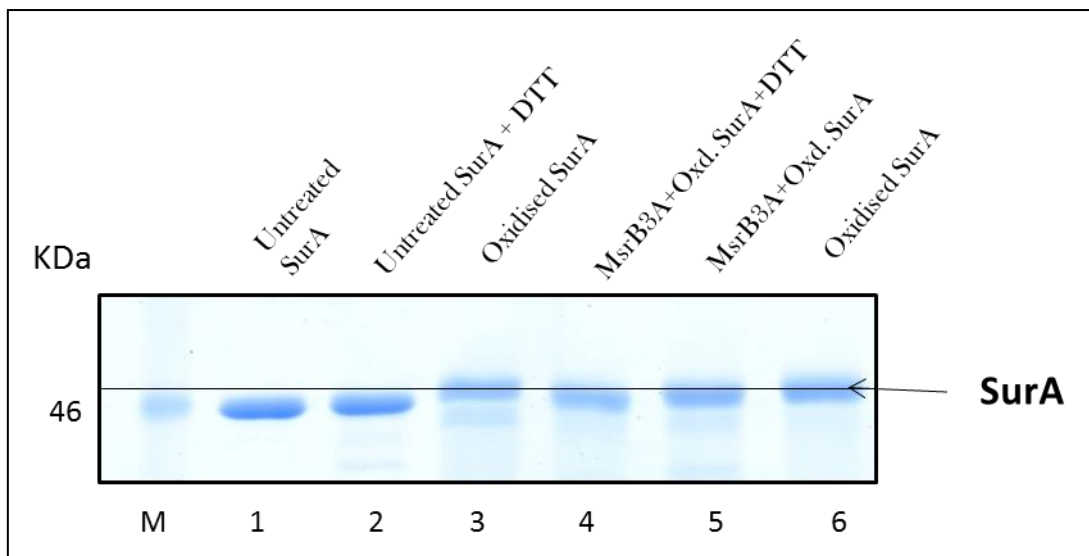


**Figure 5.5: Gel shift assay (functional assay of MsrB3A)-I.** SDS-PAGE gel depicting the different conditions of oxidised SurA when treated with MsrB3A and DTT.

Lane 1 represents SurA in its native state, lane 2 contains the SurA sample when treated with DTT, lane 3 contains the oxidised SurA sample, while lanes 4 and 5 represent the oxidised SurA sample after it was treated with equal molar concentrations of wild-type MsrB3A under reducing and non-reducing conditions in presence and absence of DTT, respectively.

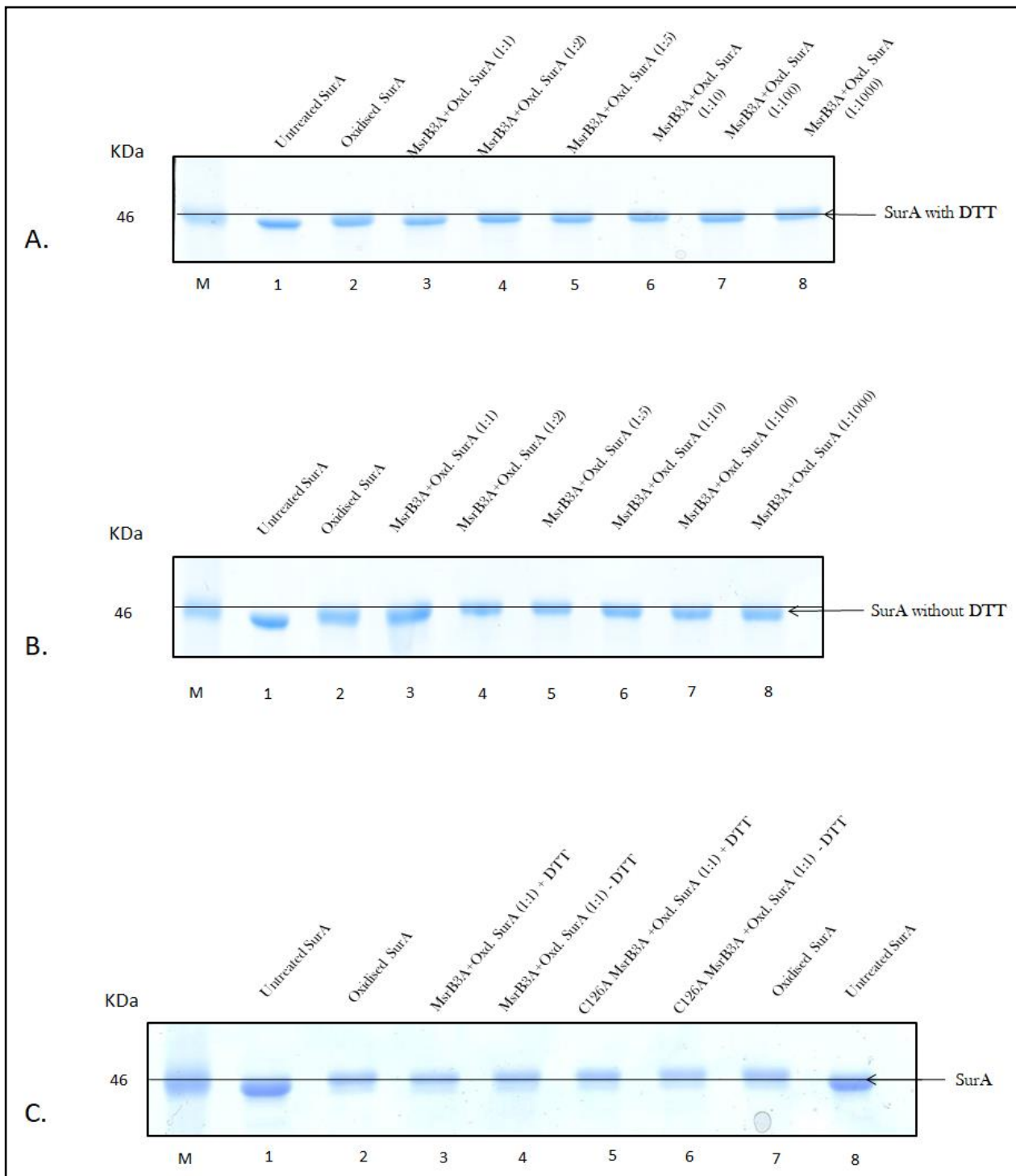


**Figure 5.6: Gel shift assay (functional assay of MsrB3A)-II**

- A. SDS-PAGE gel representing the shift in the mobility of oxidised SurA samples when treated with different concentrations (1X, 2X, 5X, 10X, 100X and 1000X dilution) of MsrB3A represented by lanes 3 to 8 under reducing conditions, in the presence of DTT. Lanes 1 and 2 contains untreated or native SurA sample and oxidised SurA samples, respectively.
- B. SDS-PAGE gel representing the shift in the mobility of oxidised SurA when treated with different concentrations (1X, 2X, 5X, 10X, 100X and 1000X dilution) of MsrB3A represented by lanes 3 to 8 under non-reducing conditions, in the in absence of DTT.
- C. SDS-PAGE gel representing shift in SurA mobility when treated with equal concentrations of MsrB3A or MsrB3A C126A mutant in presence and absence of DTT, alternatively and are represented by the lanes 3 to 6.

### **5.3 Discussions**

From the results obtained above, we could predict the following conclusions from the gel shift assay, though the results obtained do not hold much significance and are mostly not clear to draw definite conclusions. First, the MsrB3A protein might be stereo-specific in nature, as all the figures indicate a slight shift in the mobility of the oxidised SurA when it is treated with MsrB3A enzyme, but the shift does not occur all the way to the original mobility indicating that SurA is partially repaired and a fraction of methionine residues might still be oxidised. Similar situation was also observed by Gennaris et al., 2015, when they had treated the oxidised SurA with MsrP enzyme only in contrast to the treatment of the oxidised SurA by MsrPQ reduction system, which could successfully reduce the oxidised SurA back to its native form. But the stereoisomer that is reduced by MsrB3A is still not confirmed, though from literature it is said to be R-isomer of methionine sulfoxide (Kim and Gladyshev, 2004b). Hence, we need to have further experiments to prove that R-form of methionine sulfoxide is reduced by MsrB3A.

From the literature, it is known that DTT cannot reduce oxidised methionine residues in SurA and requires a reagent with higher reducing strength (Gennaris et al., 2015). The same was also observed in Fig. 5.6 panel A. The oxidised SurA had no effect in the reducing environment caused by the presence of DTT, hence, the mobility shift of oxidised SurA was observed, indicating SurA is independent of reduction by DTT and requires Msrs to be reduced back to its native state.

In Fig. 5.6 panel C, we can observe that there is no difference in the mobility shifts when oxidised SurA was treated with wild-type MsrB3A and C126A MsrB3A mutant. This indicates that either the C126A MsrB3A mutant was functional and the mutation of cysteine does not affect the protein activity of MsrB3A or there is no separation at all. This is mainly attributed for the low resolution of the gel, which could be responsible for the negligible to no separation observation.

Although, the gel shift assay is a cheap and easy way to determine the protein function of Msrs, the lack of clear and definitive separation of the oxidised and repaired forms in our experiments clearly indicates the drawbacks of this method. To obtain clear and distinct bands with good separation, the gel shift assay requires a lot of manipulation and optimisation of different factors involved with SDS-PAGE

electrophoresis. For example, the sample concentration added to the SDS-PAGE gels requires a lot of trial and error to obtain distinct and sharp bands, which could help distinguish and analyse protein function. Percentage composition of the SDS-PAGE gels and the voltage applied across the gel are some other factors which govern the success of this technique. Another major drawback of the technique is that it cannot identify the stereo-specificity of the Msr enzyme, unless a pure Msr enzyme of known origin and function with high degree of purity is used in conjugation with our target Msr. Hence, the overall conclusion which could be made is that the results obtained by gel shift assay is not credible enough to draw adequate conclusions and requires further experimentation to get better results.

Yet, with further experimentation and better understanding of the different methionine-rich proteins, the gel shift assay could be effectively used in future for establishing the function of different Msrs.

#### **5.4 Future work**

To improve the results obtained by gel shift assay, we can experiment further with different percentage gels, preferably on 7.5% and 12.5% SDS-PAGE gels to determine which offers better separation. Optimisation of the voltage applied across the gel or current flowing through the gel would help further benefit the get better resolution.

Other future experiments which could be done include the use of MsrA-MsrB3A conjugate system in presence of DTT, which might help us to determine the true stereo-specificity of MsrB3A, provided the MsrA enzyme used is from a known origin and of high purity. Use of other methionine-rich proteins which has a better separation between their oxidised and reduced states.

# Chapter 6: MsrB3A functional assay II- HPLC assay

---

## 6.1 Introduction

In the previous chapter, we discussed the different types of assays used for determining the function of different Msrs throughout literature. A recent technique which has emerged to determine the functions of Msrs is the gel shift assay which we described in detail in the last chapter. Although the gel shift assay is a cheap and easy technique to perform, it has several drawbacks. First it could not provide a clear overview of the MsrB3A function, due to the lack of definitive separation between the oxidised and repaired states of the methionine-rich proteins (in this case SurA). Secondly, it lacks the ability to identify the stereo-specificity of the Msr enzyme unless conjugated with an Msr of known function and origin. Therefore, the HPLC assay is another method which is widely used to have a better understanding of the MsrB3A function and help to evaluate the results obtained from gel shift assay.

The method utilises the dabsylated derivatives of methionine sulfoxide and methionine (Minetti et al., 1994), thus making it easier to observe the reduction of methionine sulfoxide to methionine by monitoring the absorption of light at 436 nm (Kryukov et al., 2002). Also, both dabsylated methionine sulfoxide and dabsylated methionine have different retention time within the reverse phase HPLC column. Hence, they could be separated easily from each other. The major advantage of this technique is its high accuracy and sensitivity, with minimum requirement of reaction substrates. Another advantage of this method is that, individual dabsylated isoforms, i.e., either the methionine-R-sulfoxide or methionine-S-sulfoxide or a racemic mixture of methionine-RS-sulfoxide could be synthesised for study of the Msr function. The drawback of the technique includes the utilisation of the HPLC system which requires skilled labour for handling and the substrate preparation which is difficult and time consuming. Although, recent developments in the HPLC

system has made the use of such systems more user-friendly, hence, allowing greater possibility of the use of this technique.

From sequence alignment (Fig. 3.1), we notice that the MsrB sequences have 5 sets of conserved cysteine residues. From the literature, we know that four of the cysteine residues organised in form of -CXXC- motifs are responsible for Zn<sup>2+</sup> binding (Kumar et al., 2002) and the conserved cysteine residue present towards the C-terminal region of the MsrB sequence might be responsible for enzyme catalysis due to the presence of seleno-cysteine (represented as U in the amino acid sequence) residue in mammalian MsrB1 protein which is an indication of the catalytic residue involved in the redox processes (Kim and Gladyshev, 2007, Kim and Gladyshev, 2004b). Hence, we use an improved version of the HPLC assay as described by (Kumar et al., 2002), for determining the protein function of human MsrB3A protein and the results so obtained from the technique are described below in detail.

## **6.2 Results**

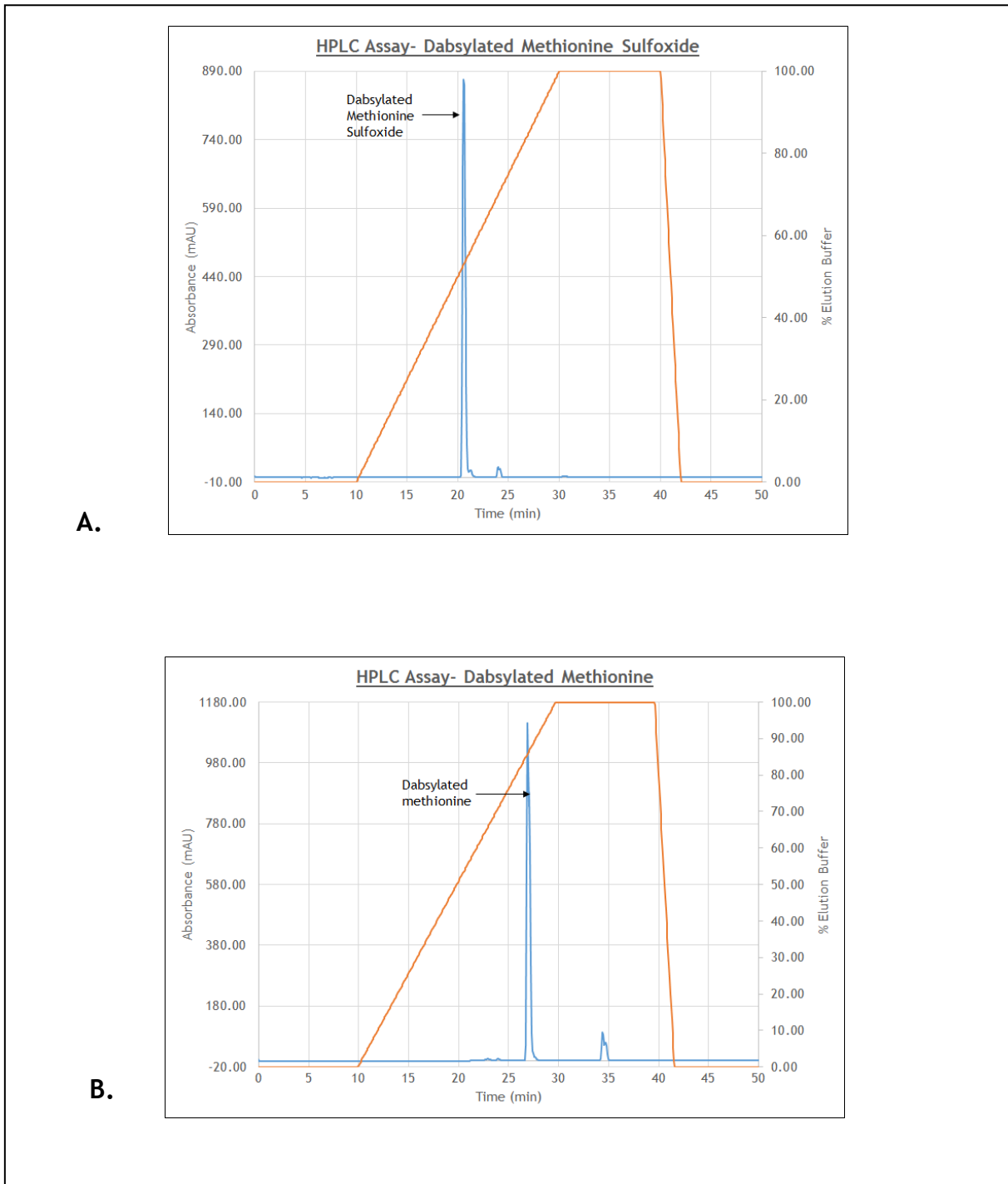
As stated earlier, the dabsyl group has maximum absorbance of light at 436 nm. Hence, the dabsylated methionine and dabsylated methionine sulfoxide were first eluted using the C-18 reverse phase column to determine their retention time in the column, to be used as reference for further experiments. Fig. 6.1 illustrates the typical HPLC elution profile of dabsylated methionine sulfoxide (panel A) and dabsylated methionine (panel B) respectively. As we can see from Fig. 6.1 panel A, dabsylated methionine sulfoxide elutes from the column after 20 minutes, while in panel B dabsylated methionine has a retention time of nearly 25 minutes.

As explained earlier in section 2.5.2, the dabsylated methionine sulfoxide was treated with MsrB3A in presence of DTT at different times- 5, 10, 20 and 30 minutes. The reaction was then stopped using 0.5% SDS and the reaction products were separated using the C-18 reverse phase chromatography column. Fig. 6.2 illustrates the elution profile of dabsylated methionine and methionine sulfoxide obtained after treatment with MsrB3A at different time intervals. As we can clearly observe in Fig. 6.2, only a part of the dabsylated methionine sulfoxide is reduced back to methionine (approximately half the peak size obtained for dabsylated methionine sulfoxide), as a racemic mixture of dabsylated methionine-RS-sulfoxide was used as substrate. This could be due to the other isoform of methionine sulfoxide which is not a substrate for MsrB3A, also verifying that the enzyme is stereo-specific in nature, as stated by (Kryukov et al., 2002) as well. Although, only half the fraction of the dabsylated methionine sulfoxide gets reduced, whether it is the R- or S- isoform of methionine sulfoxide being reduced, is still required to be proved by further experimentation.

It can also be observed that the elution peak of dabsylated methionine becomes constant after 10 minutes and no net changes are observed in the peaks, indicating that the reaction takes only about 10 minutes to complete in presence of a recycling environment (in this case provided by DTT).

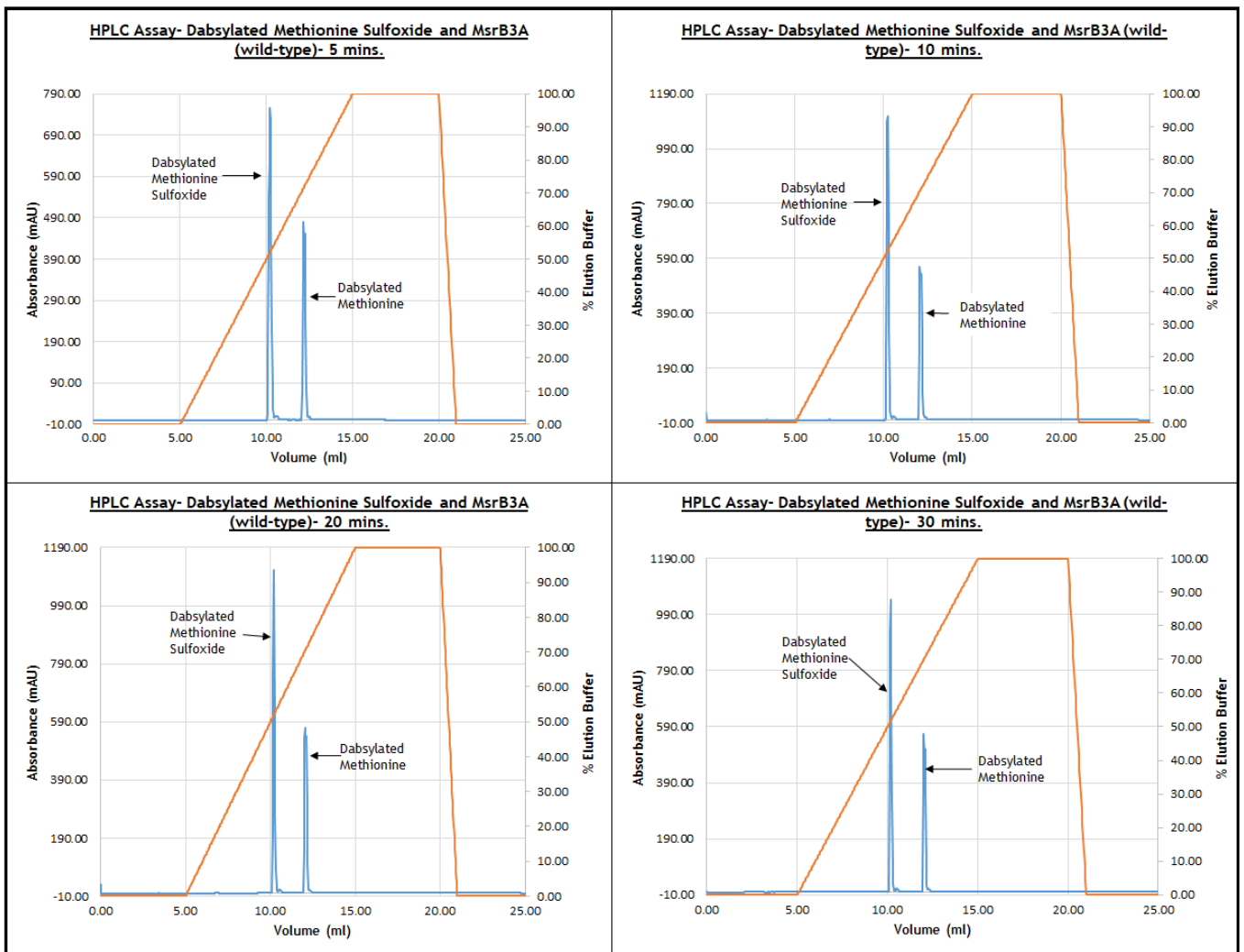
Another observation is that the peak for dabsylated methionine occurs at 25 minutes rather than after it, as shown in Fig. 6.1 panel B. This is due to difference in the flow rates. The flow rate of the reference dabsylated methionine was 0.45 ml/min, while flow rate used in the functional assay was 0.5 ml/min, resulting in the difference in the retention time.

Fig. 6.3 represents the elution profile of dabsylated methionine sulfoxide when it was treated with MsrB3A C126A mutant in presence of DTT. As we can observe, there is no difference in the elution profile between elution profile for dabsylated methionine sulfoxide and the elution profile obtained when dabsylated methionine sulfoxide was treated with the C126A MsrB3A mutant protein. This indicates 2 major aspects. First, the mutant is non-functional and is unable to reduce the dabsylated methionine sulfoxide. Secondly, the 126<sup>th</sup> position cysteine that was mutated (substituted with alanine) is required for the proper functioning of the protein, and might be present in the active site of the protein. Similar results were also obtained by (Kumar et al., 2002), indicating that the 126<sup>th</sup> position cysteine is the catalytic cysteine responsible for reducing the methionine sulfoxide to methionine.



**Figure 6.1: HPLC assay**

- A. Graph representing a typical elution profile of dabsylated methionine sulfoxide represented by the blue curve, while the gradient of the elution buffer is expressed by the orange curve.
- B. Graph representing a typical elution profile of dabsylated methionine represented by the blue curve, while the gradient of the elution buffer is represented by the orange curve.



**Figure 6.2: HPLC assay:** Graphs representing the typical elution profile of dabsylated methionine sulfoxide and methionine after treatment of dabsylated methionine sulfoxide for 5, 10, 20 and 30 minutes with MsrB3A in presence of DTT, shown by the curve in blue. The orange curve shows the gradient profile for the elution buffer.

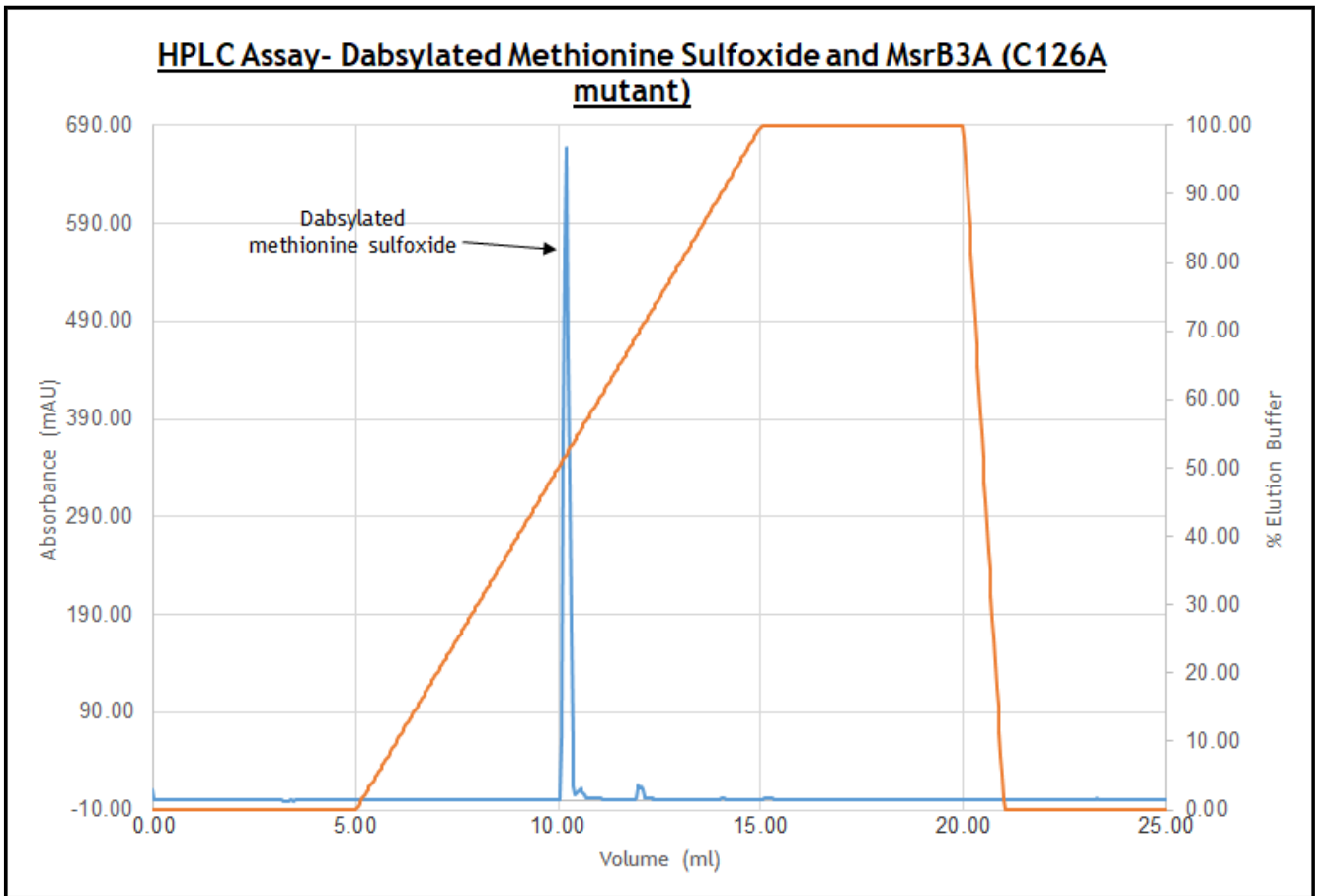


**Figure 6.3: HPLC assay:** Graph representing the typical elution profile of dabsylated methionine sulfoxide after treatment with MsrB3A C126A mutant for 30 minutes in presence of DTT, shown by the blue curve. The orange curve represents the gradient profile for the elution buffer.

### 6.3 Discussions

From the results obtained by HPLC assay, we can conclude that the MsrB3A protein is stereo-specific in nature as we can clearly observe in Fig. 6.2. Since, only a part of the dabsylated methionine sulfoxide is reduced back to methionine by treatment of dabsylated methionine sulfoxide with MsrB3A in presence of DTT, along with the appearance of dabsylated methionine curve clearly indicates that MsrB3A is stereospecific in nature. But the stereospecificity type of MsrB3A could not be answered in the experiment as dabsylated methionine-RS-sulfoxide was used as substrate for the experiment. Though from literature, we know that MsrB3A is specific for the R-form of methionine sulfoxide (Kim and Gladyshev, 2004b), but further experiments involving only dabsylated methionine-R-sulfoxide should be used as substrate for reduction (as stated by (Kumar et al., 2002)) or a MsrA protein of known function, origin and high purity should be used in conjugation with MsrB3A protein for future experiments to identify the stereo-specificity of MsrB3A protein.

Another noticeable feature is that, the reduction of dabsylated methionine sulfoxide only takes 10 minutes to complete, as observed in Fig. 6.2 panels A to D. We observe no change in the elution peak of the dabsylated methionine obtained after 10 minutes in the further experiments. This could help us determine the specific reactivity of MsrB3A protein on further experimentation by plotting the substrate consumption against the time spent for reduction at 1 minute intervals.

Fig. 6.3 illustrates the HPLC assay of dabsylated methionine sulfoxide when treated with C126A MsrB3A mutant. As we can clearly observe that there is no reduction which takes place signifying that the mutant is non-functional. Contrary to the results obtained by gel shift assay, the HPLC assay clearly suggests that the C126A MsrB3A mutant protein was non-functional and that the 126<sup>th</sup> position cysteine could be a catalytic cysteine which is present at the active site of the protein as stated by (Kumar et al., 2002) and shown as a conserved residue in multiple sequence alignment (Fig. 3.1).

Although, the HPLC assay has provided us with valuable insight in to the function of MsrB3A to understand the functional mechanism of MsrB3A enzyme, further experiments are required which are discussed in detail the next section.

## **6.4 Future work**

First step is to identify the stereo-specificity of MsrB3A protein by either analysing the reduction of dabsylated methionine-R-sulfoxide as stated by (Kumar et al., 2002) or by using MsrA enzyme of known function, origin and high purity in conjugation with MsrB3A protein to reduce the dabsylated methionine-RS-sulfoxide utilising the same procedure used initially for determination of MsrB3A function.

Following determination of MsrB3A stereo-specificity, kinetic studies to determine the specific reactivity of MsrB3A experimentally should be done by plotting the amount of substrate consumption with respect to time at 1 minute time intervals.

Similar HPLC assay experiments involving protein based reducing systems such as the thioredoxin reducing system, should be performed to represent the biological conditions present in the cell to understand the functionality of MsrB3A better.

To understand the reaction mechanism of MsrB3A, several mutants needs to be made by identifying the conserved amino acid residues from multiple sequence alignment and mutating them as stated by (Kumar et al., 2002), to better understand the reaction mechanism of MsrB3A and the corresponding structural impacts on MsrB3A protein.

# Conclusions

---

## **7.1 Introduction**

Although, we can conclude from our results that the recombinant MsrB3A protein which was expressed and purified from the recombinant *E. coli* cells was functional and might have the correct structural conformation. Yet further experimental work would be essential to determine the stereo-specificity of MsrB3A protein, its structure and the mode of action at the functional site as discussed in the chapters 3 to 4.

Despite the further works required to obtain more information to better understand MsrB3A, there are still many questions that are unanswered. As we have discussed earlier, MsrB3 protein in humans has two isoforms- MsrB3A and MsrB3B, which are located within the endoplasmic reticulum and mitochondria, respectively (Kim and Gladyshev, 2004b). This is unique only to humans, though MsrB3B homologue is also present within the mouse genome but not expressed in mice (Kim and Gladyshev, 2004a). Hence, to understand the significance of MsrB3A protein in the endoplasmic reticulum of human cells, it is important to work on the following conditions which are discussed in the following sections.

## **7.2 Potential substrates for MsrB3A in human endoplasmic reticulum**

Several studies have been made to determine methionine-rich proteins which are the active substrates for methionine sulfoxide reductases mostly in bacteria (Le et al., 2008). Recent studies have also found certain methionine-rich repeat proteins occurring in the membrane of higher organisms (Weiss et al., 2005). However, in higher organisms such as the mammalian cells, the situation is more complicated. Due to the presence of multiple isoforms of MsrB which occur individually within different cellular compartments, as well as, differ in their mode of action and substrate affinity. Unlike bacteria, the potential substrates for the MsrB protein within different cellular components of the eukaryotic cells are also not clear, because of the diverse environment within the cellular compartments. Recently, it

has been reported that methionine sulfoxide reductases are more efficient in reducing methionine sulfoxide in unfolded proteins than in folded proteins and their activities increase with greater degree of unfolding in the proteins, hence, serving the critical function in folding of proteins by repairing the damaged nascent polypeptides and unfolded proteins produced due to oxidative stress (Tarrago et al., 2012). Since, MsrB3A is present within the endoplasmic reticulum of human cells, hence, potential substrates found in the ER would be of great importance and play vital roles in understanding human diseases at molecular level.

From sequence analysis (Fig. 3.1) it was assumed that the cysteine residue at the 126<sup>th</sup> position of the MsrB3A amino acid chain is an active site residue. By help of our experiments it could be said that the 126<sup>th</sup> position cysteine is also responsible for the function of MsrB3A. Yet the structural information related to MsrB3A mutants such as, C126A MsrB3A mutant would be essential to confirm it. Also, potential substrates for MsrB3A protein within the endoplasmic reticulum of human cells are still unknown which could provide us with more insight in to MsrB3A function. Thus, using site-directed mutagenesis, we can create a mutant by substituting the asparagine residue (conserved) at the 128<sup>th</sup> position in the amino acid chain to aspartate with the aim of trapping the covalent intermediate between the enzyme and substrate through Pummerer reaction of the bound sulfoxide. This mutant would then enable us to identify potential substrates for MsrB3A in cells, as any conjugate formed could then be isolated and identified using mass spectroscopy.

Another advantage which could be achieved from finding the potential substrates would be their link with potential human disorders such as Alzheimer's disease, cancer, etc., which can then be studied further to either decrease the detrimental effects caused by the diseases or essentially cure them.

### **7.3 Enzyme kinetics and substrate affinity of MsrB3A within the ER**

From the literature, we know that, MsrB3A and MsrB3B are two isoforms of MsrB3 protein that occur exclusively in human due to alternative splicing, but are targeted to the endoplasmic reticulum and mitochondria, respectively. Genomic analysis of the matured MsrB3A and MsrB3B genes has revealed that presence of six and eight exons within MsrB3A and MsrB3B, respectively. Although the sequence of

MsrB3A and MsrB3B are almost identical, the presence of the extra two exons in MsrB3B could be the signal peptide targeting MsrB3B to the mitochondria. From the analysis of MsrB2 and MsrB3B activity in the mitochondria, it was noted that MsrB3B was highly active when the concentration of methionine sulfoxide was greater than 1 mM. From sequence analysis, it could be clearly observed that the functional portion of MsrB3A and MsrB3B were identical. Hence, it can be predicted that the activity of MsrB3A within the endoplasmic reticulum is the same as MsrB3B (Kim and Gladyshev, 2004b).

#### **7.4 Determination of physiological role of MsrB3A during oxidative stress**

With the identification of potential substrates of MsrB3A in the human cells and determination of the enzyme activity in the endoplasmic reticulum, the next step is to understand the physiological role of MsrB3A within the endoplasmic reticulum.

Throughout the literature, there are indirect references which relate methionine oxidation with human disorders such as breast cancer, Alzheimer's disease, human deafness with age and many other age-related disorders (Gonias et al., 1988, De Luca et al., 2010, Butterfield and Kanski, 2002, Ahmed et al., 2011). In most cases, it was observed that the oxidation of methionine residue caused by the ROS induced oxidative stress led to alteration in the conformation of the proteins if not repaired, thereby, leading to loss in essential protein function. Unless the oxidised methionine residues are repaired by the Msr enzymes, they tend to increase the oxidative stress. Studies related to over-expression of different Msrs has shown that there is increase in the resistance against oxidative stress, with down-regulation of age-related disorders and increase in the life-span. For example, expression studies conducted on *Drosophila* and mammalian cells over-expressing the MsrB3A protein has shown to increase the oxidative stress resistance in the cells and increasing their life-span (Kwak et al., 2012).

Hence, to understand the physiological role of MsrB3A within the endoplasmic reticulum of human cells, we need to generate knock-out cell lines from immortalised cell lines such as, HT1080, HEK293 or HeLa cell lines, which are

deficient in *Msrb3A* gene, using CRISPR-Cas 9 technology and then study the effects of the susceptibility of the ER proteins to methionine oxidation.

## **7.5 Other areas of research**

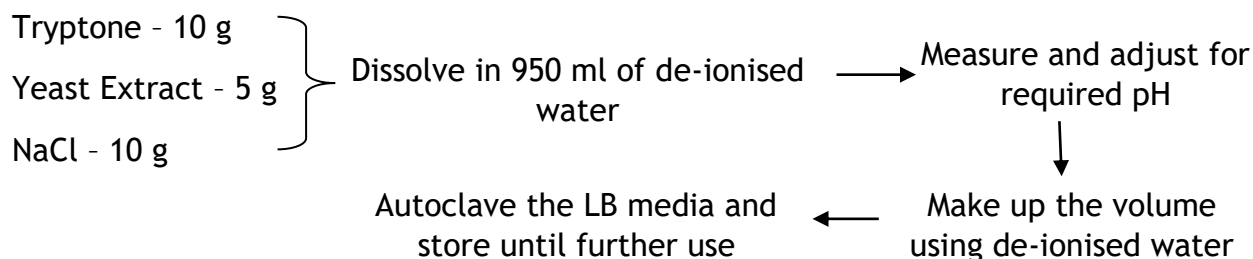
Although, we need to perform the above experiments to have a detailed understanding of the role of *Msrb3A* within the ER of human cells, there are still some areas which are unknown and require further investigation. The first being that *Msrb3A* is predicted to be involved only in the reduction of methionine-R-sulfoxide. However, in mammals there is only one gene that encodes for *Msra* and no additional genes could be revealed from BLAST analysis. It is still unclear whether the single gene is responsible to generate multiple protein products which get targeted to different cellular compartments or some unknown *Msra* gene is still present which is yet to be found. Experimental studies have shown that *Msra* is present in the mitochondria and cytosol of the cells (Hansel et al., 2002, Vouquier et al., 2003). But no such evidence has been found that supports the presence of *Msra* within the endoplasmic reticulum or the nucleus of the cell. A viable explanation to this could be the presence of certain epimerase enzyme which might be responsible for the conversion of the S-form to R-form of methionine sulfoxide, thereby, preventing the accumulation of methionine-S-sulfoxide and inhibiting oxidative stress (Kim and Gladyshev, 2004b).

Another area which needs investigation is the process by which *Msrb3A* function is recycled back. Though we will be able to know this clearly when the *Msrb3A* structure is determined, as it would provide us a detailed insight as to how the enzyme activity gets recycled within the ER. It is predicted that either a resolving cysteine is present very near to the active site cysteine or the protein activity is recycled by thioredoxin using the thioredoxin reductase reducing system which is present in the ER and would be a member of the protein disulphide reductase family.

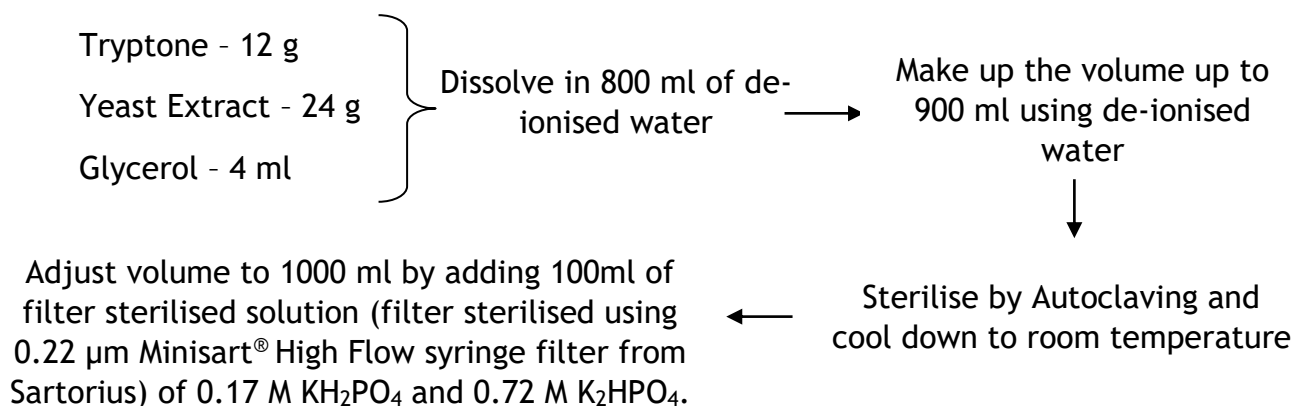
# Appendix

---

## A. Luria Broth (LB) Media (1l)



## B. Terrific Broth (TB) Media (1l)



## C. <sup>15</sup>N-labelling Media (M9 Minimal Media)

### M9 medium (10X); (for 1L)

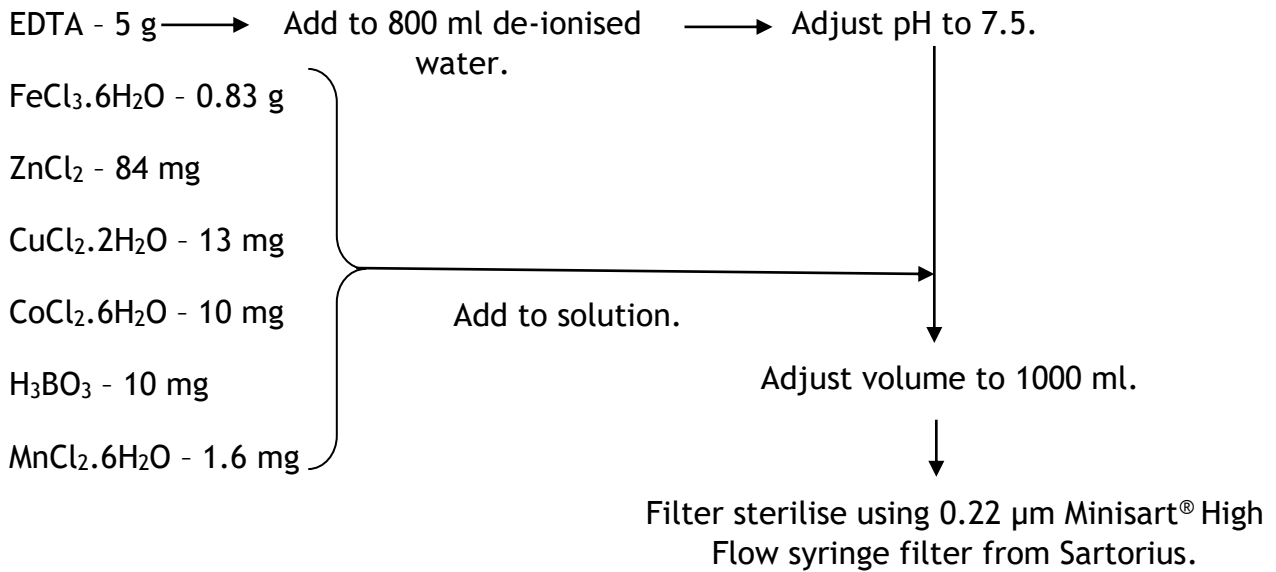
Na<sub>2</sub>HPO<sub>4</sub> - 60 g

KH<sub>2</sub>PO<sub>4</sub> - 30 g

NaCl - 5 g

<sup>15</sup>NH<sub>4</sub>Cl - 5 g (should be freshly prepared, filter sterilised using 0.22 µm Minisart® High Flow syringe filter from Sartorius and added at the end in the final medium @ 0.6 g / (L of medium)).

Trace element solution (100X); (for 1L)



<sup>15</sup>N-labelling media

M9 medium (10X) - 100 ml

Trace element solution (100X) - 10 ml

20% (w/v) glucose solution - 20 ml

1M MgSO<sub>4</sub> solution - 1 ml

1M CaCl<sub>2</sub> solution - 0.3 ml

1 mg/ml Biotin solution - 1 ml

1 mg/ml Thiamine solution - 1 ml

Filter sterilised using 0.22 µm Minisart® High Flow syringe filter from Sartorius.

Note: - The appropriate antibiotic and IPTG solution added to the media were also filter sterilised using 0.22 µm Minisart® High Flow syringe filter from Sartorius.

# List of references

---

- AACHMANN, F. L., SAL, L. S., KIM, H. Y., MARINO, S. M., GLADYSHEV, V. N. & DIKIY, A. 2010. Insights into function, catalytic mechanism, and fold evolution of selenoprotein methionine sulfoxide reductase B1 through structural analysis. *J Biol Chem*, 285, 33315-23.
- AHMED, Z. M., YOUSAF, R., LEE, B. C., KHAN, S. N., LEE, S., LEE, K., HUSNAIN, T., REHMAN, A. U., BONNEUX, S., ANSAR, M., AHMAD, W., LEAL, S. M., GLADYSHEV, V. N., BELYANTSEVA, I. A., VAN CAMP, G., RIAZUDDIN, S. & FRIEDMAN, T. B. 2011. Functional null mutations of MSRB3 encoding methionine sulfoxide reductase are associated with human deafness DFNB74. *Am J Hum Genet*, 88, 19-29.
- ANTOINE, M., BOSCHI-MULLER, S. & BRANLANT, G. 2003. Kinetic characterization of the chemical steps involved in the catalytic mechanism of methionine sulfoxide reductase A from *Neisseria meningitidis*. *J Biol Chem*, 278, 45352-7.
- BECHTOLD, U., MURPHY, D. J. & MULLINEAUX, P. M. 2004. Arabidopsis peptide methionine sulfoxide reductase2 prevents cellular oxidative damage in long nights. *Plant Cell*, 16, 908-19.
- BERLETT, B. S., LEVINE, R. L. & STADTMAN, E. R. 1998. Carbon dioxide stimulates peroxynitrite-mediated nitration of tyrosine residues and inhibits oxidation of methionine residues of glutamine synthetase: both modifications mimic effects of adenylylation. *Proc Natl Acad Sci U S A*, 95, 2784-9.
- BLACK, D. L. 2003. Mechanisms of alternative pre-messenger RNA splicing. *Annu Rev Biochem*, 72, 291-336.
- BOSCHI-MULLER, S., AZZA, S., SANGLIER-CIANFERANI, S., TALFOURNIER, F., VAN DORSSELEAR, A. & BRANLANT, G. 2000. A sulfenic acid enzyme intermediate is involved in the catalytic mechanism of peptide methionine sulfoxide reductase from *Escherichia coli*. *J Biol Chem*, 275, 35908-13.
- BOSCHI-MULLER, S. & BRANLANT, G. 2014. Methionine sulfoxide reductase: chemistry, substrate binding, recycling process and oxidase activity. *Bioorg Chem*, 57, 222-30.
- BOSCHI-MULLER, S., OLRV, A., ANTOINE, M. & BRANLANT, G. 2005. The enzymology and biochemistry of methionine sulfoxide reductases. *Biochim Biophys Acta*, 1703, 231-8.
- BROT, N. & WEISSBACH, H. 1991. Biochemistry of methionine sulfoxide residues in proteins. *Biofactors*, 3, 91-6.
- BROT, N., WEISSBACH, L., WERTH, J. & WEISSBACH, H. 1981. Enzymatic reduction of protein-bound methionine sulfoxide. *Proc Natl Acad Sci U S A*, 78, 2155-8.
- BROT, N., WERTH, J., KOSTER, D. & WEISSBACH, H. 1982. Reduction of N-acetyl methionine sulfoxide: a simple assay for peptide methionine sulfoxide reductase. *Anal Biochem*, 122, 291-4.
- BUTTERFIELD, D. A. & KANSKI, J. 2002. Methionine residue 35 is critical for the oxidative stress and neurotoxic properties of Alzheimer's amyloid beta-peptide 1-42. *Peptides*, 23, 1299-309.
- CHAO, C. C., MA, Y. S. & STADTMAN, E. R. 1997. Modification of protein surface hydrophobicity and methionine oxidation by oxidative systems. *Proc Natl Acad Sci U S A*, 94, 2969-74.
- CIORBA, M. A., HEINEMANN, S. H., WEISSBACH, H., BROT, N. & HOSHI, T. 1997. Modulation of potassium channel function by methionine oxidation and reduction. *Proc Natl Acad Sci U S A*, 94, 9932-7.
- DADO, G. P. & GELLMAN, S. H. 1993. Redox control of secondary structure in a designed peptide. *Journal of the American Chemical Society*, 115, 12609-12610.
- DE LUCA, A., SANNA, F., SALLESE, M., RUGGIERO, C., GROSSI, M., SACCHETTA, P., ROSSI, C., DE LAURENZI, V., DI ILIO, C. & FAVALORO, B. 2010. Methionine sulfoxide reductase A down-regulation in human breast cancer cells results in a more aggressive phenotype. *Proc Natl Acad Sci U S A*, 107, 18628-33.
- DOKAINISH, H. M. & GAULD, J. W. 2013. A molecular dynamics and quantum mechanics/molecular mechanics study of the catalytic reductase mechanism of methionine sulfoxide reductase A: formation and reduction of a sulfenic acid. *Biochemistry*, 52, 1814-27.
- ETIENNE, F., SPECTOR, D., BROT, N. & WEISSBACH, H. 2003. A methionine sulfoxide reductase in *Escherichia coli* that reduces the R enantiomer of methionine sulfoxide. *Biochem Biophys Res Commun*, 300, 378-82.

- EZRATY, B., AUSSEL, L. & BARRAS, F. 2005. Methionine sulfoxide reductases in prokaryotes. *Biochimica et Biophysica Acta - Proteins and Proteomics*, 1703, 221-229.
- GABBITA, S. P., AKSENOV, M. Y., LOVELL, M. A. & MARKESBERY, W. R. 1999. Decrease in peptide methionine sulfoxide reductase in Alzheimer's disease brain. *J Neurochem*, 73, 1660-6.
- GARNER, B., WALDECK, A. R., WITTING, P. K., RYE, K. A. & STOCKER, R. 1998. Oxidation of high density lipoproteins. II. Evidence for direct reduction of lipid hydroperoxides by methionine residues of apolipoproteins AI and AII. *J Biol Chem*, 273, 6088-95.
- GENNARIS, A., EZRATY, B., HENRY, C., AGREBI, R., VERGNES, A., OHEIX, E., BOS, J., LEVERRIER, P., ESPINOSA, L., SZEWCZYK, J., VERTOMMEN, D., IRANZO, O., COLLET, J. F. & BARRAS, F. 2015. Repairing oxidized proteins in the bacterial envelope using respiratory chain electrons. *Nature*, 528, 409-12.
- GETZ, E. B., XIAO, M., CHAKRABARTY, T., COOKE, R. & SELVIN, P. R. 1999. A comparison between the sulfhydryl reductants tris(2-carboxyethyl)phosphine and dithiothreitol for use in protein biochemistry. *Anal Biochem*, 273, 73-80.
- GOEMANS, C., DENONCIN, K. & COLLET, J. F. 2014. Folding mechanisms of periplasmic proteins. *Biochim Biophys Acta*, 1843, 1517-28.
- GONIAS, S. L., SWAIM, M. W., MASSEY, M. F. & PIZZO, S. V. 1988. cis-dichlorodiammineplatinum (II) as a selective modifier of the oxidation-sensitive reactive-center methionine in alpha 1-antitrypsin. *J Biol Chem*, 263, 393-7.
- GONZALEZ PORQUE, P., BALDESTEN, A. & REICHARD, P. 1970. The involvement of the thioredoxin system in the reduction of methionine sulfoxide and sulfate. *J Biol Chem*, 245, 2371-4.
- GRIMAUD, R., EZRATY, B., MITCHELL, J. K., LAFITTE, D., BRIAND, C., DERRICK, P. J. & BARRAS, F. 2001. Repair of oxidized proteins. Identification of a new methionine sulfoxide reductase. *J Biol Chem*, 276, 48915-20.
- HANSEL, A., KUSCHEL, L., HEHL, S., LEMKE, C., AGRICOLA, H. J., HOSHI, T. & HEINEMANN, S. H. 2002. Mitochondrial targeting of the human peptide methionine sulfoxide reductase (MSRA), an enzyme involved in the repair of oxidized proteins. *FASEB J*, 16, 911-3.
- HATFIELD, D. L. & GLADYSHEV, V. N. 2002. How selenium has altered our understanding of the genetic code. *Mol Cell Biol*, 22, 3565-76.
- JUNG, S., HANSEL, A., KASPERCZYK, H., HOSHI, T. & HEINEMANN, S. H. 2002. Activity, tissue distribution and site-directed mutagenesis of a human peptide methionine sulfoxide reductase of type B: hCBS1. *FEBS Lett*, 527, 91-4.
- KIM, G., COLE, N. B., LIM, J. C., ZHAO, H. & LEVINE, R. L. 2010. Dual sites of protein initiation control the localization and myristoylation of methionine sulfoxide reductase A. *J Biol Chem*, 285, 18085-94.
- KIM, H. Y. & GLADYSHEV, V. N. 2004a. Characterization of mouse endoplasmic reticulum methionine-R-sulfoxide reductase. *Biochemical and Biophysical Research Communications*, 320, 1277-1283.
- KIM, H. Y. & GLADYSHEV, V. N. 2004b. Methionine sulfoxide reduction in mammals: characterization of methionine-R-sulfoxide reductases. *Molecular Biology of the Cell*, 15, 1055-1064.
- KIM, H. Y. & GLADYSHEV, V. N. 2005a. Different catalytic mechanisms in mammalian selenocysteine- and cysteine-containing methionine-R-sulfoxide reductases. *PLoS Biol*, 3, e375.
- KIM, H. Y. & GLADYSHEV, V. N. 2005b. Role of structural and functional elements of mouse methionine-S-sulfoxide reductase in its subcellular distribution. *Biochemistry*, 44, 8059-67.
- KIM, H. Y. & GLADYSHEV, V. N. 2007. Methionine sulfoxide reductases: selenoprotein forms and roles in antioxidant protein repair in mammals. *Biochem J*, 407, 321-9.
- KRYUKOV, G. V., KUMAR, R. A., KOC, A., SUN, Z. & GLADYSHEV, V. N. 2002. Selenoprotein R is a zinc-containing stereo-specific methionine sulfoxide reductase. *Proc Natl Acad Sci U S A*, 99, 4245-50.
- KUMAR, R. A., KOC, A., CERNY, R. L. & GLADYSHEV, V. N. 2002. Reaction mechanism, evolutionary analysis, and role of zinc in *Drosophila* methionine-R-sulfoxide reductase. *J Biol Chem*, 277, 37527-35.
- KWAK, G. H., LIM, D. H., HAN, J. Y., LEE, Y. S. & KIM, H. Y. 2012. Methionine sulfoxide reductase B3 protects from endoplasmic reticulum stress in *Drosophila* and in mammalian cells. *Biochem Biophys Res Commun*, 420, 130-5.
- LE, D. T., LIANG, X., FOMENKO, D. E., RAZA, A. S., CHONG, C. K., CARLSON, B. A., HATFIELD, D. L. & GLADYSHEV, V. N. 2008. Analysis of methionine/selenomethionine oxidation and methionine sulfoxide reductase

- function using methionine-rich proteins and antibodies against their oxidized forms. *Biochemistry*, 47, 6685-94.
- LEVINE, R. L., MOSONI, L., BERLETT, B. S. & STADTMAN, E. R. 1996. Methionine residues as endogenous antioxidants in proteins. *Proc Natl Acad Sci U S A*, 93, 15036-40.
- LIU, C. Y. & KAUFMAN, R. J. 2003. The unfolded protein response. *J Cell Sci*, 116, 1861-2.
- LOWTHER, W. T., WEISSBACH, H., ETIENNE, F., BROT, N. & MATTHEWS, B. W. 2002. The mirrored methionine sulfoxide reductases of *Neisseria gonorrhoeae* pilB. *Nat Struct Biol*, 9, 348-52.
- MALHOTRA, J. D. & KAUFMAN, R. J. 2007. Endoplasmic reticulum stress and oxidative stress: a vicious cycle or a double-edged sword? *Antioxid Redox Signal*, 9, 2277-93.
- MINETTI, G., BALDUINI, C. & BROVELLI, A. 1994. Reduction of DABS-L-methionine-dl-sulfoxide by protein methionine sulfoxide reductase from polymorphonuclear leukocytes: stereospecificity towards the l-sulfoxide. *Ital J Biochem*, 43, 273-83.
- MORI, S., ABEYGUNAWARDANA, C., JOHNSON, M. O. & VAN ZIJL, P. C. 1995. Improved sensitivity of HSQC spectra of exchanging protons at short interscan delays using a new fast HSQC (FHSQC) detection scheme that avoids water saturation. *J Magn Reson B*, 108, 94-8.
- MOSKOVITZ, J. 2005. Methionine sulfoxide reductases: ubiquitous enzymes involved in antioxidant defense, protein regulation, and prevention of aging-associated diseases. *Biochim Biophys Acta*, 1703, 213-9.
- MOSKOVITZ, J., BERLETT, B. S., POSTON, J. M. & STADTMAN, E. R. 1997. The yeast peptide-methionine sulfoxide reductase functions as an antioxidant in vivo. *Proc Natl Acad Sci U S A*, 94, 9585-9.
- MOSKOVITZ, J., POSTON, J. M., BERLETT, B. S., NOSWORTHY, N. J., SZCZEPANOWSKI, R. & STADTMAN, E. R. 2000. Identification and characterization of a putative active site for peptide methionine sulfoxide reductase (MsrA) and its substrate stereospecificity. *J Biol Chem*, 275, 14167-72.
- MOSKOVITZ, J., SINGH, V. K., REQUENA, J., WILKINSON, B. J., JAYASWAL, R. K. & STADTMAN, E. R. 2002. Purification and characterization of methionine sulfoxide reductases from mouse and *Staphylococcus aureus* and their substrate stereospecificity. *Biochem Biophys Res Commun*, 290, 62-5.
- MOSKOVITZ, J., WEISSBACH, H. & BROT, N. 1996. Cloning the expression of a mammalian gene involved in the reduction of methionine sulfoxide residues in proteins. *Proc Natl Acad Sci U S A*, 93, 2095-9.
- NAKAO, L. S., IWAI, L. K., KALIL, J. & AUGUSTO, O. 2003. Radical production from free and peptide-bound methionine sulfoxide oxidation by peroxynitrite and hydrogen peroxide/iron(II). *FEBS Lett*, 547, 87-91.
- NOVOSELOV, S. V., RAO, M., ONOSHKO, N. V., ZHI, H., KRYUKOV, G. V., XIANG, Y., WEEKS, D. P., HATFIELD, D. L. & GLADYSHEV, V. N. 2002. Selenoproteins and selenocysteine insertion system in the model plant cell system, *Chlamydomonas reinhardtii*. *EMBO J*, 21, 3681-93.
- OLRY, A., BOSCHI-MULLER, S., MARRAUD, M., SANGLIER-CIANFERANI, S., VAN DORSSELEAR, A. & BRANLANT, G. 2002. Characterization of the methionine sulfoxide reductase activities of PILB, a probable virulence factor from *Neisseria meningitidis*. *J Biol Chem*, 277, 12016-22.
- POGOCKI, D. 2003. Alzheimer's beta-amyloid peptide as a source of neurotoxic free radicals: the role of structural effects. *Acta Neurobiol Exp (Wars)*, 63, 131-45.
- PROVENCHER, S. W. & GLÖCKNER, J. 1981. Estimation of globular protein secondary structure from circular dichroism. *Biochemistry*, 20, 33-7.
- RANAIVOSON, F. M., ANTOINE, M., KAUFFMANN, B., BOSCHI-MULLER, S., AUBRY, A., BRANLANT, G. & FAVIER, F. 2008. A structural analysis of the catalytic mechanism of methionine sulfoxide reductase A from *Neisseria meningitidis*. *J Mol Biol*, 377, 268-80.
- RANAIVOSON, F. M., NEIERS, F., KAUFFMANN, B., BOSCHI-MULLER, S., BRANLANT, G. & FAVIER, F. 2009. Methionine sulfoxide reductase B displays a high level of flexibility. *J Mol Biol*, 394, 83-93.
- REDDY, V. Y., DESORCHERS, P. E., PIZZO, S. V., GONIAS, S. L., SAHAKIAN, J. A., LEVINE, R. L. & WEISS, S. J. 1994. Oxidative dissociation of human alpha 2-macroglobulin tetramers into dysfunctional dimers. *J Biol Chem*, 269, 4683-91.
- REDDY, V. Y., PIZZO, S. V. & WEISS, S. J. 1989. Functional inactivation and structural disruption of human alpha 2-macroglobulin by neutrophils and eosinophils. *J Biol Chem*, 264, 13801-9.
- RILEY, M., ABE, T., ARNAUD, M. B., BERLYN, M. K., BLATTNER, F. R., CHAUDHURI, R. R., GLASNER, J. D., HORIUCHI, T., KESELER, I. M., KOSUGE, T., MORI, H., PERNA, N. T., PLUNKETT, G., RUDD, K. E., SERRES,

- M. H., THOMAS, G. H., THOMSON, N. R., WISHART, D. & WANNER, B. L. 2006. Escherichia coli K-12: a cooperatively developed annotation snapshot--2005. *Nucleic Acids Res*, 34, 1-9.
- ROBINET, J. J., DOKAINISH, H. M., PATERSON, D. J. & GAULD, J. W. 2011. A sulfonium cation intermediate in the mechanism of methionine sulfoxide reductase B: a DFT study. *J Phys Chem B*, 115, 9202-12.
- SCHONEICH, C. 2002. Redox processes of methionine relevant to beta-amyloid oxidation and Alzheimer's disease. *Arch Biochem Biophys*, 397, 370-6.
- SCHÖNEICH, C., POGOCKI, D., HUG, G. L. & BOBROWSKI, K. 2003. Free radical reactions of methionine in peptides: mechanisms relevant to beta-amyloid oxidation and Alzheimer's disease. *J Am Chem Soc*, 125, 13700-13.
- SCHÖNEICH, C., ZHAO, F., WILSON, G. S. & BORCHARDT, R. T. 1993. Iron-thiolate induced oxidation of methionine to methionine sulfoxide in small model peptides. Intramolecular catalysis by histidine. *Biochim Biophys Acta*, 1158, 307-22.
- SIGALOV, A. B. & STERN, L. J. 1998. Enzymatic repair of oxidative damage to human apolipoprotein A-I. *FEBS Lett*, 433, 196-200.
- SILHAVY, T. J., KAHNE, D. & WALKER, S. 2010. The bacterial cell envelope. *Cold Spring Harb Perspect Biol*, 2, a000414.
- SINGH, V. K., MOSKOVITZ, J., WILKINSON, B. J. & JAYASWAL, R. K. 2001. Molecular characterization of a chromosomal locus in Staphylococcus aureus that contributes to oxidative defence and is highly induced by the cell-wall-active antibiotic oxacillin. *Microbiology*, 147, 3037-45.
- SPECTOR, D., ETIENNE, F., BROT, N. & WEISSBACH, H. 2003. New membrane-associated and soluble peptide methionine sulfoxide reductases in Escherichia coli. *Biochem Biophys Res Commun*, 302, 284-9.
- SREERAMA, N. & WOODY, R. W. 2000. Estimation of protein secondary structure from circular dichroism spectra: comparison of CONTIN, SELCON, and CDSSTR methods with an expanded reference set. *Anal Biochem*, 287, 252-60.
- STADTMAN, E. R., MOSKOVITZ, J. & LEVINE, R. L. 2003. Oxidation of methionine residues of proteins: biological consequences. *Antioxid Redox Signal*, 5, 577-82.
- STADTMAN, T. C. 1996. Selenocysteine. *Annu Rev Biochem*, 65, 83-100.
- SUN, H., GAO, J., FERRINGTON, D. A., BIESIADA, H., WILLIAMS, T. D. & SQUIER, T. C. 1999. Repair of oxidized calmodulin by methionine sulfoxide reductase restores ability to activate the plasma membrane Ca-ATPase. *Biochemistry*, 38, 105-12.
- TARRAGO, L., KAYA, A., WEERAPANA, E., MARINO, S. M. & GLADYSHEV, V. N. 2012. Methionine sulfoxide reductases preferentially reduce unfolded oxidized proteins and protect cells from oxidative protein unfolding. *J Biol Chem*, 287, 24448-59.
- TÊTE-FAVIER, F., COBESSI, D., BOSCHI-MULLER, S., AZZA, S., BRANLANT, G. & AUBRY, A. 2000. Crystal structure of the Escherichia coli peptide methionine sulphoxide reductase at 1.9 Å resolution. *Structure*, 8, 1167-78.
- UVERSKY, V. N., YAMIN, G., SOUILLAC, P. O., GOERS, J., GLASER, C. B. & FINK, A. L. 2002. Methionine oxidation inhibits fibrillation of human alpha-synuclein in vitro. *FEBS Lett*, 517, 239-44.
- VERTOMMEN, D., RUIZ, N., LEVERRIER, P., SILHAVY, T. J. & COLLET, J. F. 2009. Characterization of the role of the Escherichia coli periplasmic chaperone SurA using differential proteomics. *Proteomics*, 9, 2432-43.
- VIEIRA DOS SANTOS, C., CUINÉ, S., ROUHIER, N. & REY, P. 2005. The Arabidopsis plastidic methionine sulfoxide reductase B proteins. Sequence and activity characteristics, comparison of the expression with plastidic methionine sulfoxide reductase A, and induction by photooxidative stress. *Plant Physiol*, 138, 909-22.
- VOGT, W. 1995. Oxidation of methionyl residues in proteins: tools, targets, and reversal. *Free Radic Biol Med*, 18, 93-105.
- VOLOKHINA, E. B., GRIJPSTRA, J., STORK, M., SCHILDERS, I., TOMMASSEN, J. & BOS, M. P. 2011. Role of the periplasmic chaperones Skp, SurA, and DegQ in outer membrane protein biogenesis in Neisseria meningitidis. *J Bacteriol*, 193, 1612-21.
- VON ECKARDSTEIN, A., WALTER, M., HOLZ, H., BENNINGHOVEN, A. & ASSMANN, G. 1991. Site-specific methionine sulfoxide formation is the structural basis of chromatographic heterogeneity of apolipoproteins A-I, C-II, and C-III. *J Lipid Res*, 32, 1465-76.

- VOUGIER, S., MARY, J. & FRIGUET, B. 2003. Subcellular localization of methionine sulfoxide reductase A (MsrA): evidence for mitochondrial and cytosolic isoforms in rat liver cells. *Biochem J*, 373, 531-7.
- WEISS, J. L., EVANS, N. A., AHMED, T., WRIGLEY, J. D., KHAN, S., WRIGHT, C., KEEN, J. N., HOLZENBURG, A. & FINDLAY, J. B. 2005. Methionine-rich repeat proteins: a family of membrane-associated proteins which contain unusual repeat regions. *Biochim Biophys Acta*, 1668, 164-74.
- YAMIN, G., GLASER, C. B., UVERSKY, V. N. & FINK, A. L. 2003. Certain metals trigger fibrillation of methionine-oxidized alpha-synuclein. *J Biol Chem*, 278, 27630-5.
- YERMOLAIEVA, O., XU, R., SCHINSTOCK, C., BROT, N., WEISSBACH, H., HEINEMANN, S. H. & HOSHI, T. 2004. Methionine sulfoxide reductase A protects neuronal cells against brief hypoxia/reoxygenation. *Proc Natl Acad Sci U S A*, 101, 1159-64.
- ZHANG, K. & KAUFMAN, R. J. 2008. From endoplasmic-reticulum stress to the inflammatory response. *Nature*, 454, 455-62.